# Performance Testing of Field-Aged Cured-in-Place Liners (CIPL) for Cast Iron Piping

**Final Report**

Submitted to:

NYSEARCH/Northeast Gas Association

By

HE Stewart, TD O'Rourke, BP Wham, AN Netravali, C Argyrou, X Zeng, and TK Bond

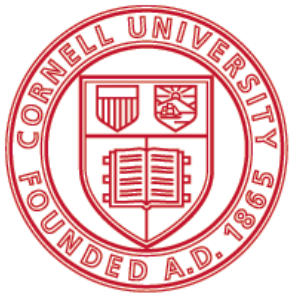


Cornell University

School of Civil and Environmental Engineering
Cornell University
Hollister Hall
Ithaca, NY 14853

December, 2015

Principal Investigators

Harry E. Stewart
Anil N. Netravali
Thomas D. O'Rourke

## LEGAL NOTICE

Periodically Northeast Gas Association ("NGA") sponsors product development and field testing efforts by providing funds or input for projects involving product specifications, design, prototype development, and laboratory or field testing. This activity is designed to assist the gas industry by providing new information to all interested parties.

Neither NGA, nor any of its members, warrant directly or indirectly, in any way or in any matter, that the reports, products, test results or information from these activities are accurate, effective or have application to the gas industry in any particular field setting, if at all.

NGA, its members, and those acting on behalf of NGA, hereby expressly disclaim any and all liability, responsibility, damages or claims, of any kind or of any nature, that may result from use of these reports, products, test results or information related thereto. Any individual, corporation or other entity which uses these reports, products, test results or the information related thereto, does so at its own risk, without reliance on the fact that NGA and/or its members sponsored these activities. Such individual, corporation or other entity assumes any and all liability that may result from such use.

This research was funded in part under the Department of Transportation Pipeline and Hazardous Materials Safety Administration's Pipeline Safety Research and Development Program. The views and conclusions contained in this document are those of the authors and should not be interpreted as representing the official policies, either expressed or implied, of the Pipelines and Hazardous Materials Safety Administration, or the U.S. Government.

## ACKNOWLEDGEMENTS

The authors express their thanks to NYSEARCH, the Northeast Gas Association (NGA), and the U.S. Department of Transportation Pipeline and Hazardous Materials Safety Administration (PHMSA) for providing support for this project. In particular, we appreciate the management and oversight provided by Daphne D'Zurko and Dave Merte of NYSEARCH/NGA, PHMSA, and members of the gas industry, including Con Edison, National Grid, PECO, and PSE&G. The authors would also like to recognize the significant contributions of the laboratory personnel and student assistants on this project. They include Blake A. Berger, Kimberley N. Buhl, Joe Chipalowsky, Addie R. Lederman, Chalermpat Pariya-Ekkasut, Dakota Price, Andrew J. Shakalis, and Reed W. Wawrzynek. Their assistance was invaluable.

## EXECUTIVE SUMMARY

This report presents the results of a project jointly supported by NYSEARCH/Northeast Gas Association and the U.S. Department of Transportation Pipeline and Hazardous Materials Safety Administration to evaluate the performance of field-aged cured-in-place pipe liners (CIPL) that had been in service for 10 to 16 years. Pipe sections with these linings were retrieved from two field sites and subjected to 100 years of mechanical aging due to vehicular traffic, undermining/backfill events, and thermal cycling simulations. Vehicular traffic simulations were equivalent to 100 years (2,000,000 cycles) of a repetitive 40-kip (180-kN) tandem axle load with an impact factor of 1.5. Thermal aging was performed by simulating the expected contraction/expansion of a round crack in cast iron (CI) pipe due to a 40 ºF (22 ºC) seasonal temperature variation in the ground at typical pipe depths.

Specimens were retrieved from two field sites. Six-in. (150-mm)-diameter specimens were retrieved from a location in the Public Service Electric and Gas service area in Elmwood Park, NJ. The CI pipeline was installed in 1949, and a Starline®2000 liner was installed inside the pipeline in 1998. The pipe specimens were extracted in spring 2014 and sent to Cornell University for mechanical aging tests and material property characterization. Twelve-in. (300-mm)-diameter specimens were retrieved from a location in the National Grid service area in South Garden City, Long Island, NY. The CI pipeline was installed in 1951, and a Starline®2000 liner was installed inside the pipeline in 2004. The pipe specimens were retrieved in summer 2014 and testing began March, 2015. The joints of the 6 in. (150 mm) pipes were sealed with cement/mortar and jute caulking. The pipe joints for the 12 in. (300 mm) sections were mechanical clamps with a rubber sealing gasket.

Mechanical aging tests included flexure testing to simulate vehicular traffic, additional bending after an undermining/backfill event, and thermal contraction/expansion cycling to simulate the effects of seasonal variations in temperature. The testing program consisted of four-point bending (flexure) tests, simulating two 50-year-sequences of testing for a total of 100 years. Input displacements representative of deformation imposed by vehicular loading were determined from analytical models, which were validated by full-scale field tests, assuming soil and flexible pavement conditions typically found in gas distribution systems.

Thermal loads in buried piping are a direct result of temperature changes. Data for New York State and other parts of the Northeast US indicate that ground temperatures can fluctuate between 70 and 30 ºF (21 and -1 ºC). Thus, the maximum design temperature change due to seasonal variations in ground temperature in the northeastern US for typical distribution pipe depths is taken as $\Delta T = 40$ºF (22ºC). The anticipated axial movement associated with this temperature fluctuation was determined analytically by assuming the existence of a full circumferential crack in a lined cast iron pipe. One hundred cycles of thermal contraction/expansion were imposed on the test specimens, simulating 100 years of service life under upper bound thermal loading conditions.

No leakage was detected in any specimen throughout all phases of the mechanical aging tests. Following mechanical aging each test specimen was pressure tested. Pressure testing was conducted to a maximum pressure of 150 psig (1,034 kPa) and 90 psig (620 kPa) for 6 in. (150 mm) and 12 in. (300 mm) specimens, respectively. There were no leaks and all pipe sections maintained pressure integrity.

After mechanical testing the pipe joints were cut longitudinally for visual inspection. The 6 in. (150 mm) joints with the CIPL showed debonding at the separation between bell and spigot that was confined to a small distance either side of the separation, less than one pipe diameter in total width. This debonding allowed the liner to stretch without experiencing excessive strain, and demonstrated that the CIPL response involves local bonding adjustments that relieve high strain concentrations in the liner. This type of strain reduction is a highly desirable aspect of CIPL performance.

The 12 in. (300 mm) specimens did experience some minor liner damage. It is believed that this distress occurred during the first thermal loading cycle, which caused substantial debonding and some visually observed fiber damage. However, the liner did not leak because the polyurethane membrane remained intact and maintained its capacity to resist high internal gas pressure. This is a very important experimental observation. Fiber damage does not mean that the CIPL will leak because additional capacity is provided by the polyurethane membrane.

Additional material property characterization tests were performed to:

l) Characterize the residual tensile properties of the composite liner system as a way to assess the effects of field and mechanical aging on the liner system and their durability, and

2) Characterize the residual liner/CI pipe bond (adhesion) strength and assess the durability of the bond strength of field and mechanically aged specimens using lap shear and peel tests.

This allowed for an evaluation of whether the longitudinal and hoop tensile strengths of bonded, field-aged (FA) liner specimens are comparable to those for both bonded and debonded field- and mechanically-aged (FMA) liner specimens. The testing showed that the liner strengths were comparable for the 6 in. (150 mm) specimens for FA and FMA liner specimens taken from bonded and unbonded sections of the liners. Thus, 100 years of mechanical aging did not have a significant effect on either the longitudinal or hoop tensile strengths of the 6 in. (150 mm) pipe liners.

For the 12 in. (300 mm) pipe liners, tensile strength reduction was measured in the immediate vicinity of damaged fibers in the debonded sections of the lining. Considerable tensile strength was still present in lining specimens with damaged fibers because the polyurethane membrane was intact, thus providing resistance to tensile test forces. In locations removed from the vicinity of damaged fibers, liner strengths were comparable for FA and FMA liner specimens taken from bonded and unbonded sections of the liners.

The testing for lap and peel strengths allows for an evaluation of whether the lap and peel strengths of the FA and FMA liner specimens are comparable to those of unaged specimens. A comparison of the lap shear strengths of FA and FMA specimens from the 6 in. (150 mm) and 12 in. (300 mm) pipe with the lap shear strengths of unaged specimens of cast iron pipe with Starline®2000 liner tested at Cornell in 2002 show no significant difference in the results. Thus, no loss of lap shear strength can be shown over the 10 to 16 years of service life in the field and for the 100 years of mechanical aging imposed on the specimens. These findings are important because the strength of the CIPL system depends strongly on the lap shear strength, especially for resistance to thermally induced contraction/expansion of the pipe at round cracks and the bell/spigot separation in a weak, deteriorated joint.

A comparison of the peel strengths of FA and FMA specimens from the 6 in. (150 mm) pipe with the peel strengths of unaged specimens of 6 in. (150 mm) cast iron pipe with Starline®2000

liner tested at Cornell in 2002 show no significant difference in the results. Peel strengths for the 12 in. (300 mm) specimens in this study are not comparable to those of the 6 in. (150 mm) specimens because installation of the liner in the field involves curing under internal pressure substantially less than that for 6 in. (150 mm) pipe. The reduced pressure will result in a lower peel strength relative to that for the 6 in (150 mm) pipe, which is confirmed by the test results in this study. Thus, a critical conclusion from the testing is that there is no evidence of significant reduction in either lap or peel strength due to field aging over 10 to 16 years in addition to 100 years of mechanical aging.

## TABLE OF CONTENTS

## TABLE OF CONTENTS (continued)

## TABLE OF CONTENTS (continued)

## TABLE OF CONTENTS (completed)



## LIST OF FIGURES

## LIST OF FIGURES (continued)

## LIST OF FIGURES (continued)

## LIST OF FIGURES (completed)



## LIST OF TABLES

## LIST OF TABLES (completed)

# Section 1
# Performance Testing of Field-Aged Cured-in-Place Liners (CIPL) for Cast Iron Piping

## 1.1 Introduction

This report provides the results of full-scale tests to evaluate the performance of cast iron (CI) gas pipelines that have been in service with cured-in-place liners (CIPL) for 10 to 16 years. Mechanical aging tests to simulate an additional 100 years of in-service life have been completed, and tests to evaluate key material properties of the field and mechanically aged liners have been performed.

NYSEARCH provided two sections of lined 6-in. (150-mm)-diameter CI pipe and two sections of lined 12-in. (300-mm)-diameter CI pipe with joints in good working condition. All sections were approximately 8 ft (2.4 m) long with the joint at the center. After removal of the pipe sections from excavations in the service areas of gas distribution companies participating in the study, the sections were placed into cradles for protection during truck transportation to Cornell University.

Two sets of mechanical tests were performed on the 6-in. (150-mm) and 12-in. (300-mm)-diameter CI joints. The joints are intended to act as a proxy for CI round cracks, as well as weak and degraded joints in the field. Mechanical aging tests include flexure and axial compression/tension tests on CI specimens obtained from the two field sites. These mechanical aging tests were complemented by a suite of longitudinal and hoop tensile strength tests of the liners in addition to lap shear and peel tests of the CI/liner interface.

Flexure tests were performed to simulate truck loading over two 50-year service life cycles for a total of 100 additional years. Axial pull-push tests were performed to simulate the effects of annual temperature changes on the pipe over the two 50-year service life cycles, simulating an additional 100 years of service. The methodology of the testing is as described in O'Rourke, et al. (1996) and Netravali, et al. (2003).

Specimens for laboratory testing both before and after the mechanical aging tests were removed from four CI pipe sections that were sampled at the field sites. Tests were performed to evaluate liner characteristics a) after roughly 10-16 years of service life, and b) an additional 100 years of simulated field traffic and thermal cyclic loading.

This report is organized in seven sections. The first of which provides introductory comments. Section 2 provides a description of the CIPLs and a summary of previous CIPL research. Section 3 presents the methodology developed to simulate aging in the laboratory. A general description of the analytical methods is provided, along with justification for the approach based of field measurements. Sections 4 and 5 present the results of the mechanical aging tests performed on 6- and 12-in. (150- and 300-mm)-diameter CI pipeline segments, respectively, which had been lined with Starline®2000 CIPL. The retrieval of the pipeline segments is described, and the test results simulating 100+ years of vehicle loading and thermal cycles are provided. The results of internal pressurization tests following the aging tests are described. Section 6 presents the results of material property testing on the polymeric liner materials from the test pipelines. Several types or tensile strength, lap shear, and peel tests on the liner materials were performed after field retrieval of the specimens and after the additional 100+ years of mechanical aging. The test results are compared with the results of prior testing of similar liners. Section 7 presents a summary of the test and research findings, and recommends areas for further investigation.

## Section 2
## Cured-in-Place Liner Systems and Previous Cornell Research

### 2.1 Introduction

The overall objective of the project is to develop a rigorous engineering and science-based framework for using cured-in-place linings (CIPL) as a safe and practical option in the gas industry. Over the past two decades, *in situ* pipe linings have evolved into a well-established technology (AWWA, 2001; Bainbridge, et al., 2005) that increases the service life of existing utilities without expensive and disruptive excavation and replacement. The concept is to install polymeric linings remotely inside existing, underground pipelines with minimum outside disturbance through trenchless construction procedures (Downey and Heavens, 2007; Kramer et al., 1992). The linings secure continuity of pipeline flow, prevent leakage and intrusion, and provide variable degrees of structural reinforcement. R&D efforts have focused on developing advanced equipment and installation techniques, establishing limit state design approaches for the linings (Alam and Allouche, 2010; Guan et al., 2007), and quantifying the effects of imperfections that may result from the installation process (Bruzzone et al., 2007; Dhar and Moore, 2001). Cured-in-place linings (CIPL) have benefitted from previous research (Bainbridge et al., 2005; Bruzzone et al., 2007; Guan et al., 2007; Herzog et al, 2007), and have been used for nearly two decades for *in situ* pipeline rehabilitation. These CIPLs are tubes of woven polyester fabric saturated with thermosetting resin and inserted and cured in existing pipelines. They provide for rapid installation and can accommodate bends and changes in pipe cross-section.

Figure 2.1 provides a three-dimensional cut-away view of the Starline®2000 CIPL system, which was used in this work. Typical installation lengths, pipe diameters, and liner thicknesses are summarized in the figure.

### 2.2 Previous Cornell Research

A substantial body of research exists on CI properties, field performance of CI pipelines, and rehabilitation/repair methods for CI pipe. Over 20 reports have been prepared and circulated by Cornell research-

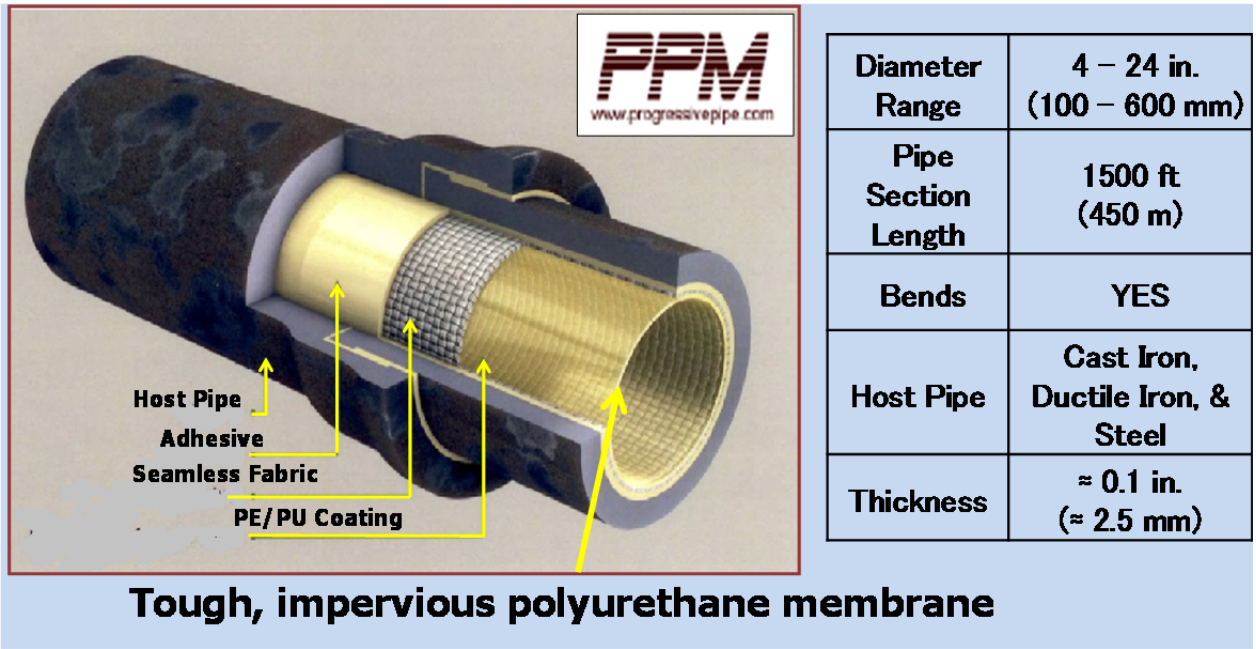


| | |
|---|---|
| Diameter Range | 4 – 24 in. (100 – 600 mm) |
| Pipe Section Length | 1500 ft (450 m) |
| Bends | YES |
| Host Pipe | Cast Iron, Ductile Iron, & Steel |
| Thickness | ≈ 0.1 in. (≈ 2.5 mm) |

Figure 2.1. Cured-in-Place Lining System (after PPM)

**Cast Iron Pipelines**

- Response of Jointed Cast Iron Pipelines to Parallel Trench Construction, NYGAS, 1983
- Factors Affecting the Performance of Cast Iron Pipe, NYGAS, 1984
- Field Tests of Cast Iron Pipeline Response to Shallow Trench Construction, NYGAS, 1984
- Manual for Assessing the Influence of Excavations on Parallel Cast Iron Gas Mains, NYGAS, 1984
- Field Monitoring of Cast Iron Gas Main Response to Deep Trench Construction, NYGAS 1987
- Evaluation of Cast Iron Pipeline Response at Excavation Crossings, NYGAS, 1988

**Mechanical Aging & CIPL Systems**

- Evaluating Service Life of Cast Iron Joint Sealing Products and Techniques, NYGAS, 1985
- Evaluating Service Life of Anaerobic Joint Sealing Products and Techniques, Gas Research Institute, 1996
- Advanced Pipeline Support and Stabilized Backfill for Gas Mains, New York Gas Group, 2000
- Evaluation of Starline Cured-in-Place Lining System for Cast Iron Gas Distribution Pipelines NYSEARCH/NGA, 2003
- Longevity Testing of Anaerobic Sealants in Cast Iron Pipe Joints, National Grid, LCC, 2011

Figure 2.2. Major Cornell Research on Cast Iron Pipelines and Mechanical Aging and CIPL Systems

on CI pipeline performance and rehabilitation technologies. Figure 2.2 lists select research projects that Cornell has undertaken for gas industry research organizations. Testing regimes have been developed for qualifying polymer lining products and for estimating the design life of rehabilitated pipelines (Netravali et al., 2000, 2003). Special testing has been conducted to evaluate seasonal thermal expansion/contraction and traffic load effects on CI mains and joints as well as ground deformation related to undermining and parallel deep trenches and excavations. The testing procedures also involved chemical and material aging assessments of the polymers. Experimental and analytical work by Netravali et al. (2000, 2003) and Jeon et al. (2004) demonstrate the effectiveness of polymer linings for pipelines that have full circumferential cracks and weak joints.

In subsequent sections of this report, the methodologies developed in prior research at Cornell are described with respect to the testing variables for mechanical aging tests, including:

- Pipe joint displacements and rotations for flexure tests that represent 100 years of vehicular traffic effects, and
- Pipe axial displacements that simulate the effects of seasonal temperature changes, representing 100 years of thermal contraction/expansion effects.

Material property tests are discussed in subsequent report sections, which were performed to:

- Characterize the residual tensile properties of the composite liner system as a way to assess the effects of field and mechanical aging on the liner system and its durability, and
- Characterize the residual liner/CI pipe bond (adhesion) strength and its durability using lap shear and peel tests of field and mechanically aged specimens.

Thus, the testing procedures used in this report are the same as those used for over two decades of testing CI pipelines and CIPLs at Cornell. They assure that the methods, as well as the interpretations, are consistent with previous testing and CIPL product development. Of particular importance is the ability to compare the current test results with previous test data to enhance our understanding of the aging effects on complex composite liners and liner/CI interfaces.

# Section 3
# Methodology for Mechanical Aging Tests

## 3.1 Crack Openings in Cast Iron Piping due to Thermal Effects

This section describes the analytical models that were developed to relate axial and vertical displacements and rotations imposed on a CI pipeline with a CIPL installed in pipe sections with a round (circumferential) crack or a weak and degraded bell and spigot joint. Previous Cornell research has shown that round cracks will develop in previously lined CI pipe without damaging the lining (Netravali et al., 2000, 2003). One of the attributes of CIPLs, in fact, is their ability to bridge defects, like round cracks, that develop subsequent to liner installation. The introduction of a round crack, however, interrupts the structural continuity of the CI main so that the effects of repetitive traffic loads and thermal expansion/contraction are concentrated at the lined crack locations. Similar mechanical effects will occur at lined pipe sections with weak and degraded bell and spigot joints. The analytical models developed to simulate lined pipe performance at round cracks and weak joints were used to establish laboratory test procedures to simulate repetitive loadings associated with those imposed by the thermal expansion and contraction effects, traffic loading, undermining excavations for services, and backfill effects.

Pipelines are affected by seasonal changes in soil temperature that cause expansion and contraction of the pipe. Jeon et al. (2004) present the details of a design methodology to predict the opening of a round crack due to temperature changes in the ground for lined CI piping. Two assumptions were adopted in the development of the analytical models:

1) It was assumed that a lined round crack or weak joint occurs in a section of CI pipe adjacent to pipe sections in good repair with CI joints that are stiff and strong. This establishes an upper bound on crack opening displacement due to thermal contraction because the axial movement cannot be distributed to other nearby cracks or weak joints, and thus must be concentrated at one location only.

2) The axial stiffness of the CIPL is negligible compared to that of the CI piping. Full-scale laboratory tests at Cornell have shown that neglecting the stiffness of the lining provides a good representation of the mechanical characteristics of the CIPL system. This model

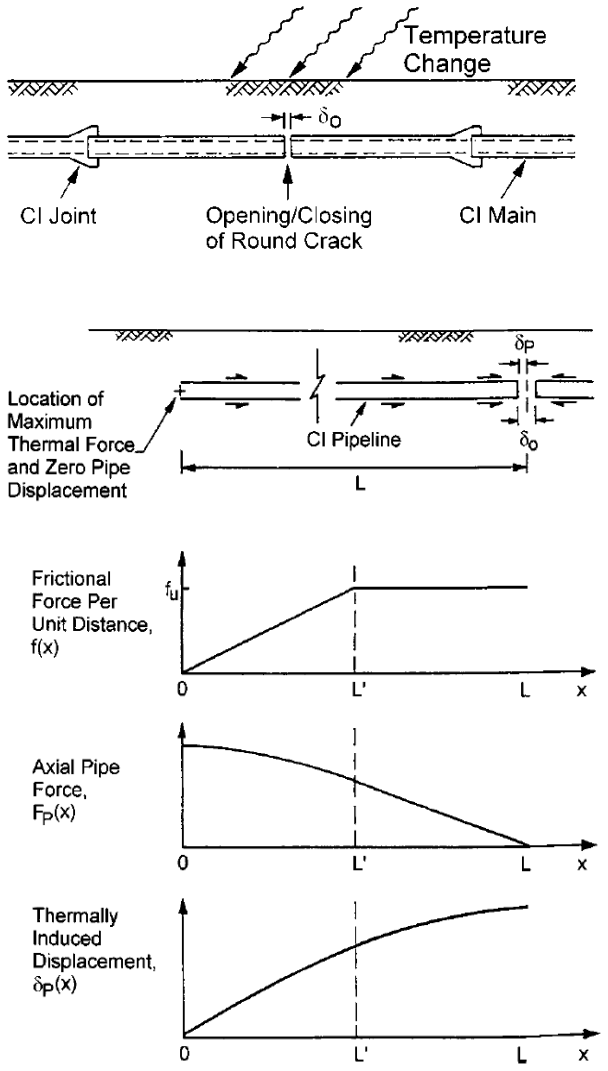


Figure 3.1. Thermally Induced Movements at Round Cracks in Buried Cast Iron Piping (after Jeon et al., 2004)

has a small conservative bias because the relatively low liner resistance to crack opening and joint pullout is discounted.

Additional considerations in this approach, and characteristic movements, are shown in Figure 3.1. In the figure $\delta_O$ is the maximum width of the crack opening. Other important considerations are the frictional force, $f_u$, developed along the pipe, and the design temperature change. The pipe/soil frictional force is based on the pipe geometry, depth of burial, and soil properties, as described by Jeon et al. (2004.)

### 3.1.1 Design Temperature Change

Thermal loads in buried piping are a direct result of temperature changes. Stewart et al. (1999) summarized the seasonal thermal variation, representative of temperature change in New York State and other parts of the Northeast US that would be experienced by buried pipelines. Data were collected at soil depths between 30 and 49 in. (0.8 and 1.2 m), which is in the range of burial depths for typical gas distribution pipe. Table 3.1 describes the information available for each data set evaluated, including the location and depth of data collection, soil conditions, and the reference source for the data set.

Table 3.1. Background Information for Ground Temperature Data Sets

| Location | Depth of Data Collection | Soil Conditions | Reference |
|---|---|---|---|
| Ithaca, NY, NRCC[a] | 20 in.<br>510 mm | Bare ground at surface, sod to 8 in. (200 mm), glacial till at 20 in. (510 mm). | NRCC (1992-97) |
| Ithaca, NY, Burns Rd.[b] | 31 to 33 in.<br>790 to 840 mm | Paved surface, medium to fine sand backfill, glacial till *in situ* soil. | Stewart, et al. (1989) |
| Naumburg, NY | 30, 42, and 49 in.<br>760, 1070, and 1240 mm | Paved surface, silty soil to 49 in. (1240 mm). | Erlingsson (1971) |
| Portland, ME | 36 and 48 in.<br>915 and 1220 mm | Paved surface, not specified below surface. | Monie and Clark (1974) |
| Potsdam, NY | 30 and 49 in.<br>760 and 1240 mm | 4 in. (102 mm) deep gravel bed at surface, poorly graded sand at 6 in. (150 mm), silty or clayey sand and gravel at 48 in. (1220 mm). | Carroll, et al. (1966) |

a – Northeast Regional Climate Center, Ithaca, NY
b – Cornell field site for CI research

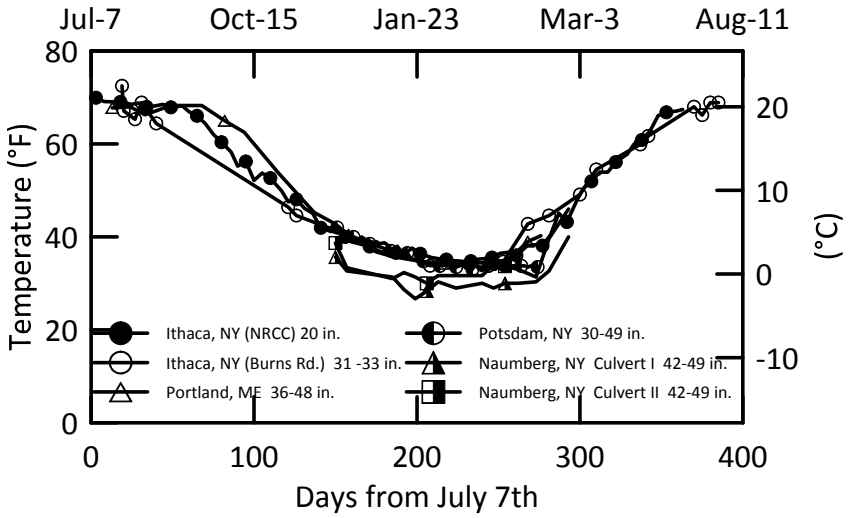


Figure 3.2. Measured Ground Temperatures in Northeastern United States

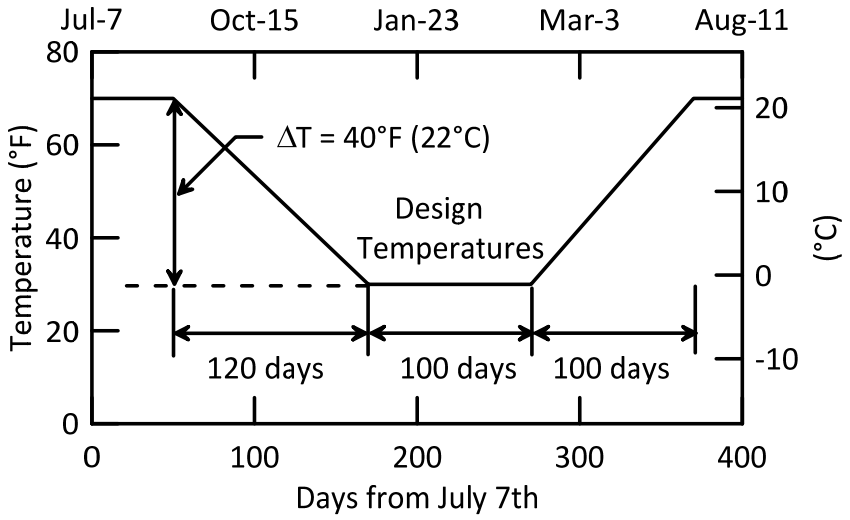


Figure 3.3. Design Seasonal Temperature Variations for Shallow Piping

Figure 3.2 illustrates ground temperature data for these locations. A comparison of data sets reveals a relatively consistent trend in seasonal temperature for the different conditions included in the study. Ground temperatures can fluctuate between 70 and 25 °F (21 and -4 °C) over a period of 6 to 7 months. More typically, the data show that ground temperatures vary between 70 and 30 °F (21 and -1 °C).

Table 3.2. Geometric and Material Properties of 6- and 12- in. (150- and 300-mm)-Diameter CI

| | Nominal Diameter, D | |
|---|---|---|
| | 6 in. | 12 in. |
| External Diameter, $D_{out}$ (in.) | 6.9 | 13.2 |
| Wall Thickness, $t_w$ (in.) | 0.46 | 0.60 |
| Internal Diameter, $D_{in}$ (in.) | 5.98 | 12.0 |
| Cross-Sectional Area, A ($in.^2$) | 9.31 | 23.56 |
| Young's Modulus, E (psi)[a] | 10 to 13 x $10^6$ | |

1 in. = 25.4 mm; 1 psi = 6.89 kPa

Figure 3.3 shows the recommended seasonal design temperature variations for shallow piping. The typical lower temperature is on the order of 30 °F (-1 °C). The maximum design temperature change due to seasonal variations in ground temperature in the northeastern US for typical distribution pipe depths is taken as $\Delta T = 40°F$ (22°C).

### 3.1.2 Testing Procedure

The imposed joint opening for the axial pull-push tests on 6- and 12-in. (150- and 300-mm)-diameter cast iron (CI) lined pipe specimens was based on the analytical solutions presented by Jeon et al. (2004), which were used in prior CI testing at Cornell University. To perform the analyses, pipe geometric and material properties are required. Table 3.2 summarizes the geometric characteristics of the pipe specimens.

Test specimens taken from CI gas distribution pipes in New York State have shown initial tangent Young's moduli between 10 and 13 x $10^6$ psi (69 and 90 GPa) (Taki and O'Rourke 1984; Stewart et al., 1989.) In the analysis, the lower and upper bounds for Young's modulus were considered. The coefficient of thermal expansion, $\alpha_T$, for CI is taken as 6.2 x $10^{-6}$ / ºF (11.4 x $10^{-6}$ / °C).

Material properties used for the soil and pipe-soil interaction conditions are based on experience both in the field and laboratory. The soil behavior is assumed to follow a linearly elastic, perfectly plastic force vs. displacement curve. Two parameters are necessary to characterize the curve: 1) the maximum axial soil frictional resistance per unit pipe length, $f_u$, and 2) the relative

Table 3.3. Parameters for Determination of Soil Frictional Resistance

| | Nominal Diameter, D | |
|---|---|---|
| | 6 in. | 12 in. |
| Depth of Soil Cover (in.) | 32 | 32 |
| Depth to Pipe Centerline (in.) | 35.4 | 38.6 |
| Soil Friction Angle, $\phi^o$ | 40 | 40 |
| Interface Friction Ratio, $\delta/\phi$ | 0.80 | 0.80 |
| Soil Unit Weight, $\gamma$ (lb/ft$^3$) | 125 | 125 |
| Coefficient of Lateral Earth Pressure, $K_o$ | 1.0 | 1.0 |
| Pipe Displacement at Limiting Friction, $\delta_u$ (in.) | 0.04 | 0.04 |
| Frictional Resistance, $f_u$ (lb/ft) | 420 | 870 |

1 in. = 25.5 mm; 1 lb/ft$^3$ = 0.157 kN/m$^3$, 1 ft = 0.305 m

soil/pipe displacement, $\delta_u$, required to fully mobilize soil resistance. The maximum frictional resistance was evaluated according to the methods described by Jeon et al. (2004) and consistent with recommendations established by the Committee on Gas and Liquid Fuel Lifelines (1984). Table 3.3 summarizes the assumptions for the soil properties. As for the displacement, $\delta_u$, three different values were considered; 0, 0.04 and 0.1 in. (0, 1.0 and 2.5 mm). The value of $\delta_u$ = 0.04 in. (1.0 mm) was selected for the final evaluations.

The analytical model gives the opening, $\delta_o$, of a round crack for different temperature changes. Using the pipe and soil characteristics described above and the design temperature change of $\Delta T$ = 40 ºF (22 ºC), the crack openings for 6- and 12-in. (150- and 300-mm)-diameter CI piping were determined. Figures 3.4(a) and 3.4(b) show the results for these CI pipelines for the two bounding values of axial stiffness, EA.

For the 6-in. (150-mm)-diameter piping, the crack opening ranges between 0.25 and 0.34 in. (6.4 and 8.6 mm). For the 12-in. (300-mm)-diameter piping, the crack opening ranges between 0.30 and 0.43 in. (7.6 and 10.9 mm). These openings represent upper bound seasonal expansions/contractions of round cracks in CI pipe at typical burial depths.

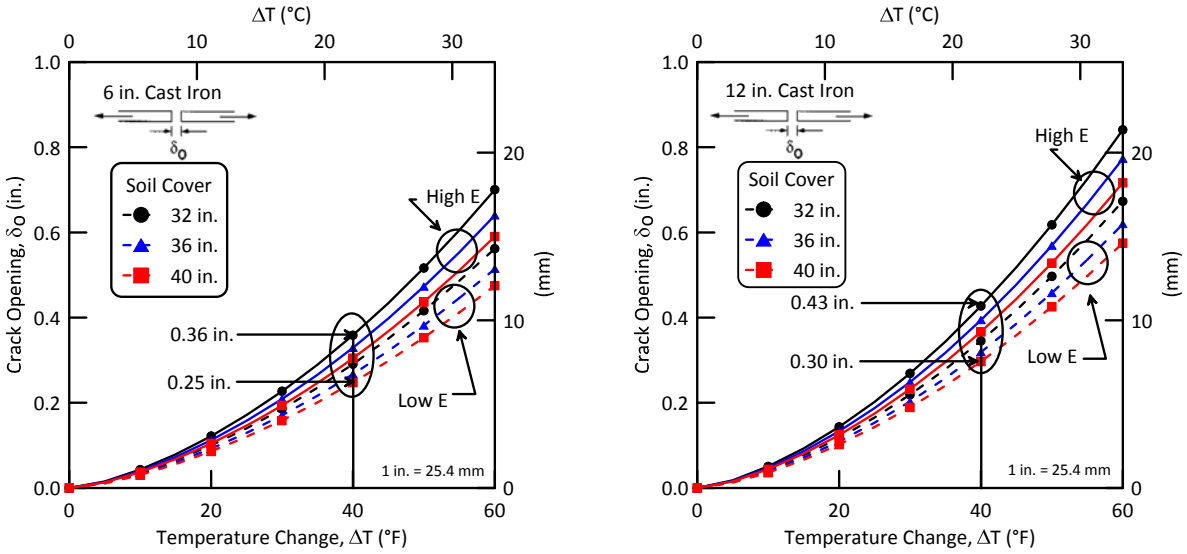


a) 6-in.(150-mm)-Diameter b) 12-in.(300-mm)-Diameter

Figure 3.4. Crack Opening for CI Piping vs. Temperature Change

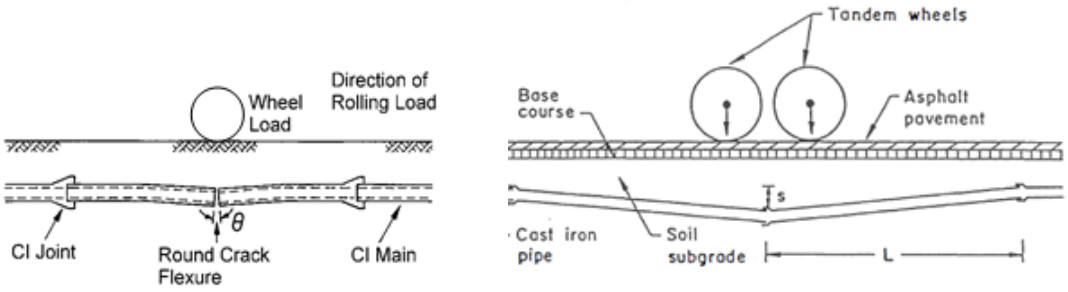


Figure 3.5. Illustrations of Buried Pipeline Deformation due to Applied Traffic Loading

## 3.2 Traffic Loading Approach

The purpose of the traffic loading simulation tests is to characterize the performance of the lined joints under repetitive deformations caused by traffic loads during the pipeline service life. Figure 3.5 shows the types of loading and pipeline deformations which might occur due to vehicular traffic. Vehicular surface loads are transmitted through the pavement and soil to the underground pipelines imposing flexure and joint rotation. Among other factors, the magnitude of pipeline deformation and joint rotation depend on the applied load, relative stiffness of the

pipeline with respect to the surrounding soil that supports it, depth of burial, and stiffness of the joint between individual lengths of pipe. The two important factors for the performance of joints are (1) the magnitude of joint rotation due to the applied load, and (2) ability of the joint to handle the imposed rotation.

To evaluate the effect of traffic loads on the CIPLs, 4-point bending tests were conducted. The deformations imposed were designed to represent the worst-case levels of pipeline deformation in the field. This section of the report describes the process used to determine the quantity and magnitude of deformations imposed during the flexure tests that represent field aging of CI pipelines in dense urban environments.

### 3.2.1 Traffic Loading Test Setup

Figure 3.6 presents a schematic of a 4-point bending test typical of the testing program. The dashed vertical line marks the center of the joint, which is assumed to be located 2.5 in. (64 mm) from the bell face. The vertical thick lines indicate the locations of the supports. To create conditions of constant moment along the joint, the specimen in the lab tests was divided into

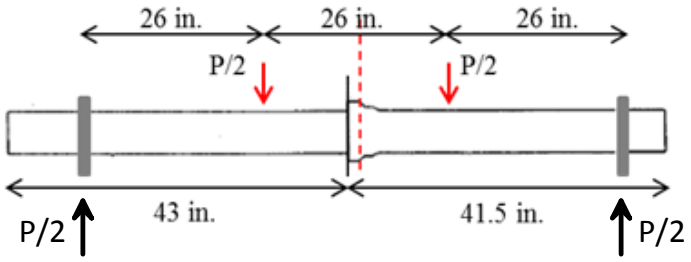


a) Loading Diagram

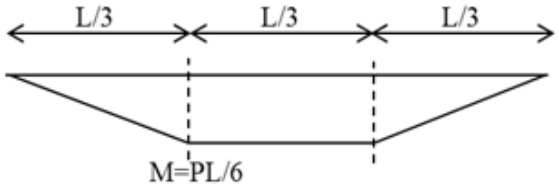


b) Moment Diagram

Figure 3.6. Schematic of 4-Point Bending Test

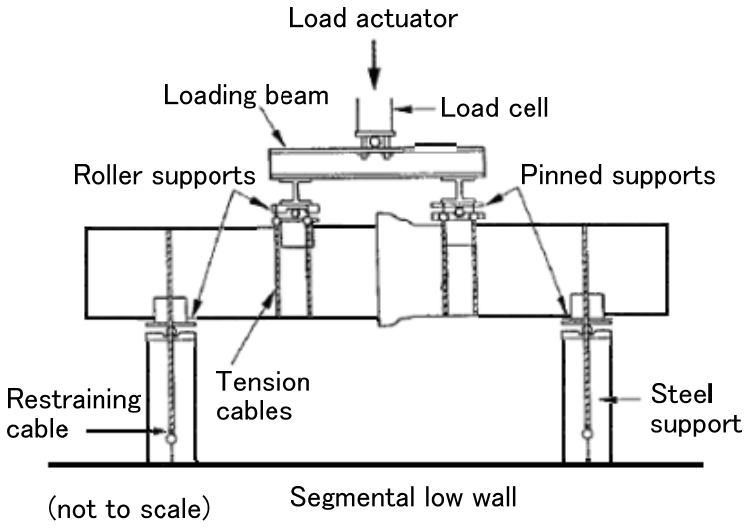


Figure 3.7. Loading Apparatus for Flexure Tests

three spans of approximately equal length [typically 24-in. (610-mm)-long] and two equal loads are applied at symmetric locations with respect to the joint center. More precisely, a vertical displacement is imposed with the aid of a 22-kip (97.9 kN) capacity actuator via a stiff spreader beam. Figure 3.7 shows the loading apparatus for the tests.

During the test, the actuator force and vertical displacement are recorded. Based on the bending moment diagram presented in Figure 3.6(b), the moment M at the joint can be calculated using the actuator force P as follows:

$$M=\frac{P\,L}{6} \tag{3.1}$$

in which L is the length of the pipe specimen.

### 3.2.2 Number of Applied Traffic Loading Cycles

The number of displacements and rotations accumulating at a round crack or pipeline joint over a service life of 50 years was determined by estimating the number of heavy truck loadings which would occur during this time. A New York State maximum weight limitation of 36 kips (160 kN) per double tandem axle, an impact factor of 1.5, and 3 ft (0.9 m) depth of cover were assumed. The 36 kip (160 kN) maximum weight limitation was rounded up to 40 kip (178 kN) to account for overloading, then halved and multiplied by an impact factor of 1.5 to represent a

single wheel set with an equivalent load of 30 kip (133 kN). The number of axles, vehicular volume, and the percentages of trucks and fully loaded trucks were used to compute a value of 780,000 heavy trucks per 50 years, which was rounded up to one million cycles (O'Rourke et al., 1985). One millions cycles applied over a 50 year aging life equates to 20,000 cycles per year.

### 3.2.3 Inputs for Traffic Loading Tests

CI pipelines are subjected to surface loads from vehicular traffic. When surface loading is conveyed to a lined CI main, the CIPL lining will experience maximum deformations (i.e., relative displacement and rotation) at the weakest discontinuity along a pipeline. The presence of a full circumferential fracture, or round crack, is representative of a worst-case discontinuity along a CI pipeline. The following analysis determines upper bound displacement levels for traffic loading assuming the presence of a round crack. This deformation level is imposed during mechanical aging to CIPL lined joints, which represent the weak discontinuities at which the liner will be subjected to large loading levels. The following text uses the terms round crack, joint, and weak discontinuity as synonymous.

Deformation at the round crack may occur by rolling loads traveling parallel, oblique, or perpendicular to the longitudinal axis of the pipeline. Previous studies have shown that wheel loads positioned directly over the pipe and traveling parallel to the pipeline longitudinal axis will generate stresses and deformations representative of worst case conditions (O'Rourke et al., 1988). Deformation at the round crack occurs as a relative rotation, $\theta$, and relative vertical offset, $\delta_V$. As the wheel loads travel across the crack along the pipeline, both $\theta$ and $\delta_V$, will vary. Maximum values of $\theta$ and $\delta_V$ will occur at different locations of the wheel load with respect to the round crack.

### 3.2.4 Analytical Model for Traffic Loading

The magnitude of traffic loading was determined based on analytical models, field test measurements, and recommendations presented by O'Rourke et al. (1996). The interaction between traffic loads conveyed to a CI pipeline at depth and the pipeline response in terms of bending and joint rotation was modeled by means of a beam-on-elastic foundation approach (Hetenyi, 1974) using the coefficient of subgrade reaction to represent the appropriate force-displacement behavior of the buried pipeline. Loads were conveyed to the pipeline according to the recommendations of Carder, Nath, and Taylor (1981) who evaluated buried CI pipeline

response to truck loads during field experiments at the U.K. Transport Research Laboratory. Stewart et al. (1989) found that this approach, which is based on a classical Boussinesq formulation, gave good results when modeling jointed CI pipeline response to surface truck loads during field experiments at Cornell University.

Undermining occurs when trenches are excavated and backfilled beneath existing CI mains. In this study, soil backfill was assumed to be lightly compacted, resulting in low density and stiffness. Investigations at the British Transport and Road Research Laboratory (Pocock et al., 1980) have shown that the coefficients of subgrade reaction appropriate for typical roadway bedding and loose underlying backfill are 100 and 20 t/ft$^3$ (31.4 and 6.3 MN/m$^3$), respectively.

### 3.2.5 Procedure for Evaluating Magnitude of Traffic Loading

The traffic load (flexure) testing was divided into three loading phases. The procedure outlined below was followed for each lined CI pipe specimen with diameters of 6 and 12 in. (150 and 300 mm). The following procedure presents numerical values associated with Specimen 6-1.

#### 3.2.5.1 Testing Phase A: Specimen 6-1

Phase A is conducted to characterize the rotational stiffness of the 6 in. (150 mm) joint prior to removal of cement caulking. A manual loading cycle to 0.0038$^o$ (0.000067 rad) was slowly applied to the joint. The resulting moment was 10.4 in.-kip (1.2 m-kN/rad). This yielded an initial rotational stiffness of approximately $k_\theta$ = 167,000 in.-kip./rad (19,000 m-kN/rad). The stiffness was defined as the secant slope between the peaks of the loading cycles. This stiffness was used with Figure 3.8 to provide an estimate of the appropriate level of joint rotation associated with field behavior.

#### 3.2.5.2 Testing Phase B: Specimen 6-1

During Phase B the specimen is subjected to one million (1,000,000) cycles of joint rotations to reflect 50 years of service life. The amount of rotation that the joint experiences in the field, and should be applied during the test, is a function of joint rotational stiffness, $k_\theta$, pipe diameter, D, mechanical properties of the cast iron (i.e., Young's modulus, E), subgrade soil reaction, $k_{s1}$, burial depth, z, and applied surface load, P. Parametric analyses were carried out with respect to the above factors. The pipeline is analyzed as a beam on elastic foundation, following Hetenyi's approach (Hetenyi,1939).

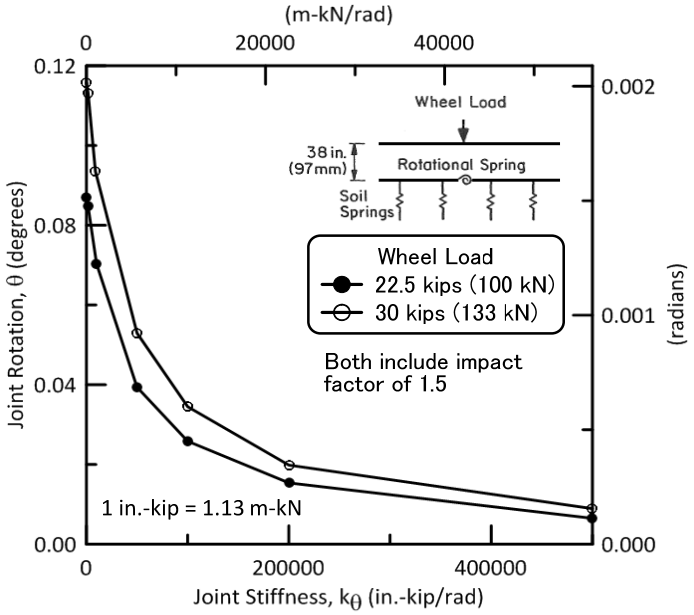


Figure 3.8. Predicted CI Joint Rotations Induced by Traffic Loads (after O'Rourke, et al., 1996)

The coefficient of subgrade reaction was taken as 100 t/ft$^3$ (31.4 MN/m$^3$), which has been shown by full-scale field experiments to be typical of normal roadway bedding conditions. Using a burial depth, z = 32 in. (0.8 m) and surface load, P = 30 kips (133 kN kN) (impact factor of 1.5 included), the imposed vertical displacement was determined using Figure 3.9. Based on the estimate for the initial joint stiffness during Phase A, the vertical displacement that needs to be imposed during Phase B is approximately equal to 0.035 in. (0.89 mm), for a pipeline with nominal diameter of 6 in. (150 mm.) The joint rotation is expected to be between 0.005$^o$ to 0.010$^o$.

### 3.2.5.3 Testing Phase C: Specimen 6-1

During the last loading phase the effect of undermining excavation for services is investigated. Trenching and subsequent backfilling, illustrated in Figure 3.10, disturbs the bedding conditions of the pipeline. In Figure 3.10 $L_P$ is the distance from the load point to the circumferential crack and LC is the position of the crack relative to the CI joint. These parameters were varied to determine the worst case conditions for relative crack rotation, $\theta$, and vertical crack offset, $\delta_V$.

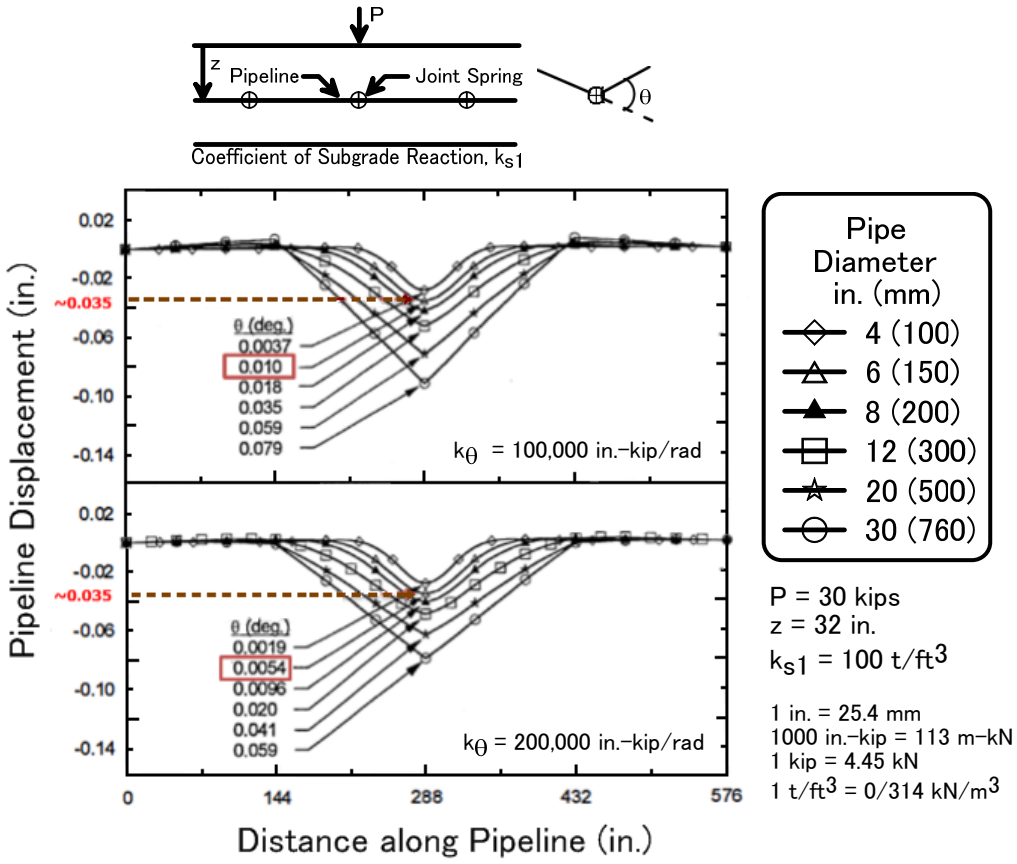


Figure 3.9. Effect of Pipe Size and Joint Stiffness on Pipeline Displacement and Joint Rotation

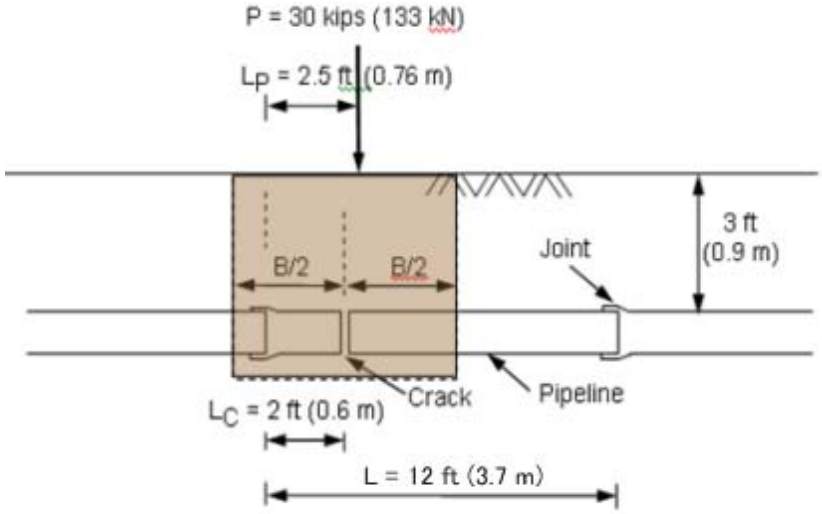


Figure 3.10. Schematic of Undermining Event Conditions

This load phase included a load cycle representative of undermining/backfill followed by an additional 100,000 cycles (+ 0.5 years) of traffic load. The procedure used to determine joint rotations and vertical displacements representative of an undermining excavation is based on analytical results presented by O'Rourke et al. (1996). To simulate the effects of an undermining excavation, the following conservative assumptions were made:

a) trench width, B, is equal to the joint separation, L, in the field where L = 12 ft in. (3.66 m). In this case the width ratio is B/L = 1.

b) subgrade reaction for the backfill at this portion of the pipeline is $k_{sb1}$ = to 20 t/ft$^3$ (6.4 MN/m$^3$), representing loose to moderate backfill conditions.

Figure 3.11(c) summarizes the analytical results in terms of normalized joint rotation relative to B/L ratio for a 6 in. (150 mm) pipe. The rotations for the undermined case, $\theta_u$, are normalized with respect to the joint rotation for uniform subgrade reaction, $k_{s1}$, along the pipeline.

For the maximum joint stiffness shown in Figure 3.11, i.e. $k_\theta$ = 50,000 in.-kip/rad (5,650 m-kN/rad), the anticipated joint rotation for the undermined condition is 2.1 times larger than the rotation for the condition of uniform subgrade reaction, as calculated for the loading Phase B.

To provide a useful metric for performing the undermining/backfill simulation this rotation needs to be equated to a representative imposed vertical displacement. In this work an interpolation was made between the existing analytical solutions for displacement of a 4- and 12-in. (100-mm and 300-mm)-diameter pipelines to determine the displacement for a 6-in (150-mm)-diameter pipeline.

Figures 3.11(a) and (b) provide the undermining joint rotation ratios for 4- and 12-in. (100- and 300-mm)-diameter pipes, respectfully. Under the assumptions previous described the joint rotation ratio, $\theta_u/\theta$, is 2.125 and 2.15 for the 4- and 12-in. (100-mm and 300-mm)-diameter pipeline, respectively. These results suggest that the normalized rotation does not vary significantly with the pipe diameter.

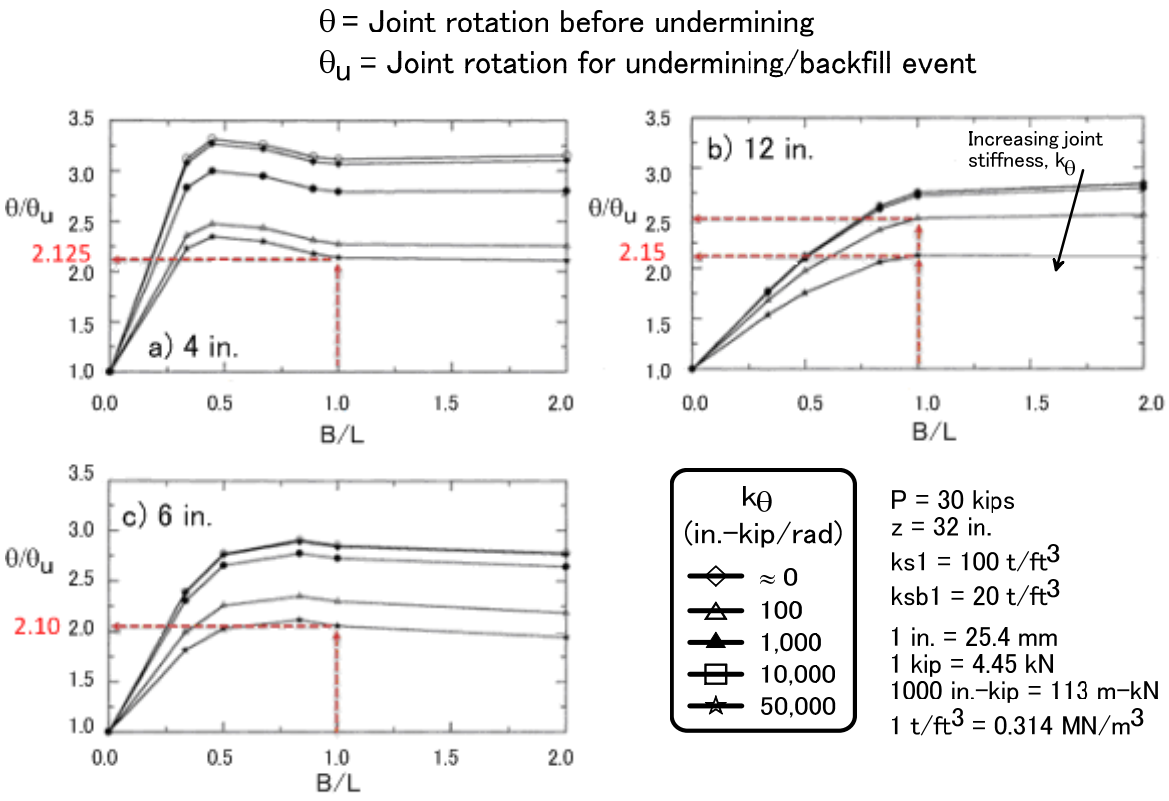


Figure 3.11. Effect of Undermining Trench Width on Joint Rotation

The bottom of Figure 3.12 provides the vertical displacements associated with various pipeline diameters with a joint stiffness $k_\theta$ = 50,000 in-kip/rad. Figure 3.13 provides the vertical pipeline displacements for the undermined condition for 4- and 12-in. (100- and 300-mm)-diameter pipelines. Combining the results of Figures 3.12 and 3.13 for 4- and 12-in. (100- and 300-mm)-diameter pipes the ratio of vertical joint displacements in the undermined case, $\delta_u$, to the displacement for the uniform case, $\delta$, can be determined as follows:

For 4-in. (100-mm)-diameter pipeline: $\frac{\delta_u}{\delta} = \frac{0.11\text{ in.}}{0.03\text{ in.}} = 3.5$

For 12-in. (300-mm)-diameter pipeline: $\frac{\delta_u}{\delta} = \frac{0.16\text{ in.}}{0.06\text{ in.}} = 2.67$

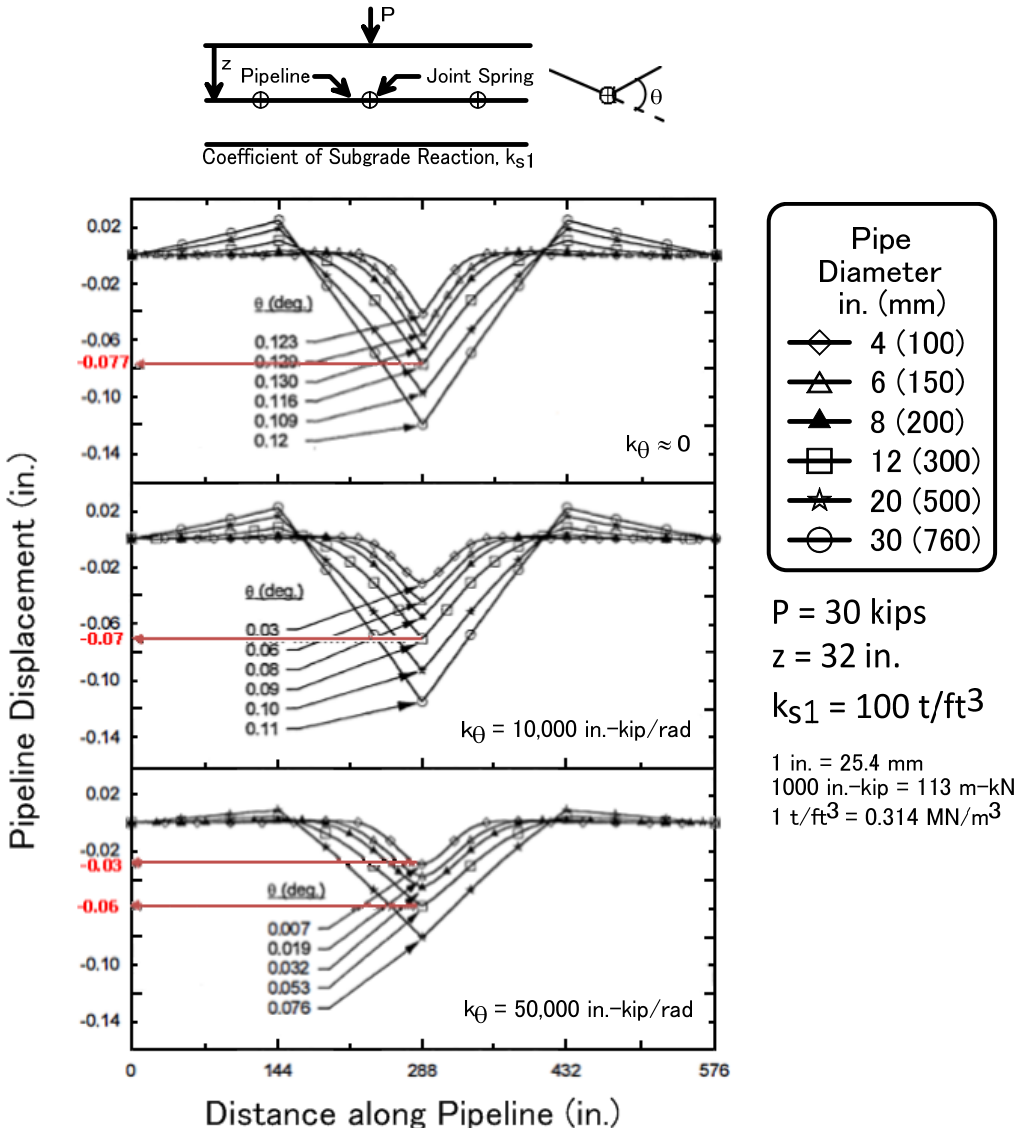


Figure 3.12. Effect of Pipe Size and Joint Stiffness on Joint Rotation and Pipeline Displacement

Assuming that the corresponding ratio for a 6-in. (150-mm)-diameter pipeline lies within this range (i.e., 2.67 - 3.5), a value of 3 is taken as a reasonable estimate. Therefore, the imposed vertical displacement at loading Phase C, the undermining/backfill event, is 0.105 in. (0.38 mm).

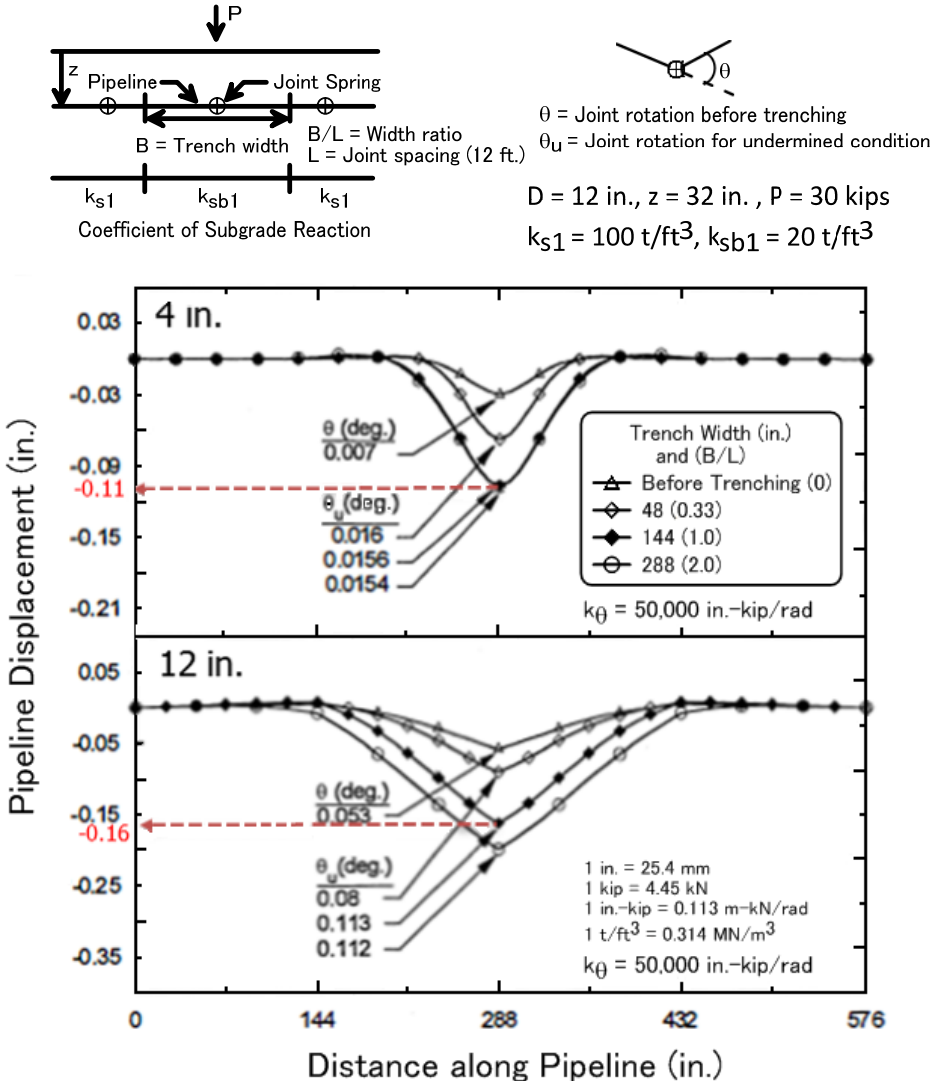


Figure 3.13. Effect of Trench Width on Joint Rotation and Pipeline Displacement for a 4- and 12-in. (100-mm and 300-mm)-Diameter Pipeline

### 3.2.5.4 Testing Phase A: Specimen 12-1

The following three sections describe the procedure for determining imposed displacements for traffic and undermining test phases for the 12-in. (300-mm)-diameter joint. Phase A was conducted to characterize the rotational stiffness of the joint prior to cyclic loading. A manual loading cycle to 0.176° (0.0031 rad) was applied slowly to the joint. The developed moment was equal to 45.9 kip-in. (5.2 m-kN). This result yields an initial rotational stiffness of 14,920 kip-in./rad (1,685 m-kN/rad).

#### 3.2.5.5 Testing Phase B: Specimen 12-1

The methodology described previously for the 6 in. (150 mm) pipe joint was similarly used to determine displacements and rotations for Specimen 12-1 with a 12 in. (300 mm) pipe joint. Using a burial depth of z = 32 in. (0.81 m), subgrade reaction, $k_{s1}$ = 100 t/ft$^3$, (31.4 MN/m$^3$), and a surface load P equal to 20 kips (89 kN) with an impact factor of 1.5, the imposed vertical displacement was determined as shown in Figure 3.12. Based on the estimate for the initial joint stiffness during Phase A, the vertical displacement that needs to be imposed during Phase B is approximately equal to 0.07 in. (1.78 mm) for a nominal 12-in. (300-mm)- diameter CI pipeline. The joint rotation is expected to be greater than $\theta = 0.09^o$ (0.00157 rad).

#### 3.2.5.6 Testing Phase C: Specimen 12-1

During the last loading phase, the effect of trenching operations is investigated. Trenching and subsequent backfilling disturbs the bedding conditions of the pipeline. This load phase included a load cycle representative of a trenching event followed by an additional one hundred thousand (100,000) cycles of traffic load. The procedure used to determine joint rotations and vertical displacements representing undermining/backfill are based on analytical results presented by O'Rourke et al. (1996). For the flexure tests, the following assumptions were made:

a) trench width, B, is equal to the joint separation, L, in the field [L is equal to 12 ft (3.66 m). In this case the width ratio is B/L = 1.

b) subgrade reaction, $k_{sb1}$, at this portion of the pipeline is equal to 20 t/ft$^3$ (6.3 MN/m$^3$), representing loose to moderate backfill conditions.

Figure 3.11(b) summarizes the analytical results in terms of normalized joint rotation relative to B/L ratio for a 12 in. (300 mm) pipe. The rotations for the undermined case, $\theta_u$, are normalized with respect to the joint rotation, $\theta$, for uniform subgrade reaction along the pipeline. For joint stiffness of $k_\theta$ = 10,000 in.-kip/rad (1,130 m-kN/rad), which is the closest value to the stiffness calculated in Phase A, the anticipated joint rotation for the undermined condition is 2.5 times larger than the rotation for the condition of uniform subgrade reaction, as calculated for the loading Phase B. However, this rotation needs to be translated into vertical imposed displacement for the loading Phase C.

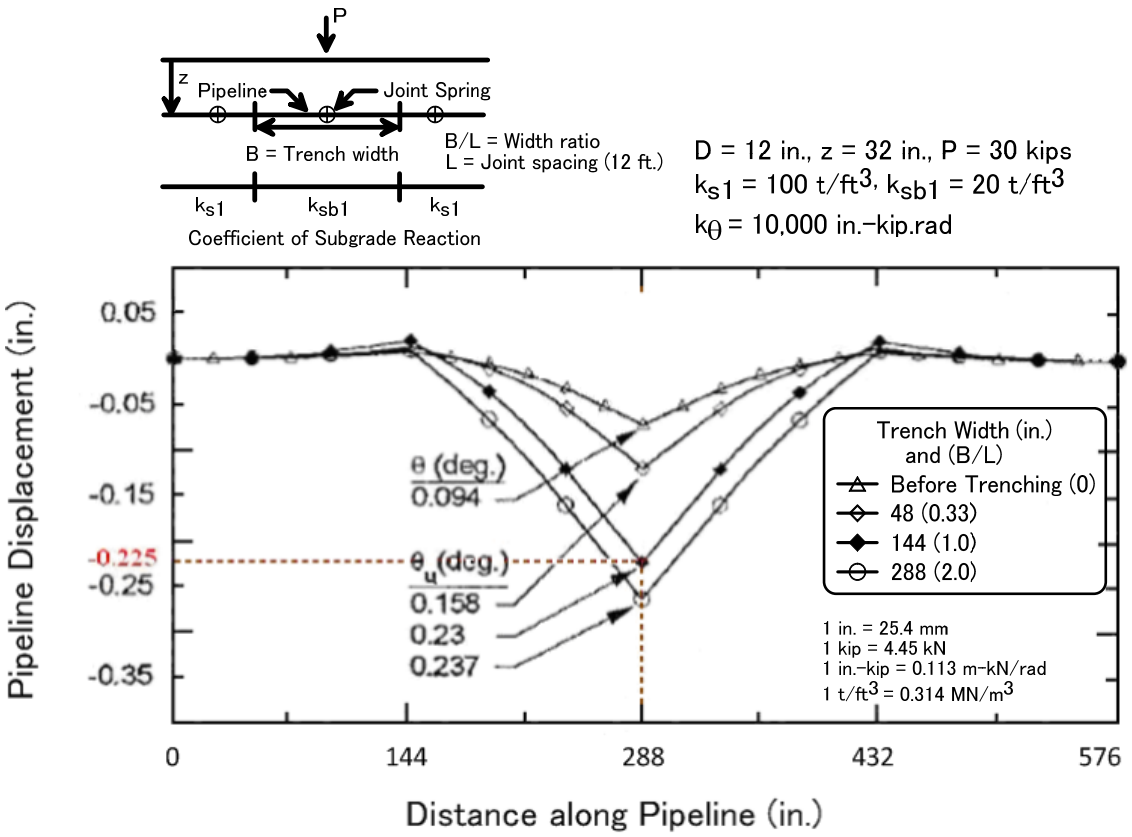


Figure 3.14. Effect of Trench Width on Joint Rotation on a 12-in. (300-mm)-Diameter Pipeline

Figure 3.14 provides the vertical pipeline displacements for the undermined condition for 12-in. (300-mm)-diameter pipeline. The imposed vertical displacement of the trenching event for loading Phase C is equal to 0.225 in. (5.72 mm).

### 3.2.6 Summary of Traffic Loading Methodology

The previous Section 3.2.5 outlined the procedure for determining input displacements for the traffic load tests on Specimen 6-1, before removal of cement calking, and Specimen 12-1. A similar procedure was followed for Specimen 6-1 (after weakening of joint), Specimen 6-2 and Specimen 12-2. Due to similar initial rotational stiffnesses, the procedure for determining input displacements is similar that of Specimen 12-1, with only slight variations. Table 3.4 summarizes all relevant inputs necessary to determine displacements for the mechanically aging traffic load tests. The table also provides values of imposed rotation during each phase of testing. For all cases the imposed rotation is at or exceeds the level of deformation suggested by the outlined procedure.

Table 3.4. Summary of Traffic Loading Analysis for Cast Iron Specimens

| | | | Specimen and Joint Condition | | | |
|---|---|---|---|---|---|---|
| | Variable | Units | 6-1 Cement | 6-1 & 6-2 Cement Removed (Weakened) | 12-1 Mechanical (Inner-Tite) | 12-2 Mechanical (Inner-Tite) |
| General | Nominal Pipe Diameter | in. | 6 | 6 | 12 | 12 |
| | | mm | 150 | 150 | 300 | 300 |
| | Elastic Modulus | ksi | 11000 | 11000 | 11000 | 11000 |
| | | GPa | 76 | 76 | 76 | 76 |
| Phase A | Initial Rotation (Manual Cycle) | deg | 0.003800 | 0.140 | 0.1760 | 0.275 |
| | | rad | 0.000067 | 0.0024 | 0.0031 | 0.0048 |
| | Initial Moment | in.-kip | 10.4 | 36 | 45.9 | 80.0 |
| | | m-kN | 1.18 | 4.07 | 5.19 | 9.04 |
| | Initial Rotational Stiffness, $k_\theta$ | in-kip/rad | 167,000 | 13,500 | 11,760 | 11,525 |
| | | m-kN/rad | 19,000 | 1,530 | 1,330 | 1,300 |
| Phase B | Subgrade Soil Reaction, $k_{s1}$ | $t/ft^3$ | 100 | 100 | 100 | 100 |
| | | $kN/m^3$ | 31.4 | 31.4 | 31.4 | 31.4 |
| | Burial Depth, z | in. | 32 | 32 | 32 | 32 |
| | | m | 1.3 | 1.3 | 1.3 | 1.3 |
| | Applied Surface Load, P | kips | 30 | 30 | 30 | 30 |
| | | kN | 133 | 133 | 133 | 133 |
| | Impact Factor | | 1.5 | 1.5 | 1.5 | 1.5 |
| | Joint Stiffness Fig. 3.9 or 3.12 | in.-kip/rad | 100K-200K | 10,000 | 10,000 | 10,000 |
| | | m-kN/rad | 11.3-22.6K | 1,130 | 1,130 | 1,130 |
| | Applied Vertical Disp., $\delta_V$ | in. | 0.035[a] | 0.045[d] | 0.07[d] | 0.07[d] |
| | | mm | 0.89 | 1.14 | 1.78 | 1.78 |
| | Joint Rotation (Fig. 3.9 & 3.12) | deg | 0.005-0.010 | 0.06 | 0.09 | 0.09 |
| | | rad | 0.0001-0.0002 | 0.00105 | 0.0016 | 0.0016 |
| | Imposed Rotation during Testing | deg | 0.0051 | 0.149 | 0.298 | 0.286 |
| | | rads | 0.00009 | 0.0026 | 0.0052 | 0.005 |

Table 3.4. Summary of Traffic Loading Analysis for Cast Iron Specimens (completed)

| | | | Specimen and Joint Condition | | | |
|---|---|---|---|---|---|---|
| | Variable | Units | 6-1 Cement | 6-1 & 6-2 Cement Removed (Weakened) | 12-1 Mechanical (Inner-Tite) | 12-2 Mechanical (Inner-Tite) |
| Phase C | Trench Width / Joint Separation, B/L | | 1 | 1 | 1 | 1 |
| | Backfill Subgrade Reaction, $k_{sb1}$ | $t/ft^3$ | 20 | 20 | 20 | 20 |
| | | $MN/m^3$ | 6.3 | 6.3 | 6.3 | 6.3 |
| | Joint Stiffness Fig. 3.13 & 3.14 | in.-kip/rad | 50,000 | 10,000 | 10,000 | 10,000 |
| | | m-kN/rad | 5,650 | 1,130 | 1,130 | 1,130 |
| | Undermined Rotation. Ratio, $\theta_u/\theta$ | | 2.1[c] | 2.25[c] | 2.5[b] | 2.5[b] |
| | Min. Imposed Rotation, $\theta_{min}$ | deg | 0.011 | 0.135 | 0.225 | 0.225 |
| | | rad | 0.00019 | 0.00236 | 0.00393 | 0.00393 |
| | Applied Vertical Displacement, $\delta_v$ | in. | 0.105[d,e] | 0.17[--] | 0.225[f] | 0.225[f] |
| | | mm | 2.67 | 4.32 | 5.72 | 5.72 |
| | Imposed Rotation during Testing | deg | 0.012 | 0.344 | 0.745 | 0.773 |
| | | rad | 0.00021 | 0.006 | 0.013 | 0.0135 |

a - Value determined from Figure 3.9
b - Value determined from Figure 3.11(b)
c - Value determined from Figure 3.11(c)
d - Value determined from Figure 3.12
e - Value determined from Figure 3.13
f - Value determined from Figure 3.14

## Section 4

## Mechanical Aging Tests on Six-In. (150-mm)-Diameter Cast Iron Pipe

### 4.1 Specimen Retrieval for 6 in. (150 mm) CI Joints

NYSEARCH/NGA provided two sections of lined 6-in. (150-mm)-diameter cast iron pipe with joints in good working condition. All sections were approximately 8 ft (2.4 m) long with a joint at the center. An additional straight section of CI also was retrieved for additional testing as necessary.

The 6-in. (150-mm)-diameter specimens were retrieved from a Public Service Gas & Electric (PSE&G) location in Elmwood Park, NJ. The CI pipeline was initially installed in 1949. A Starline®2000 liner was installed by Progressive Pipeline Management in 1998. The pipe specimens were acquired in May, 2014. After removal from the excavations the pipes were placed in protective cradles and shipped to Cornell University. Mechanical aging tests began in July, 2014. Table 4.1 lists the specimen retrieval locations. The two CI sections for testing were identified as Specimens 6-1 and 6-2.

Figure 4.1(a) – (c) shows the excavation and CI pipe at Elmwood Park, NJ. The CI joint is shown in the figures. This was a live gas cut-out. The PSE&G CI line was operating at a low pressure of about 15 in. of water column (102 kPa.) Figure 4.1(d) shows a pipe section immediately after removal. The lining appears very clean with no obvious defects after 16 years of service.

### 4.2 Joint Configuration for 6 in. (150 mm) CI Joints

Figure 4.2 shows a schematic of the joint in the 6-in. (150-mm) CI pipe. The joints were caulked with cement mortar and jute packing. They were very stiff joints.

Table 4.1. Six-in. (150-mm)-Diameter Cast Iron Joint Retrieval Location

| Specimen No. | Diameter and Length | Lined Pipe Location | Liner Installation | Specimen Retrieval Date | Cornell Begins Testing |
|---|---|---|---|---|---|
| 6-1 and 6-2 | 6 in. dia., 8 ft (150 mm, 2.4 m) | Elmwood Park, NJ | 1998 | May 21, 2014 | July, 2014 |

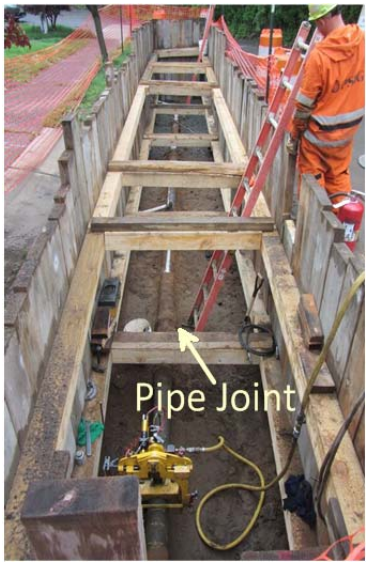


a) Six-in. (150-mm)-Diameter CI Joint in Elmwood Park, NJ


b) Six-in. (150-mm)-Diameter CI Joint Being Cut Out


c) Six-in. (150-mm)-Diameter CI Joint Showing End Cap and Live Gas Plastic Replacement


d) Six-Inch (150-mm)-Diameter CI Section after Removal in May, 2014

Figure 4.1. Pipe Retrieval from PSE&G Site in Elmwood Park, NJ

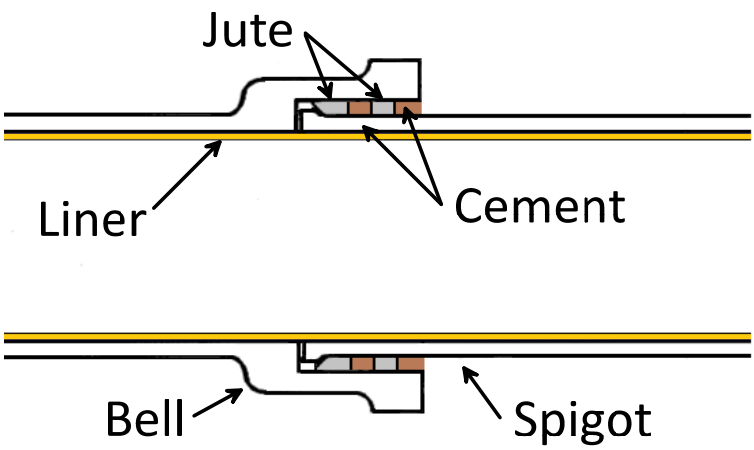


Figure 4.2. Schematic of Cement Caulked Joint for 6 in. (150 mm) Pipe Specimens

### 4.3 Mechanical Aging Test Results for Specimen 6-1

The purpose of the flexural testing was to simulate the rotation that would be induced in the pipe joint from heavy truck traffic and to apply this rotation to the joint repetitively to simulate loading effects over a 50-year service life. The test setup consisted of orienting the pipe specimen to be simply supported in the vertical direction. Each pipe was orientated as it had been in the ground. The pipes were fitted with Dresser 711 end caps. The overall length of the sections was approximately 8 ft (2.4 m). The supports were near the ends of the sample and the load applied at distances equal to 1/3 the sample length either side of the joint. A vertical load was applied using a hydraulic actuator through a spreader beam such that equal load was applied to the pipe on either side of the pipe joint. By applying the load in this fashion, the area between the applied load locations, which includes the pipe joint, is an area of zero shear. This loading configuration results in constant bending moment applied across the pipe joint. A photograph of the flexure test setup is shown in Figure 4.3. The inset in the upper right corner of the figure shows the constant moment across the central portion of the pipe section.

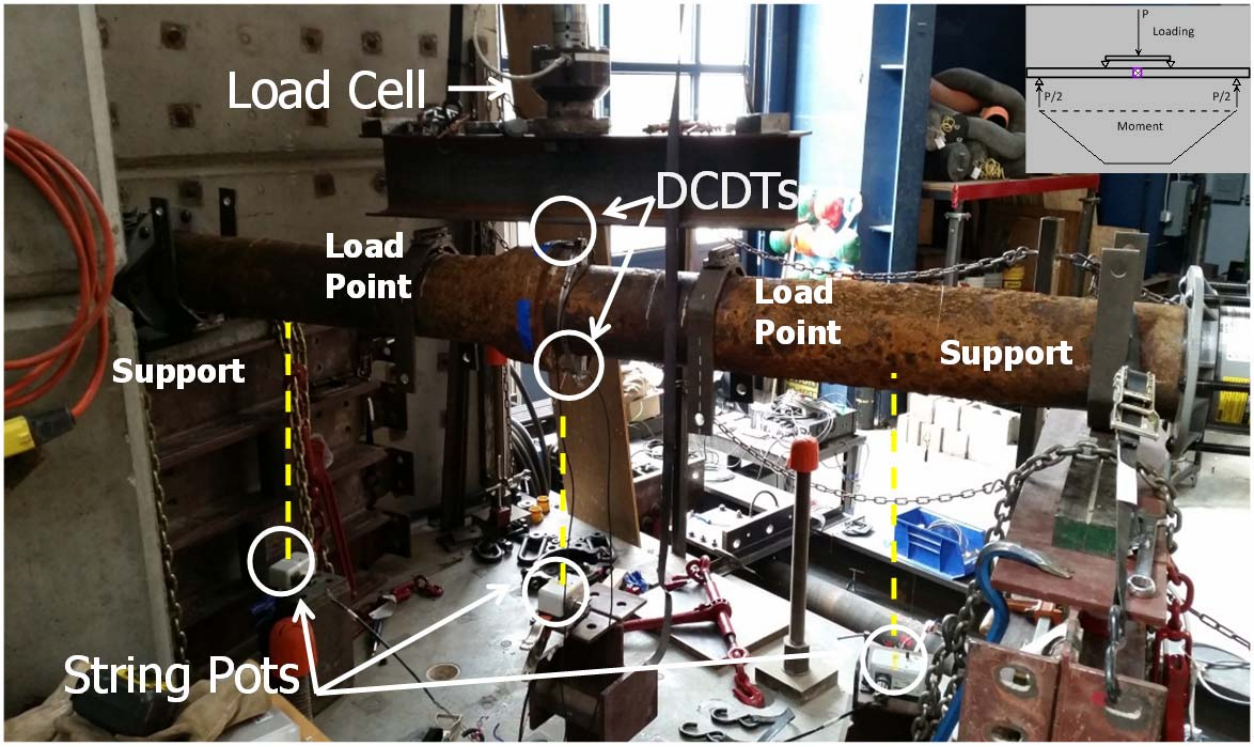


Figure 4.3. Flexure Test Apparatus with 6-in. (150-mm)-Diameter Test Specimen

The pipe specimens were pressurized for the flexure test to 15 in. of water column pressure (102 kPa) using nitrogen. This pressure was selected to be consistent with the low operating pressure of a 6 in. (150 mm) distribution pipeline. This also is consistent with other testing performed at Cornell on distribution-sized CI piping. Instrumentation was used that measured both the central force from the actuator and the deflection of the joint. Load was measured using an MTS 22-kip (97.9-kN) load cell conditioned with an MTS FlexTest SE servo-control system. Displacement at the joint was measured with both DC/DC LVDTs (DCDTs) and string potentiometers (string pots). Rotations of the joint were calculated using either the measured DCDT or string pot displacements.

After the pipe and instrumentation were in place a nominal deflection was applied to the pipe joint and the force necessary to produce this deflection was recorded. As described in Section 3, this served to characterize the stiffness of the joint. Using the applied load and the induced rotation, a rotational stiffness was calculated in units of moment/rotation (kip-inches or m-kN of moment per radian of rotation). Secure connection of the specimen included both a stiff support

at the outboard ends of the specimen and a stiff tie down at the four-point loading points, which allowed the pipe section to be returned to its initial level position under tension. Please note that the pipeline in soil returns to its initial horizontal position after the rolling traffic load has moved away from the pipe. To simulate this response, some tensile force was required to counterbalance the dead weight of the pipe in the test. These measurements of initial joint stiffness were used in analytical models to refine the predictions of pipe deflections/rotation that would be used for the bending tests.

Consistent with previous testing, one million cycles of pipe deflections simulated truck loading on the joint over a 50-year service life. As described previously, 20,000 cycles of vehicular loading is equivalent to one year of service. During the test the load cycles were applied at a rate of approximately one cycle per second. At this rate the test duration for each 50-year service period was approximately 12 days.

The testing regimen for the 6 in. (150 mm) specimens is given in Table 4.2. The testing consisted of vehicular loading followed by thermal cycles, representing 50 years of service. Both sets of aging tests were then repeated, representing an additional 50 year of service, followed by pressure test verification. The data from the testing will be presented in this order. Before presenting the test results, it is useful to place the applied deformations into perspective. The deformations applied to the pipe sections to simulate vehicular traffic and undermining/backfill events are relatively small. Figure 4.4 shows the typical range of applied deflections and resulting rotations for the vehicular loading tests. For vehicular traffic loading the pipe deflections are on the order of 0.04 to 0.06 in. (1.0 to 1.5 mm). For the excavation/backfill loadings, where there is less soil support beneath the pipe, the deformations range from approximately 0.25 to 0.35 in. (6.4 to 8.9 mm). The angular rotations at the joint are proportional to the deflections at the pipe center (joint) for these tests and range from 0.003 to 0.005 radians (0.2 to 0.3 degrees) for the vehicular loadings and 0.006 to 0.009 radians (0.35 to 0.50 degrees) for the undermining/backfill events.

Table 4.2. Testing Conditions for 6-in. (150-mm)-Diameter Cast Iron Pipe Specimens

| | Years | Pressure[b] |
|---|---|---|
| Vehicle loadings/bending cycles (1 M cycles) | Up to 50 | 15 in. water |
| Undermining excavation event (1) | 1 | 15 in. water |
| Additional vehicle loadings/bending cycles (100 K cycles) | +5 | 15 in. water |
| Thermal expansion/contraction cycles (50 cycles)[a] | 1 - 50 | 15 in. water |
| Vehicle loadings/bending cycles (another 1 M cycles) | 50 - 100 | 15 in. water |
| Excavation event (1) | 1 | 15 in. water |
| Additional vehicle loadings/bending cycles (another 100 K cycles) | +5 | 15 in. water |
| Thermal expansion/contraction cycles (another 50 cycles) | 50 - 100 | 15 in. water |
| Post-Testing Verification Pressure[b] | 1 | 90 psig (then + 60 psig) |

1 psig = 6.89 kPa.

a – For Specimen 6-1 the cement/jute caulking was removed to provide a weak joint condition after the first 50 years of vehicle loading. The stiff caulking for Specimen 6-2 was removed prior to all mechanical aging tests.

b – Nitrogen gas used for internal pressure during mechanical aging tests, water used for post-testing verification. Only Specimen 6-2 was high-pressure tested after mechanical aging.

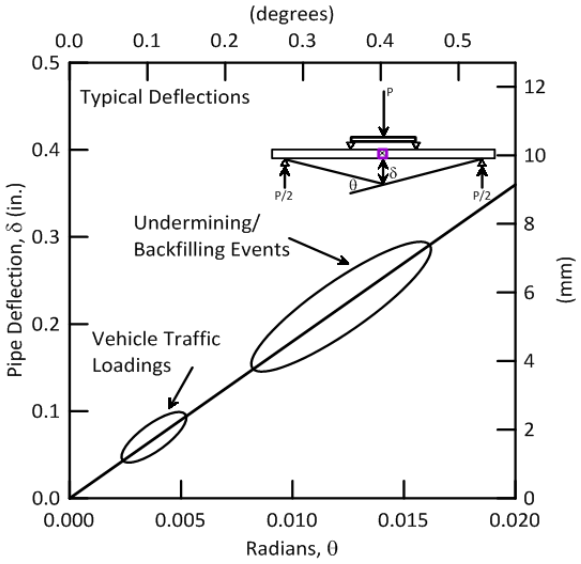


Figure 4.4. Typical Range of Deflections for Vehicular Loading Effects

### 4.3.1 Specimen 6-1: First 50 Years of Vehicular Loadings

The test results for cycles 1, 10, 100, and 1,000 for Specimen 6-1 are shown in Figure 4.5(a). For these low cycles, they are not converted to years (divide cycles by 20,000) because the converted values would not show the intended information. The data for the first 100 cycles are nearly identical. An important observation for the data in Figure 4.5 is that the rotational stiffness of the joint is very high, on the order of $k_\theta$ = 166,760 in.-kip/rad (18,500 m-kN/rad). This stiffness is typical for a 6 in. (150 mm) cast iron joint with cement/jute caulking. Recall that the joint, at this point, had not yet had the cement caulking removed. This was the "as-received" condition of the pipe section. Figure 4.5(b) shows the testing measurements for years 0.5 – 50 (cycles 10,000 – 1,000,000). There is not a significant change in the joint response during the 50-year-equivalent testing.

### 4.3.2 Specimen 6-1: First Undermining/Backfill Event

The undermining/backfill event represents a more severe loading condition, as described in Section 2. Here, the backfill is not as stiff as before, and provides less pipe support. The test results for Specimen 6-1 in response to the vehicle loading for the undermining/backfilling event are given in Figure 4.6. Note that there is a scale change in Figure 4.6 as compared to the data shown in Figure 4.5. The response to the undermining/backfilling event is roughly twice as large as the prior cyclic loading. Figure 4.7 gives the results for vehicular loading for an additional 5 years, equivalent to 100,000 cycles, beyond the undermining/backfilling event. Also note that the rotational stiffness of Specimen 6-1 is nearly constant during the first 50 years of vehicular loading testing.

### 4.3.3 Specimen 6-1: First 50 Years of Thermal Loadings

Section 3 described the approach to modeling the CI pipe subject to seasonal temperature variations. Retrieving a pipe section having had a round crack, then lined with CIPL is not feasible under any rational conditions. So, the joint is intended to simulate a round crack with very small rotational stiffness. Specimen 6-1 was a stiff, cement mortar joint. When the pipe section was first moved to the thermal loading test frame, the forces necessary to impose a joint opening were large. It was a risk that the epoxy resin in the joint opening could suddenly fail, or the interface bond between the liner and the pipe slip rapidly, causing the CIPL to abruptly rupture. This condition would not have been representative of the magnitude of loading or rate

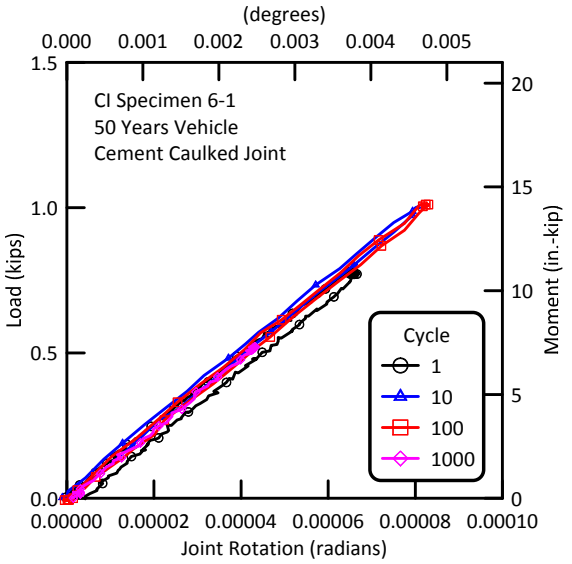


a) Specimen 6-1, Cycles 1 – 1,000

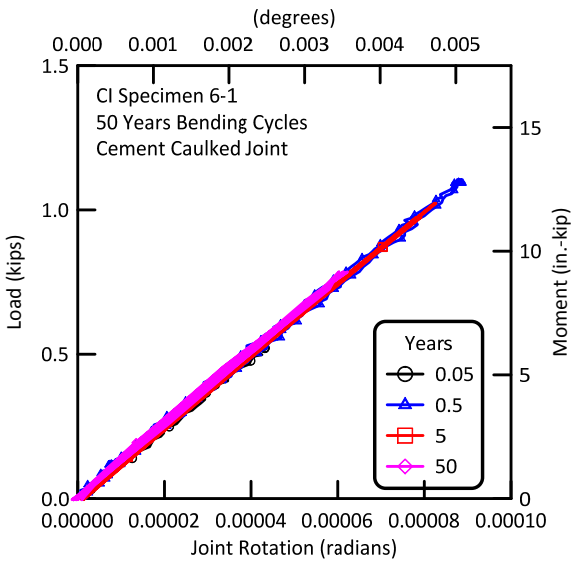


b) Specimen 6-1, Years 0.5 – 50,

Figure 4.5. First 50 Years Vehicle Loading Results for Specimen 6-1

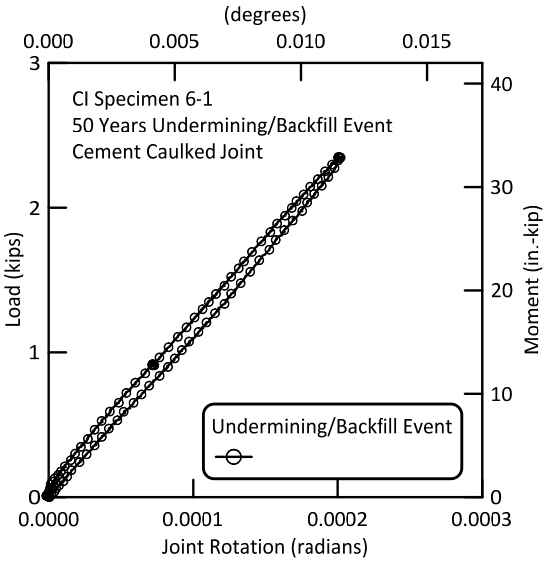


Figure 4.6. First Vehicle Loading for Undermining/Backfill Event for Specimen 6-1

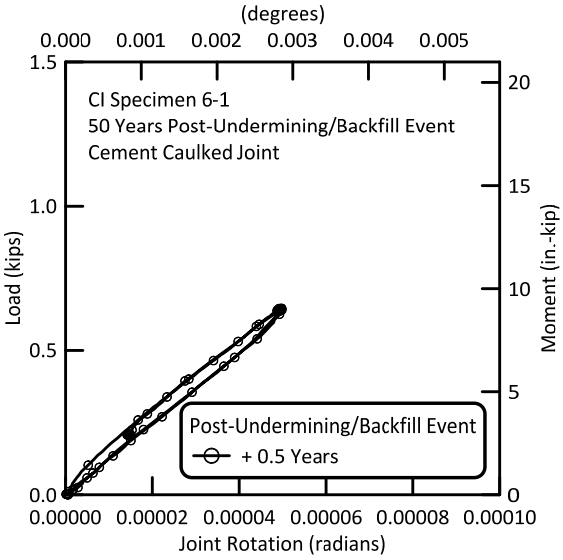


Figure 4.7. First Post-Undermining + 0.5 Years Vehicle Loading for Undermining/Backfill Event for Specimen 6-1

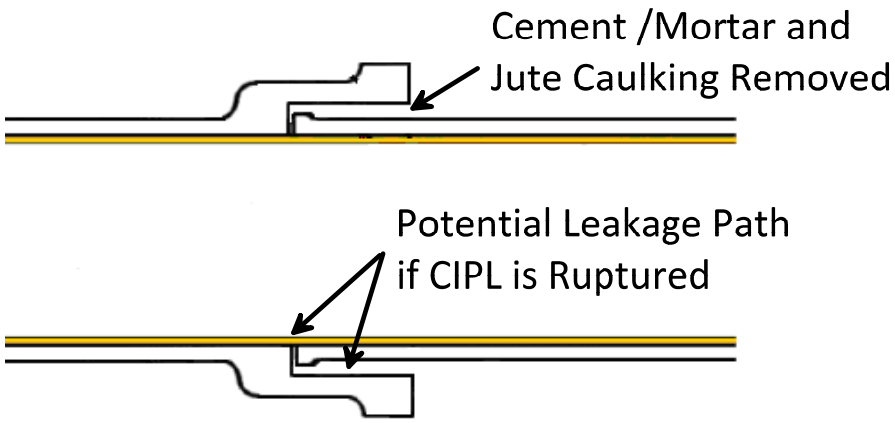


Figure 4.8. Schematic of Weakened Joint for 6 in. (150 mm) Pipe Specimens

of displacement imposed across a round crack with CIPL liner under seasonal temperature variations.

Thus, the cement/mortar joint material was removed to weaken the joint. As was shown in Figure 4.2, this PSE&G joint was first packed with a round of jute, followed by cement, then another round of jute, followed by additional cement. These multiple layers were removed, resulting in a much softer joint, which was more consistent in behavior with that of a weak joint or CI pipe round crack. This is shown schematically in Figure 4.8. This process was performed on both 6-in. (150-mm)-diameter specimens. After this procedure the joints are referred in this report as "weakened joints." This had the additional testing benefit of providing a potential leakage path for internal pressure drop (indicating leakage) if the CIPL ruptured. The intact cement/mortar in the test joint may have prevented this, and leakage may not have been detected if the CIPL had ruptured.

Figure 4.9 shows photographs of Specimen 6-1 in the test frame used to apply thermal cycles. The joint openings were applied by the actuator. Forces were measured using load cells, and joint openings were measured using DCDTs, as show in the Figure 4.9.

The initial thermal cycle for Specimen 6-1 is shown in Figure 4.10(a). At this point, the cement/mortar had not yet been removed. A relatively large force of roughly 6 kips (26.7 kN) was required to open the joint (tension positive). The "jagged" opening forces upon initial

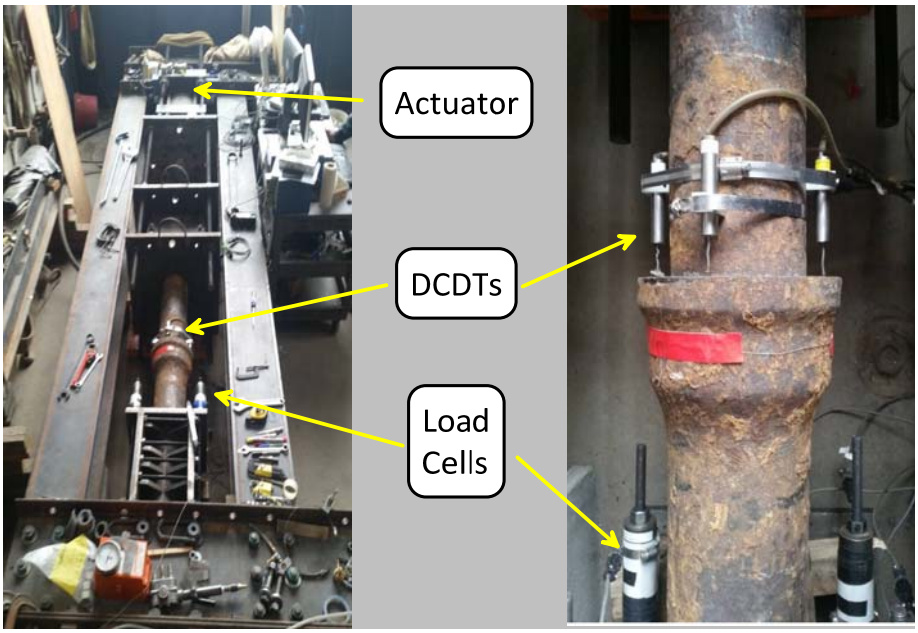


a) Experimental Setup Overview b) Top View of the Joint

Figure 4.9. Specimen 6-1 in Test Frame for Thermal Loadings

opening are a function of the inconsistent and high shear forces between the cement/mortar caulking and the CI. The unloading relationship is much smoother. During the unloading phase, the joint was pushed very close to the initial position prior to loading. Compressive force was required to complete the cycle for each subsequent year. There is a tendency for the closing force to migrate to larger values of compression during the cyclic loading. This is attributable to the migration of remnant epoxy and scaling debris into the opening between the bell and spigot during successive opening/closing cycles. Figures 4.10(b) and 4.10(c) show the joint openings vs. force for years 2 through 50. After the first and second years (cycles) the forces required to open and close the joint remain about the same. Clearly, beyond the initial cycle, the joint strength is considerably weakened, beyond that of simply removing the cement/mortar. There is debonding of the CIPL from the pipe caused by these laboratory equivalent thermal loadings, as described below.

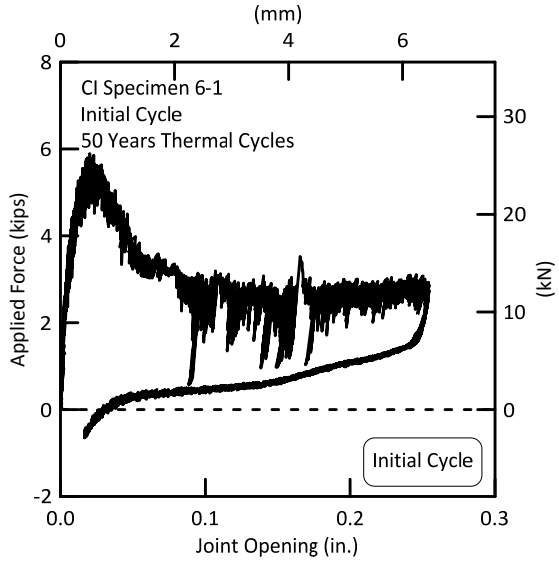


a) Initial Thermal Cycle

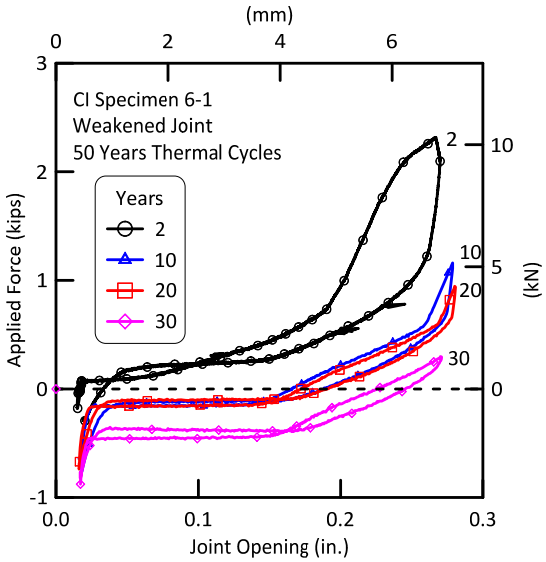


b) Years 2, 10, 20, and 30

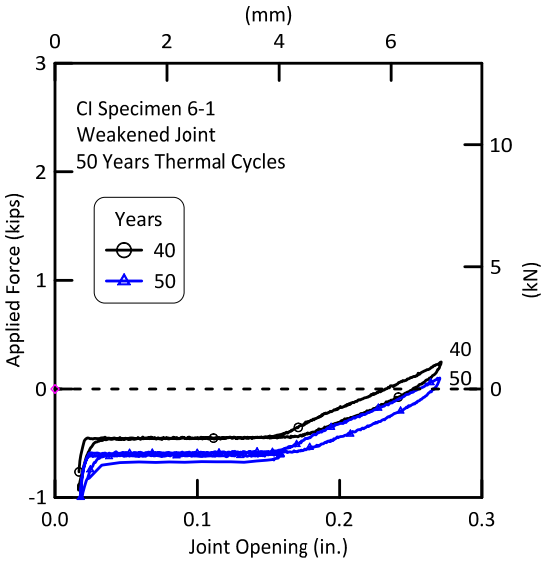


c) Years 40 and 50

Figure 4.10. Thermal Cycle Joint Openings the First 50 Years, Specimen 6-1

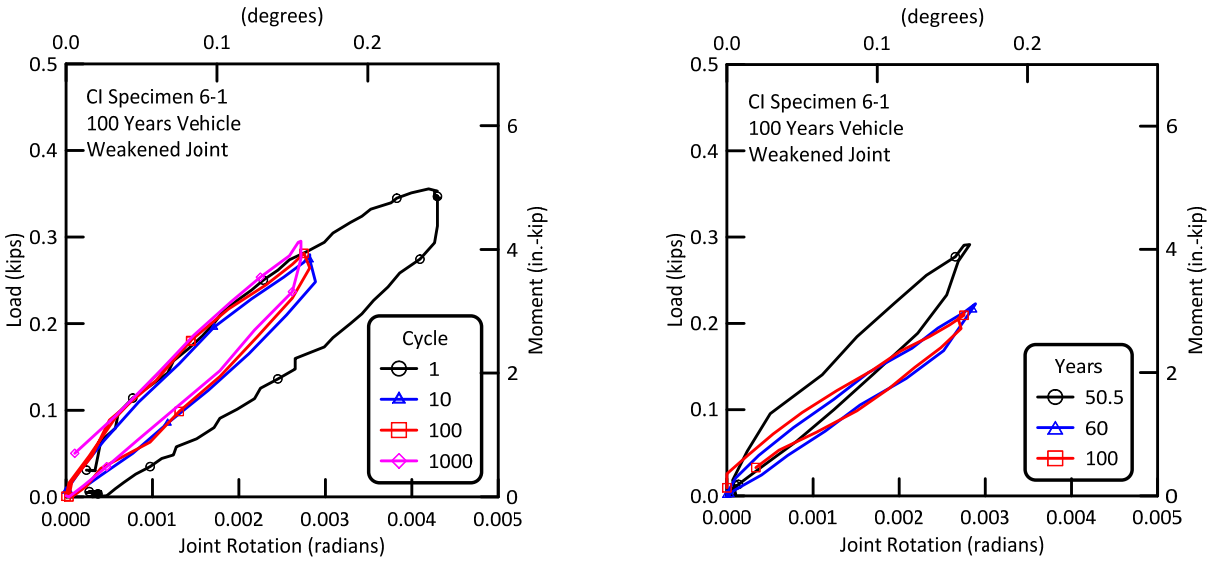


a) Specimen 6-1, Cycles 1 – 1,000

b) Specimen 6-1, Years 50.5 – 50,

Figure 4.11. Second 50 Years (100 Years Total) Vehicle Loading Results for Specimen 6-1

### 4.3.4 Specimen 6-1: Second Fifty Years of Vehicular Loadings

After the first 50 years of thermal loading, the specimen was returned to the flexural testing load frame, and subjected to an additional 50 years of vehicular traffic. Figure 4.11(a) shows the first few cycles in the second sequence of vehicular loadings, and Figure 4.11(b) shows the force-pipe deflection measurement for equivalent years 50.5 through 100 years. The rotational stiffness for the second 50 years on Specimen 6-1 is now approximately $k_\theta$ = 1,360 kip-in./rad (150 m-kN/rad). This is much lower than that measured on Specimen 6-1 with the intact cement/mortar joint, without prior thermal cycles. The initial rotational stiffness was roughly $k_\theta$ = 166,760 kip-in./rad (18,500 m-kN/rad). This is another indication that the joint was significantly weakened by both the removal of the cement/mortar and the first cycle of thermal loading.

### 4.3.5 Specimen 6-1: Second Undermining/Backfill Event

The response of Specimen 6-1 to the vehicle loading for the second undermining/backfilling episode, which occurs in the 100 year testing regimen, are given in Figure 4.12. Again note that there is a scale change in Figure 4.12 as compared to the data shown in Figure 4.11. The response to the undermining/backfilling event is again roughly twice as large as the prior cyclic loading. Figure 4.13 gives the results for vehicular loading for an additional 5 years beyond the undermining/backfilling event. Also note that the rotational stiffness of Specimen 6-1 is nearly constant during the first 50 years of vehicular loading testing.

### 4.3.6 Specimen 6-1: Second 50 Years of Thermal Loadings

The data for the second 50 years of thermal aging for Specimen 6-1 are shown in Figures 4.14(a) and 4.14(b). The cyclic load-unload curves for the second 50 years of thermal aging are the same shape for the additional 50 cycles. This indicates no major changes in cyclic degradation beyond that which occurred in the very first few cycles of thermal aging.

### 4.3.7 Specimen 6-1: Post-Test Inspection

Figure 4.15 shows photographs of the joint following all mechanical aging tests. The "before" photo is Specimen 6-1 before any mechanical aging tests. The "after" photo shows that there was substantial debonding of the CIPL from the pipe in the area of the joint. In all cases debonding at the separation between bell and spigot was confined to a small distance either side of the separation, less than one pipe diameter in total width. This debonding is a highly desirable characteristic of a well-installed CIPL liner system. The pipe had been cleaned sufficiently to allow robust adhesion without excessive bonding of the epoxy to CI surfaces. By allowing debonding, the liner could accommodate axial deformations by allowing extension. Without this ability to strain over a debonded length, the liner can be highly strained and rupture prematurely. Figure 4.16 again shows this local wrinkling of the liner inside a "cut-apart" joint. The bonded and de-bonded sections are clearly visible. This photo also shows the area between the spigot and bell where the cement/mortar caulk was removed, weakening the joint and providing a pathway for potential leakage.

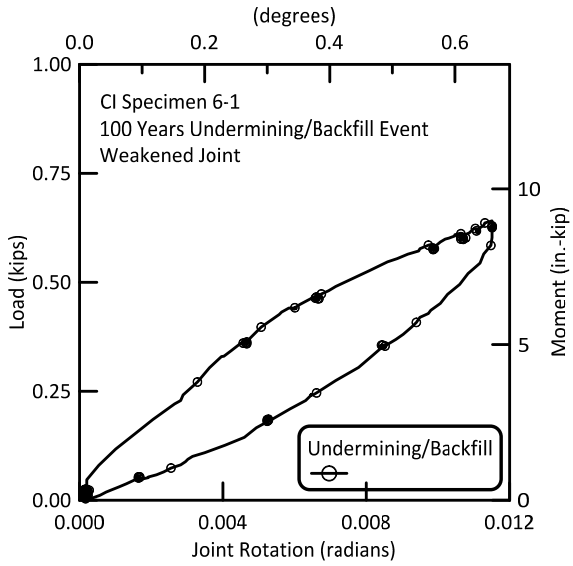


Figure 4.12. Second Vehicle Loading for Undermining/Backfill Event for Specimen 6-1

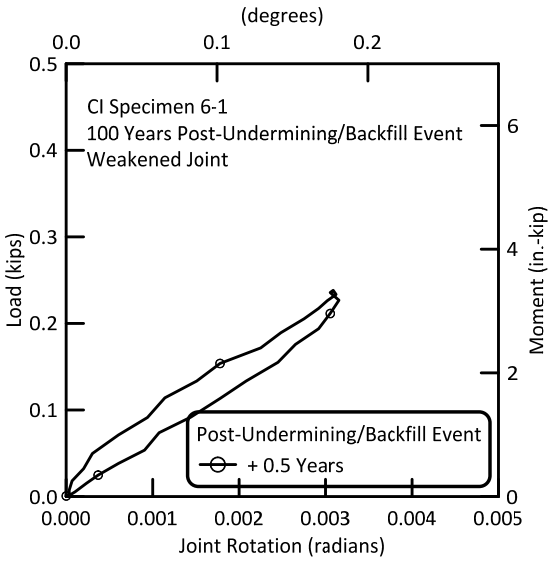


Figure 4.13. Second Post-Undermining + 0.5 Years Vehicle Loading for Undermining/Backfill Event for Specimen 6-1

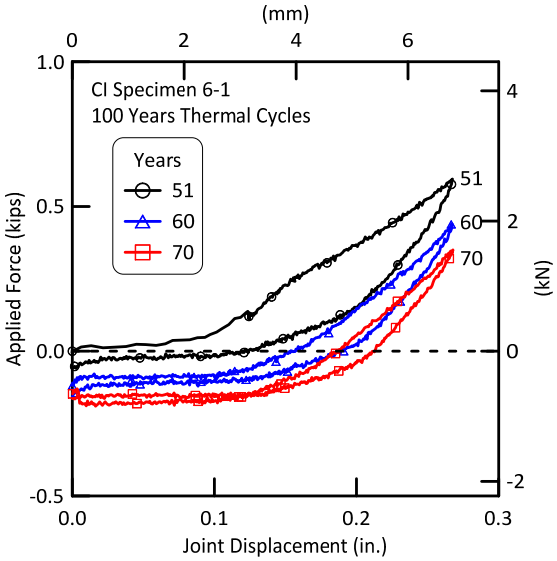


a) Years 51, 60, and 70

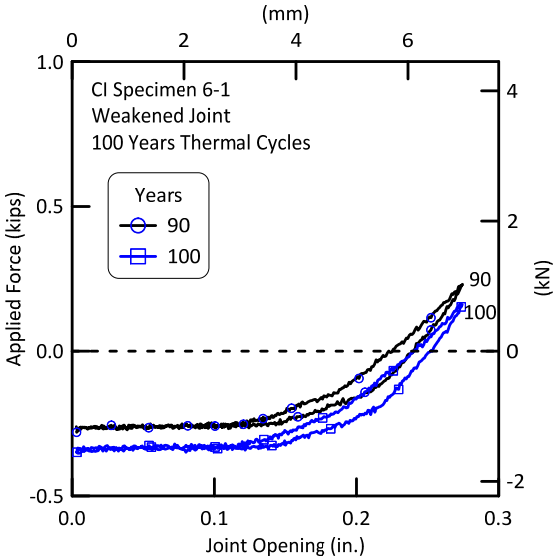


b) Years 90 and 100

Figure 4.14. Thermal Cycle Joint Openings the Second 50 Years (100 Years Total) for Specimen 6-1

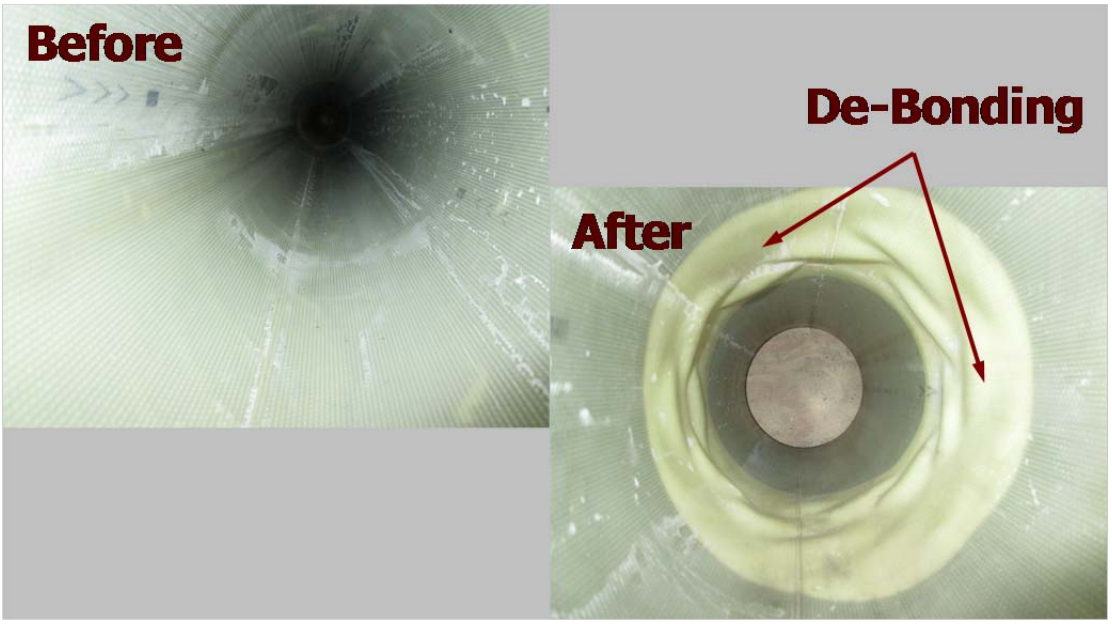


Figure 4.15. Internal Photos of Specimen 6-1 Before and After Mechanical Aging

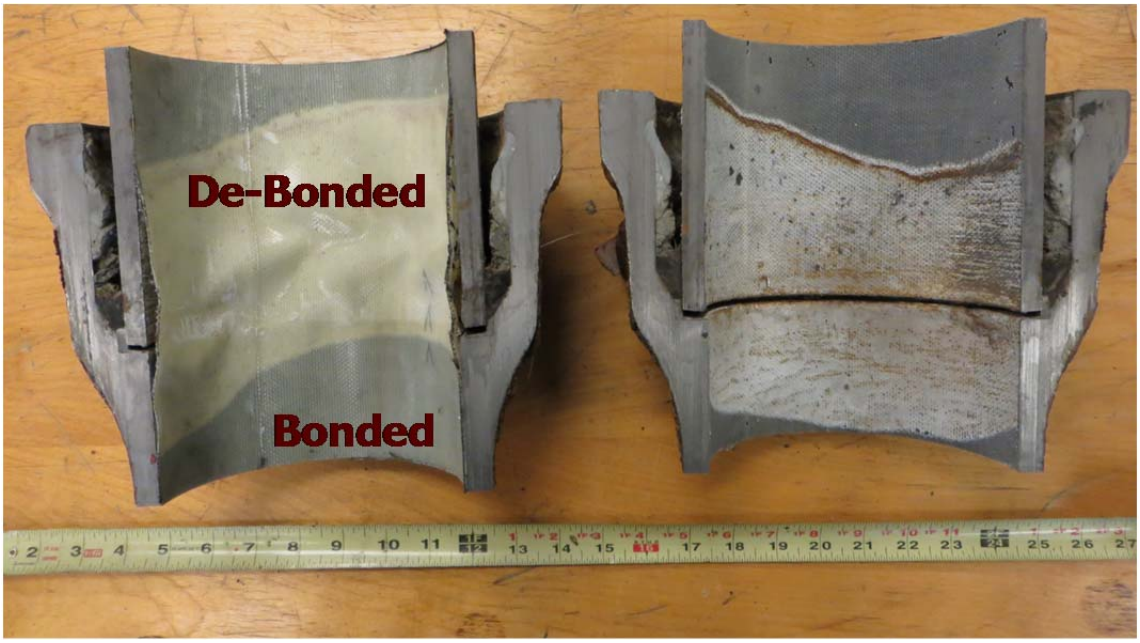


Figure 4.16. Photo of Cut-Apart Joint 6-1

Specimen 6-1 did not leak throughout all of the mechanical aging tests. Further, the interior of the pipe section showed the highly desirable effect of local debonding of the liner in the vicinity of the joint.

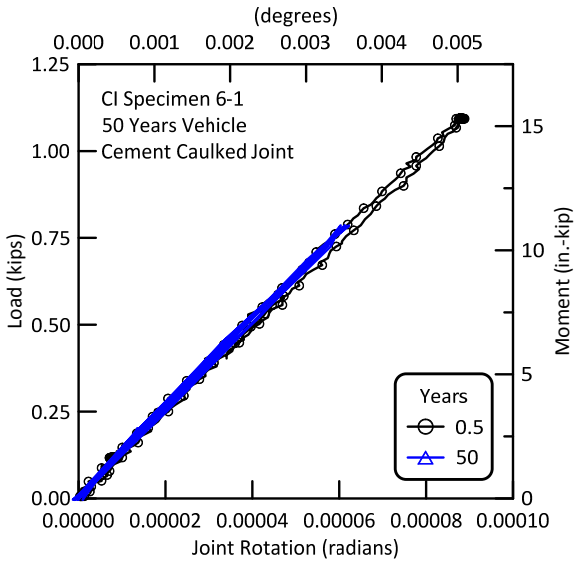


b) Specimen 6-1, Years 0.5 and 50

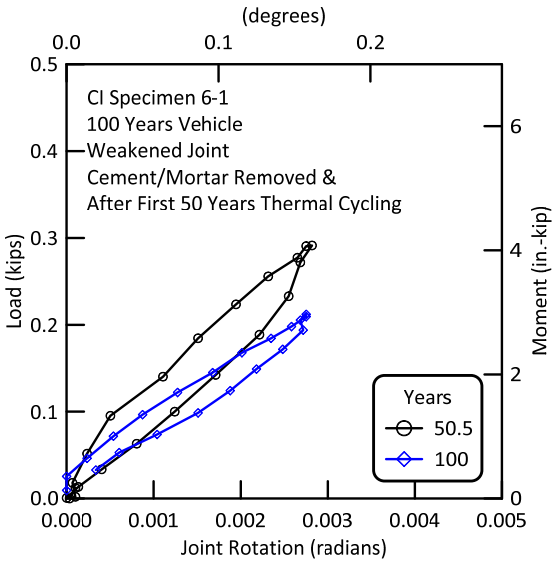


b) Specimen 6-1, Years 50.5 and 100

Figure 4.17. First 50 Years and Second 50 Years of Vehicle Loadings for Specimen 6-1

### 4.3.8 Specimen 6-1: Additional Comparisons of Mechanical Aging

#### 4.3.8.1 Specimen 6-1: 0 to 100 Years of Vehicular Traffic

Figures 4.17(a) and (b) compare the response of Specimen 6-1 to vehicular loadings for the first and second 50 years of mechanical aging. Note the significant differences in the scales between the two figures. In Figure 4.17(a), the cement/mortar packing in the joint was intact. The rotational stiffness was very high, consistent with this type of joint. In Figure 4.17(b) the cement/mortar packing had been removed **and** the specimen had been subjected to 50 years of thermal aging. This resulted in a rotational stiffness roughly two orders of magnitude lower than that in Figure 4.17(a), and consistent with the very low stiffness associated with a round crack, which was intended in these additional mechanical aging tests.

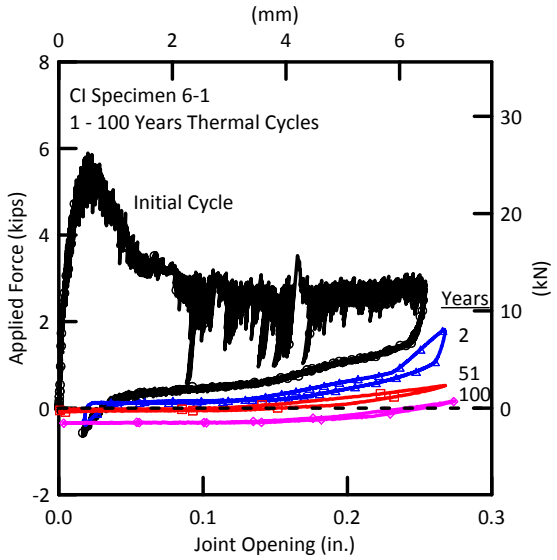


Figure 4.18. Years One through 100 of Thermal Cycling for Specimen 6-1

#### 4.3.8.2 Specimen 6-1: Years One through 100 of Thermal Cycling

Joint weakening by thermal cycles is further demonstrated in Figure 4.18. Here, the initial thermal cycle pull force is shown for Specimen 6-1, along with the softened joint pull/push results for years 2 through 100.

### 4.4 Mechanical Aging Test Results for Specimen 6-2

Specimen 6-2 was taken from the same PSE&G location in Elmwood Park, NJ. Thus, the sampling methodology is the same as described previously. The specimen underwent the same loading sequence as Specimen 6-1. The main difference between Specimen 6-1 and 6-2 is that the cement/mortar caulking was removed in Specimen 6-2 prior to any mechanical aging. This allowed the joint to behave as a weakened joint from the start of the vehicular loading. Specimen 6-2 also exhibited additional weakening due to the first thermal cycle.

#### 4.4.1 Specimen 6-2: First 50 Years of Vehicular Loadings

The test results for cycles 1, 10, 100, and 1,000 for Specimen 6-2 are shown in Figure 19(a). These cycles are not converted to years (divide cycles by 20,000) because the converted values would not show the intended information. The data for the first 1,000 cycles are nearly identical. An observation from the data in Figure 4.19 is that the rotational stiffness of the joint is about

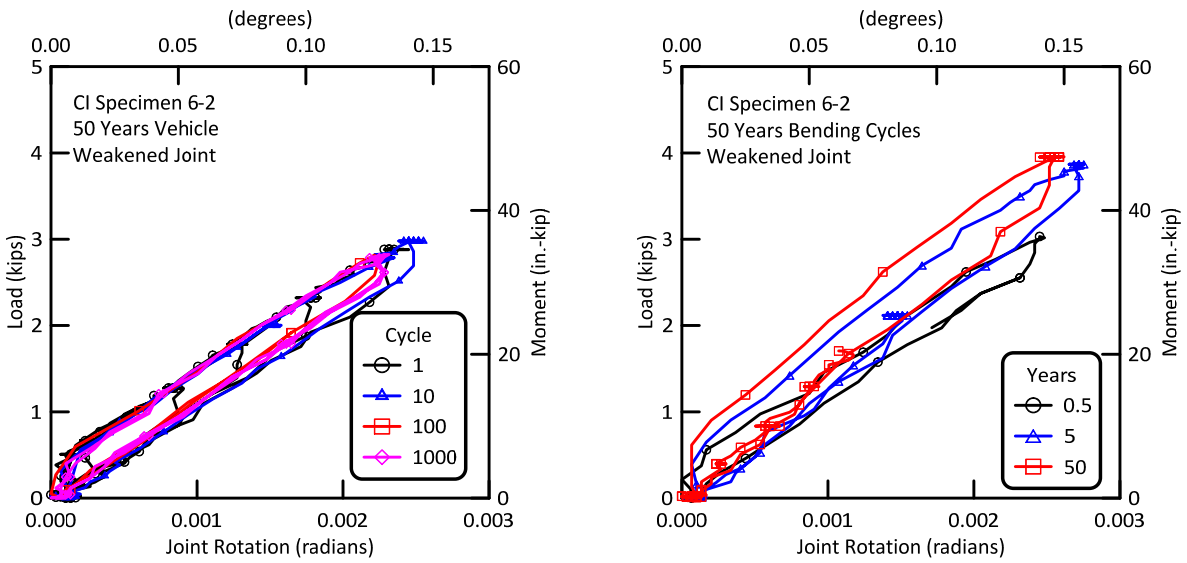


a) Specimen 6-2, Cycles 1 – 1,000 b) Specimen 6-2, Years 0.05 – 50

Figure 4.19. First 50 Years Vehicle Loading Results for Specimen 6-2

$k_\theta$ = 13,500 in.-kip/rad (1,530 m-kN/rad). This stiffness is substantially lower than the initial stiffness of Specimen 6-1 with the cement/mortar joint, which was $k_\theta$ =166,760 in.-kip/rad (18,850 m-kN/rad), typical for a 6 in. (150 mm) cast iron joint with cement/jute caulking. Figure 4.20(b) shows the testing measurements for years 0.5 – 50 (cycles 10,000 – 1,000,000). There is not significant change in Specimen 6-2 joint response during the first 50-year-equivalent testing.

### 4.4.2 Specimen 6-2: First Undermining/Backfill Event

The test results for Specimen 6-2 in response to the vehicle loading for the undermining/backfilling event are given in Figure 4.20. Note that there again is a scale change in Figure 4.20 as compared to the data shown in Figure 4.19. The response to undermining/backfilling is roughly twice as large as the prior cyclic loading (similar to Specimen 6-1). Figure 4.21 gives the results for vehicular loading for an additional 5 years beyond the undermining/backfilling event. Also note that the rotational stiffness of Specimen 6-2 is nearly constant during the first 50 years of vehicular loading testing.

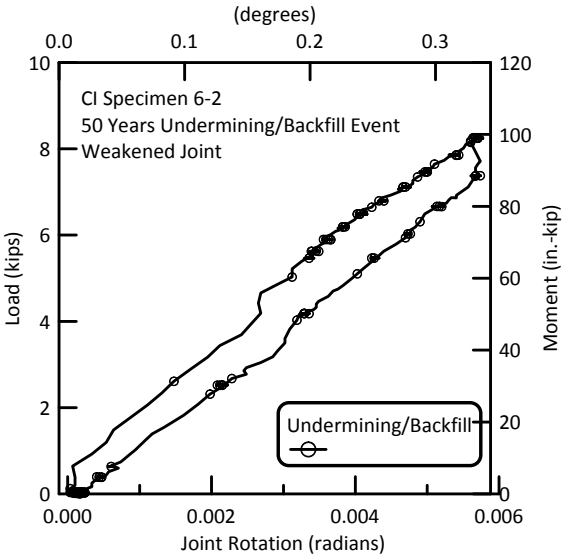


Figure 4.20. First Vehicle Loading for Undermining/Backfill Event for Specimen 6-2

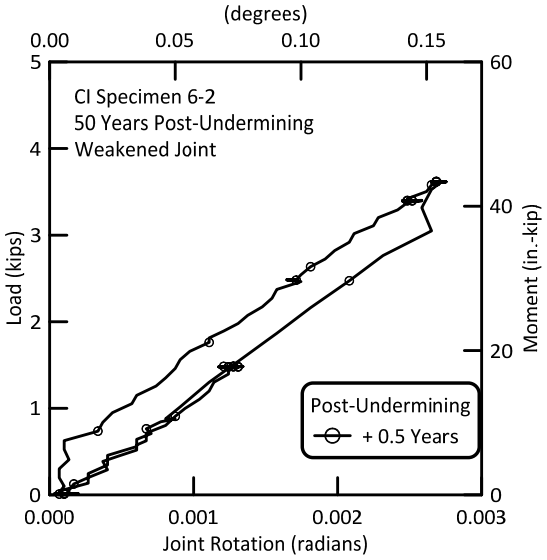


Figure 4.21. First Post-Undermining + 0.5 Years Vehicle Loading for Undermining/Backfill Event for Specimen 6-2

### 4.4.3 Specimen 6-2: First 50 Years of Thermal Loadings

Prior to the first thermal loading Specimen 6-2 already has a weakened joint due to the removal of the cement/mortar caulking. As previously described, this had the additional testing benefit of providing a potential leakage path for internal pressure drop (indicating leakage) if the CIPL ruptured.

The initial thermal cycle for Specimen 6-2 is shown in Figure 4.22(a). During the unloading phase, the joint was pushed close to the initial spigot position before loading, generating compressive force. Figures 4.22(b) and 4.22(c) show the joint openings vs. force for 2 through 50 years. As was observed in Specimen 6-1, the joint strength is weakened considerably after the initial expansion/compression cycle. There again is debonding of the CIPL from the pipe caused by these laboratory equivalent thermal loadings.

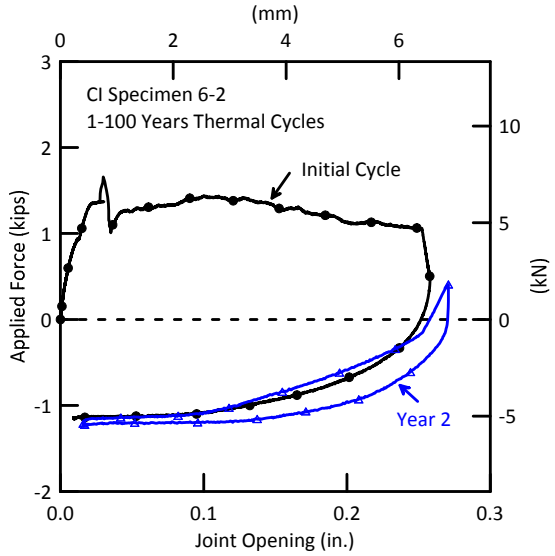


a) Initial Thermal Cycle and Year 2

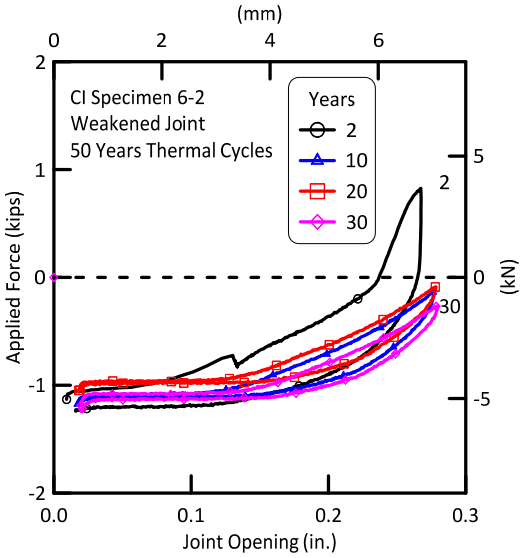


b) Years 2, 10, 20, and 30

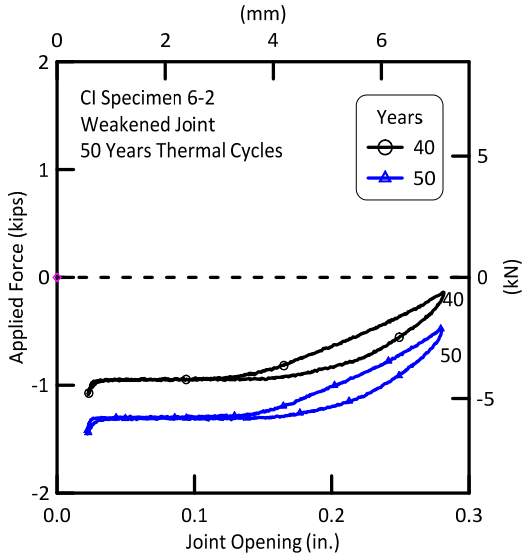


c) Years 40 and 50

Figure 4.22. Thermal Cycle Joint Openings the First 50 Years for Specimen 6-2

### 4.4.4 Specimen 6-2: Second 50 Years of Vehicular Loadings

After the first 50 years of thermal loading the specimen was returned to the flexural testing load frame and subjected to an additional 50 years of vehicular traffic. Figure 4.23(a) shows the first few cycles in the second sequence of Specimen 6-2 vehicular loadings, and Figure 4.23(b) shows the force-pipe deflection measurement for equivalent years 50.5 through 100 years. The rotational stiffness for years 50-100 on Specimen 6-2 is approximately $k_\theta$ = 850 kip-in./rad (100 m-kN/rad), lower than the rotational stiffness of roughly $k_\theta$ = 1,360 kip-in./rad (150 m-kN/rad) without prior thermal cycles. This again indicates that the joint was weakened by both the removal of the cement/mortar and the first cycle of thermal loading. Figure 4.23 also indicates no effect of cyclic degradation in Specimen 6-2.

### 4.4.5 Specimen 6-2: Second Undermining/Backfill Event

The test results for the second undermining/backfill event for Specimen 6-2, which occurs in the 100 year testing regimen, are given in Figure 4.24. Again note that there is a scale change in Figure 4.24 as compared to the data shown in Figure 4.23. The response to the undermining/backfilling event is again roughly twice as large as the prior cyclic loading. Figure 4.25 gives the results for vehicular loading for an additional 5 years beyond the undermining/backfilling event. Also note that the rotational stiffness of Specimen 6-2 is nearly constant during the first 50 years of vehicular loading testing.

### 4.4.6 Specimen 6-2: Second 50 Years of Thermal Loadings

The data for the second 50 years of thermal aging for Specimen 6-2 are shown in Figures 4.26(a) and 4.26(b). The cyclic load-unload curves for the second 50 years of thermal aging are the same shape for the additional 50 cycles. This indicates no major changes in cyclic degradation beyond that which occurred in the first few cycles of thermal aging.

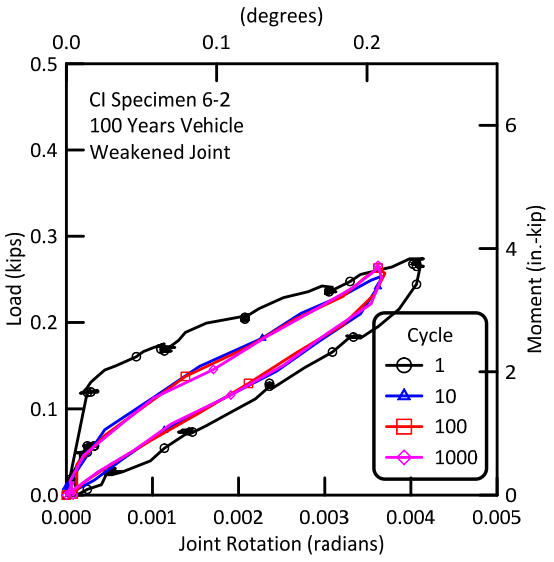


a) Specimen 6-2, Cycles 1 – 1,000

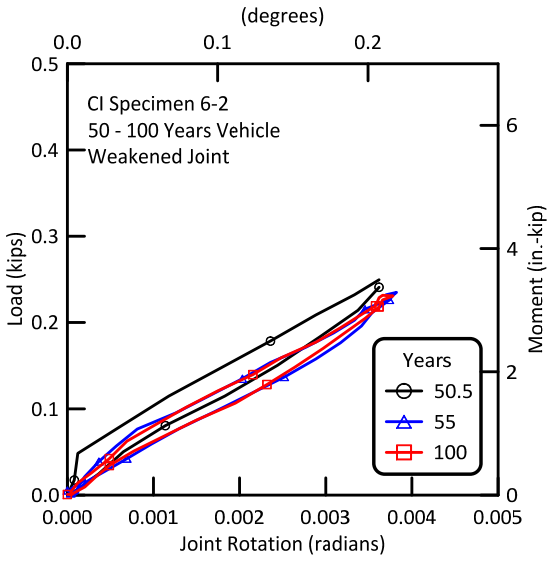


b) Specimen 6-2, Years 50.5 – 100

Figure 4.23. Second 50 Years (100 Years Total) Vehicle Loading Results for Specimen 6-2

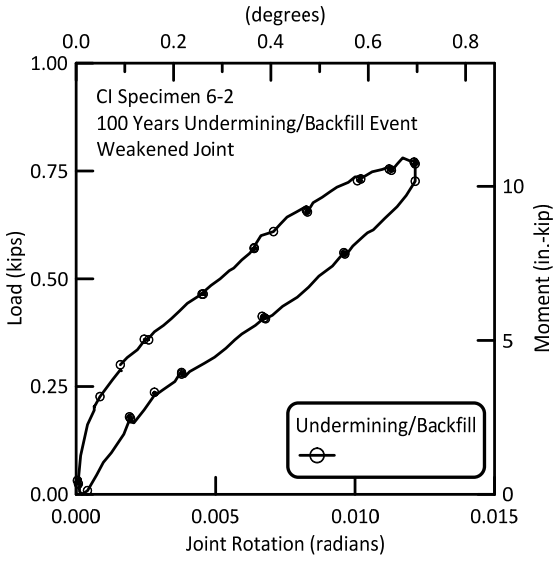


Figure 4.24. Second Vehicle Loading for Undermining/Backfill Event for Specimen 6-2

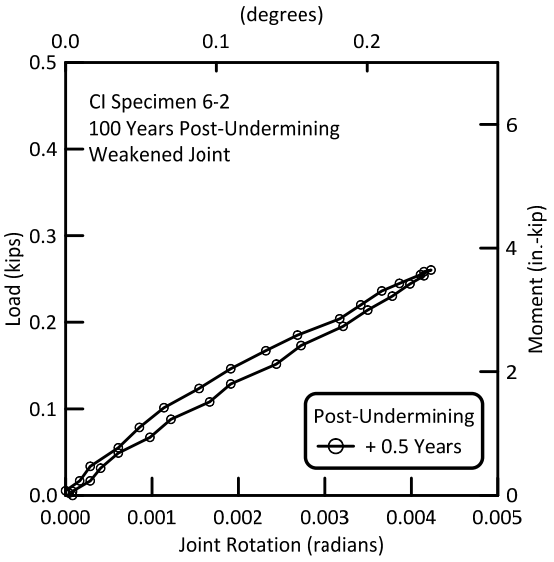


Figure 4.25. Second Post-Undermining + 0.5 Years Vehicle Loading for Undermining/Backfill Event for Specimen 6-2

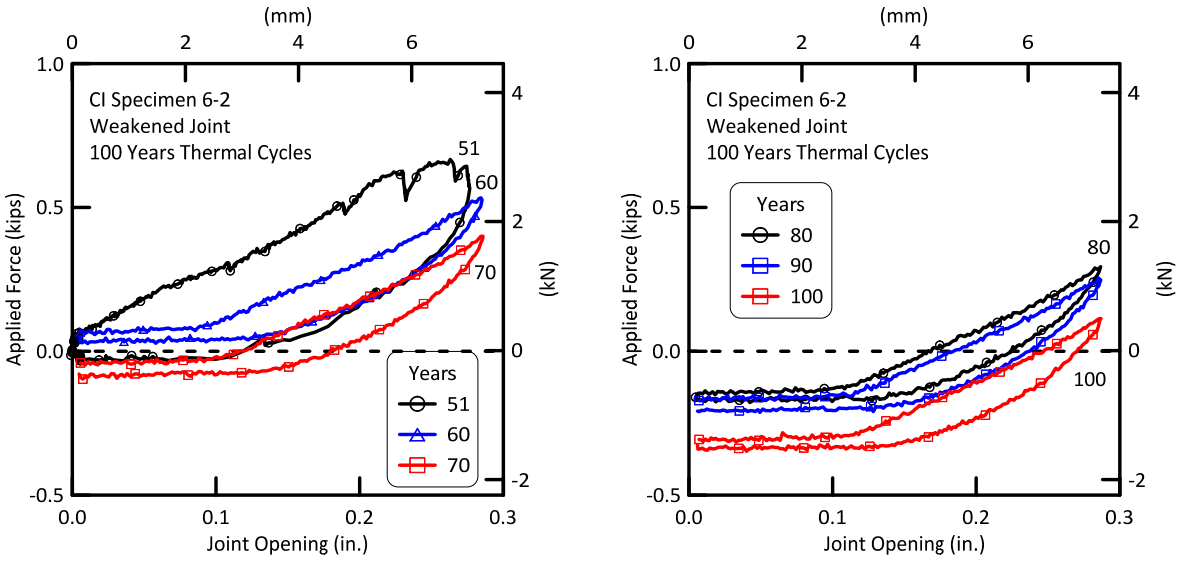


a) Years 51, 60, and 70 b) Years 80 - 100

Figure 4.26. Thermal Cycle Joint Openings the Second 50 Years (100 Years Total) for Specimen 6-2

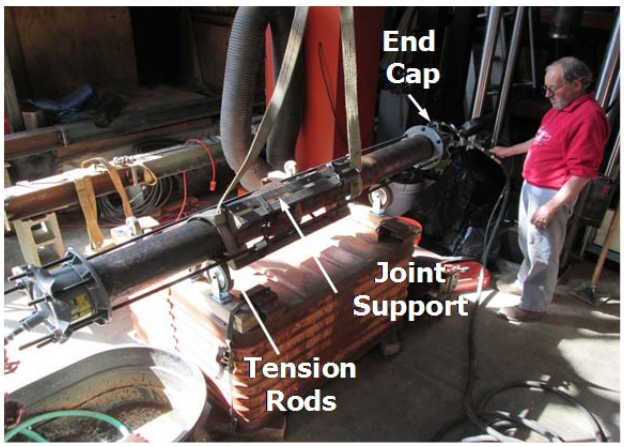


Figure 4.27. Photo of Pressure Test on Specimen 6-2

### 4.4.7 Specimen 6-2: Post-Test Pressurization

Following the entire mechanical aging sequence on Specimen 6-2, a pressure verification test was conducted to assure that the liner had not ruptured during the test. Figure 4.27 is a photo of the pressure test on Specimen 6-2. The pipe was pressure tested to 90 psig (620 kPa) in roughly

10 psig (7 kPa) increments. There was no leakage. Then the pressure was increased to 150 psig (1,034 kPa). Pipe Specimen 6-2 did not leak after all mechanical aging tests and did not leak after a pressure verification test to 150 psig (1,034 kPa). Visual observations of the liner in the pipe indicated no liner damage.

### 4.4.8 Specimen 6-2: Additional Comparisons of Mechanical Aging

#### 4.4.8.1 Specimen 6-2: 0 to 100 Years of Vehicular Traffic

Figures 4.28(a) and 4.28(b) compare the response of Specimen 6-2 to vehicular loadings for the first 50 years of mechanical aging and the second fifty years of mechanical aging. Note that there are different vertical scales in the figures. In Figure 4.28(a) the cement/mortar packing in the joint was removed when the specimen had no prior thermal cycles. In Figure 4.28(b) the cement/mortar packing had been removed **and** the specimen had been subjected to 50 years of thermal aging.

#### 4.4.8.2 Specimen 6-2: Years One through 100 of Thermal Cycling

The joint weakening by thermal cycles is further demonstrated in Figure 4.29. Here, the initial thermal cycle of force vs. displacement for Specimen 6-2 is compared with the softened joint pull/push results for the second year through year 100. Note that the specimen was removed from the load frame after the first 50 years or cycling, placed in a separate loading system for the second 50 years of vehicular loading, and re-positioned in the thermal testing frame for years 51 through 100. The load-displacement relationships for the second 50 years of thermal cycling reflect a small change in position of the test specimen.

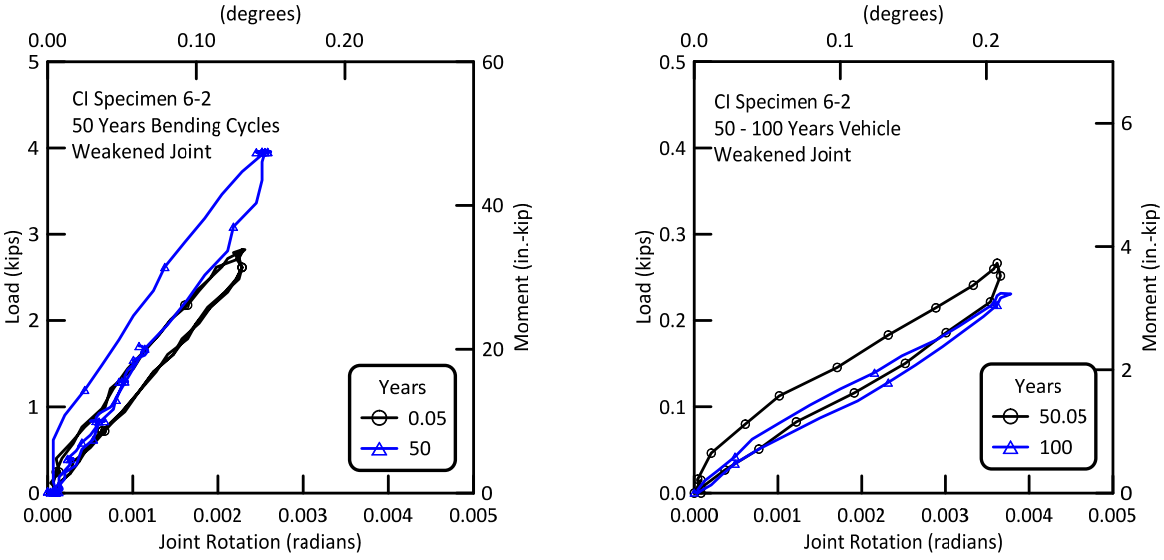


a) Specimen 6-2, Years 0.5 and 50

b) Specimen 6-2, Years 50.5 and 100

Figure 4.28. First 50 Years and Second 50 Years Vehicle Loadings for Specimen 6-2

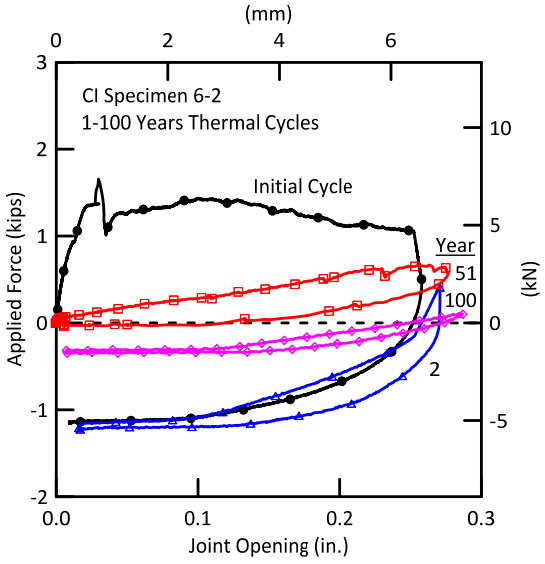


Figure 4.29. Years One through 100 of Thermal Cycling for Specimen 6-2

#### 4.4.8.3 Specimen 6-2: Rotational Stiffness Changes and Comparison to Specimen 6-1

During the vehicular loading sequences, the moment-rotation relationships for the 6-in. (150-mm)-diameter CI joints can be determined based on the force-displacement test results given above. The applied moments can be calculated knowing the force and the geometry of the flexure test setup. Figure 4.30 shows these rotational stiffnesses for several phases of the testing vs. number of loading cycles. In Figure 4.30(a) the upper solid line labeled "6-1 Pre-Thermal Cycles" shows $k_\theta$ for Specimen 6-1 when the joint was packed with the cement/mortar and jute. The typical stiffness is $k_\theta$ = 166,760 in.-kip/rad (18,850 m-kN/rad) over the range of cycles representing 50 years. The dashed line labeled "6-1 Post-Thermal Cycles" shows that the rotational stiffness of Specimen 6-1 has dropped to about 1,360 in.-kip/rad (1,530 m-kN/rad) due to the combined effect of the cement/mortar removal **and** the thermal cycles. Figure 4.30(b) shows the rotational stiffness changes for Specimen 6-2. Here, the "6-2 Pre-Thermal Cycles" data are for testing the joint that had the cement/mortar removed but had not yet experienced and thermal cycles. The drop in $k_\theta$ for Specimen 6-2 to the "6-2 Post-Thermal Cycles" represents the change due only to thermal cycling. Figure 4.30(c), showing "6-1 Pre-Thermal Cycles" and "6-2 Pre-Thermal Cycles", demonstrates the effect on rotational stiffness from removing only the cement/mortar/jute caulking. The very low stiffnesses of both Specimen 6-1 and 6-2 after thermal cycling again indicate that the testing was representative of a weakened joint, and consistent with the concept of using the very weak joint as a stand-in for a round crack.

The rotational stiffnesses of the other 6-in (150-mm)-diameter CI joints are listed in Table 4.3. In this table a range of values is presented for several different types of CI joints. The results given by Jeon et al. (2004) are given, along with those from this study for the range of conditions tested.

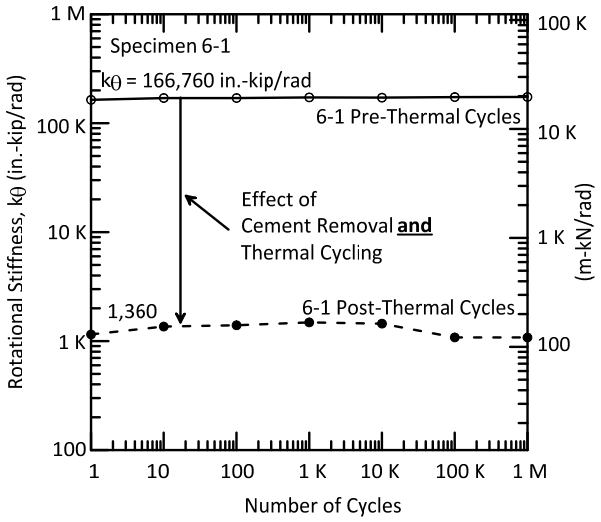


a) Effect of Cement Removal and Thermal Cycling

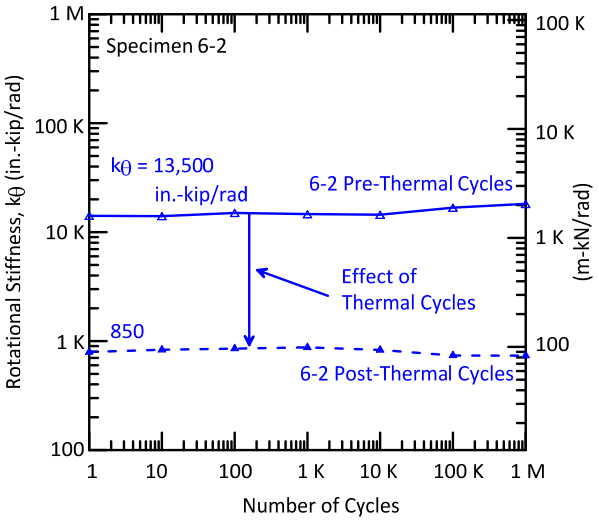


b) Effect of only Thermal Cycling

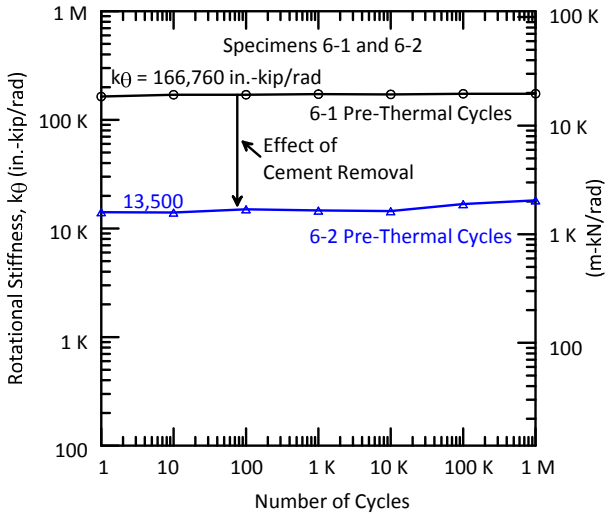


c) Effect of only Cement Removal

Figure 4.30. Rotational Stiffnesses of Specimens 6-1 and 6-2

Table 4.3. Six-in. (150-mm)-Diameter Cast Iron Joint Rotational Stiffnesses

| CI Joint Description | Rotational Stiffness | |
|---|---|---|
| | (in.-kip/rad) | (m-kN/rad) |
| Jeon, et al., (2004) | | |
| Lead with Deteriorated Jute | ≈ 0 | ≈ 0 |
| Lead with Soft Jute | 7,000 | 790 |
| Lead with Hard Jute | 60,000 | 6,780 |
| Cement Caulked | 120,000 | 13,560 |
| Continuous Pipe (infinitely stiff joint) | Infinite | Infinite |
| This Study | | |
| Cement Caulked, with CIPL[a], No Prior Thermal Cycling (Specimen 6-1) | 166,760 | 18,850 |
| No Cement Caulking, with CIPL[a], **and** Prior Thermal Cycling (Specimen 6-1) | 1,360 | 150 |
| No Cement Caulking, with CIPL[a], No Prior Thermal Cycling (Specimen 6-2) | 13,500 | 1,530 |
| No Cement Caulking, with CIPL[a], **and** Prior Thermal Cycling (Specimen 6-2) | 850 | 100 |

a – Starline®2000

## 4.5 Summary of Mechanical Aging Test Results for Specimen 6-1 and 6-2

Two 6-in. (150-mm)-diameter specimens were retrieved from a PSE&G location in Elmwood Park, NJ. The CI pipeline initially was installed in 1949 and lined with Starline®2000 in 1998. This pipeline was operating at 15 in. of water column pressure. The pipe specimens were taken in May, 2014. A testing program was developed to simulate 100 years of vehicular loading, several undermining/backfill (trenching) operations followed by additional traffic loadings, and 100 years of thermal expansion/contraction cycling using a design temperature range of $\Delta T = 40^{o}F$ (22ºC). The CI joints had cement/mortar and jute packing, which resulted in a very high moment-rotational stiffness. The caulking was removed after the first 50 years of vehicle traffic because:

1) The stiffness was very high, and not representative of a round crack with a liner. The purpose of the testing was to simulate aging at a section of lined CI pipe with a round crack or weak and degraded bell and spigot joint.

2) Removal of the cement/mortar and jute provided a clear path for leakage should a rupture occur in the liner material, causing a drop in pressure diagnostic of liner failure.

The testing program consisted of four-point bending (flexure) tests, simulating two 50-year-rounds of testing. The deflections and rotations of the joints were measured carefully, and any changes in pipe characteristics of the 100-year period were noted. The flexure tests were performed using displacements and joint rotations consistent with those derived using previous Cornell analytical research. Special undermining/backfill (trenching) events were also replicated in the laboratory testing. The deformations imposed in the pipe from these loading were about two to three times that used for the normal vehicular loadings. Additional loadings following these events did not indicate any changes in the performance of the CIPL system.

Both CI specimens showed a dramatic change in axial pull-push stiffness after the very first thermal cycle. The first thermal cycle, performed over about 6 hours for the first tension portion, and 4 hours for the completion of the compression cycle, caused substantial debonding of the liner from the pipe. This rate of temperature drop is much faster that the $\Delta T = 40^{o}F$ (22ºC) decrease in about 120 days, the typical rate of cooling at gas pipeline depths in the northeast.

This debonding was also reflected as a decrease in rotational stiffness from the first 50 years of vehicular traffic, which had not been subject to thermal cycling, to the second 50 years, which had experienced the first round of 50 years of thermal cycles. The rotational stiffness of Specimen 6-1 was reduced nearly two orders of magnitude, from $k_{\theta}$ = 166,760 to 1,360 in.-kip/rad (18,500 to 1530 m-kN/rad), due to <u>both</u> the removal of the cement/mortar caulk <u>and</u> thermal cycling. This is a very large reduction. The rotational stiffness of Specimen 6-2, which started with the stiff caulking removed, was reduced from $k_{\theta}$ = 13,500 to 850 in.-kip/rad (1,530 to 100 m-kN/rad) due to thermal cycling.

During all phases of the mechanical aging tests the specimens did not leak. Following these mechanical aging tests, Specimen 6-2 was pressure tested to 90 psig (620 kPa) using water, and

the pipe did not leak. The pressure was increased to 150 psig (1,034 kPa) and the pipe continued to maintain pressure integrity.

The pipe joints were cut longitudinally for visual inspection. The 6 in. (150 mm) joints with the Starline®2000 CIPL showed debonding at the bell/spigot connection. This debonding allowed the liner to stretch without experiencing excessive strain, which could cause damage to the fibers in the liner. This level of debonding indicates that the CIPL system was performing in a highly desirable way and that after all mechanical testing there was no leakage and no damage to the liner.

# Section 5
# Mechanical Aging Tests on Twelve-in.- (150-mm)-Diameter Cast Iron Pipe

## 5.1 Specimen Retrieval for 12 in. (300 mm) CI Joints

NYSEARCH/NGA provided two sections of lined 12-in. (300-mm)-diameter cast iron pipe with joints in good working condition. All sections were approximately 8 ft (2.4 m) long with a joint at the center. An additional straight section of lined CI pipe was also retrieved for additional testing as necessary.

The 12-in. (300-mm)-diameter specimens were retrieved from a National Grid location in South Garden City, Long Island, NY. The CI pipe was installed in 1951. The liner in the pipe was a Starline®2000 liner installed by Progressive Pipeline Management in 2004. The pipe specimens were retrieved in August, 2014. After removal from the excavation the pipes were shipped to Cornell University where mechanical aging tests commenced in March, 2015. Table 5.1 lists the specimen retrieval locations. The two CI sections for testing are identified as Specimens 12-1 and 12-2.

Figure 5.1(a) – (c) show the excavation and CI pipeline at South Garden City. The CI joint is shown in the photos. The National Grid CI pipeline was operating at 60 psig (414 kPa) pressure. Figures 5.2(a) and (b) show two views of a pipe section immediately after removal. Figure 5.2(a) shows the location of the mechanical clamp on the pipe joint. Figure 5.2(b) shows a "bubble" feature, or local protrusion of the liner, at a joint near the pipe crown. The visual appearance of the pipe interior appears quite clean. Figure 5.3(a) shows the pipe joint after field retrieval, with corrosion and scale apparent on the mechanical clamp. Figure 5.3(b) shows the joint after it had been cleaned carefully and de-scaled in the laboratory.

## 5.2 Joint Configuration for 12 in. (300 mm) CI Joints

Figure 5.4 shows a schematic of the 12 in. (300 mm) CI pipe joint. The joints had an Inner-Tite (or equivalent) mechanical clamp. The rubber gasket is compressed by the cast iron gland, providing a pressure-tight seal.

Table 5.1. Twelve-in. (300-mm)-Diameter Cast Iron Joint Retrieval Location

| Specimen No. | Diameter and Length | Lined Pipe Location | Liner Installation | Specimen Retrieval Date | Cornell Begins Testing |
|---|---|---|---|---|---|
| 12-1 and 12-2 | 12 in. dia., 8 ft (300 mm, 2.4 m) | South Garden City, LI, NY | 2004 | August 21, 2014 | March, 2015 |


Figure 5.1. Pipe Retrieval from National Grid Site in South Garden City, LI, NY


a) Joint Showing Mechanical Clamp b) Pipe Interior

Figure 5.2 Twelve-in. (300-mm)-Diameter Cast Iron Joint after Field Retrieval

a) Field Retrieval b) After Lab De-Scaling

Figure 5.3 Twelve-in. (300-mm)-Diameter Joint Condition

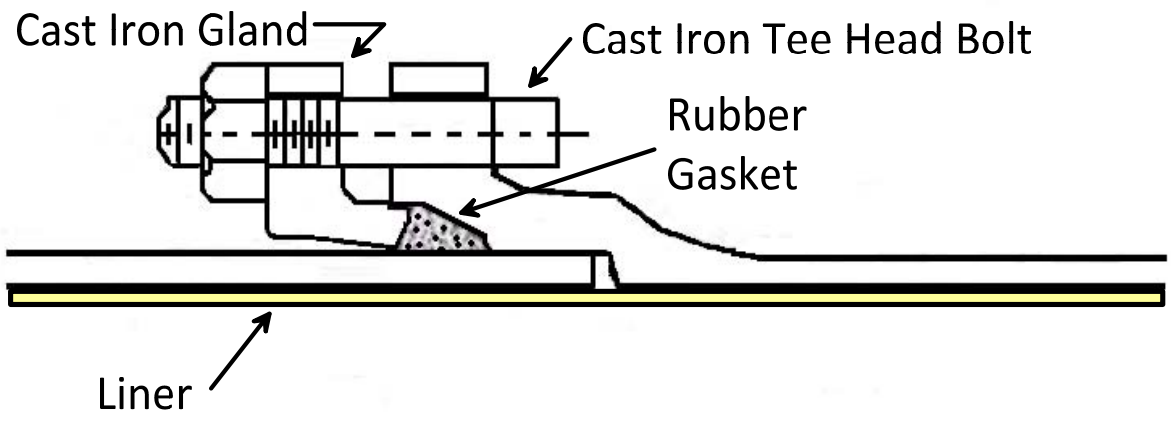


Figure 5.4. Schematic of Mechanical Clamp on 12 in. (300 mm) Pipe Specimens

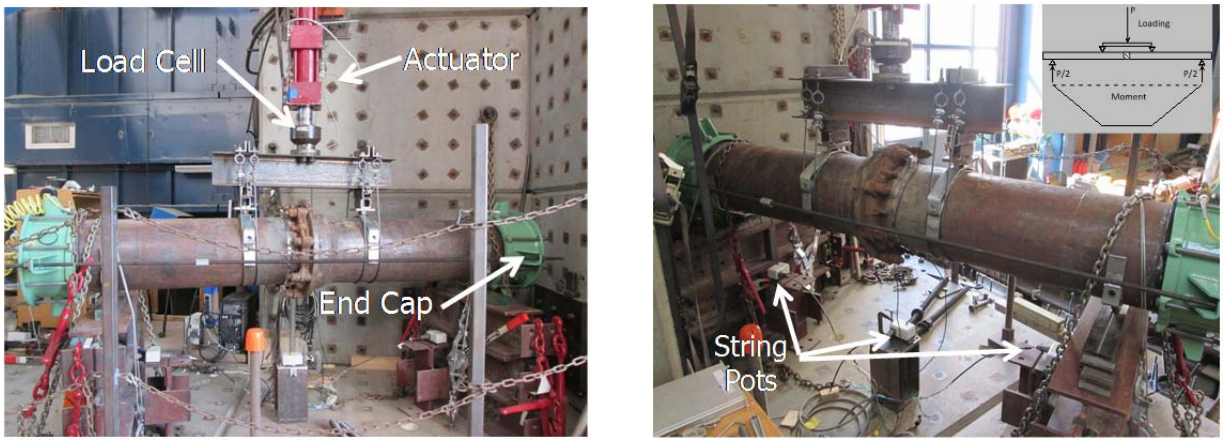


Figure 5.5. Flexure Test Apparatus with 12-in. (300-mm)-Diameter Test Specimen

### 5.3 Mechanical Aging Test Results for Specimen 12-1

As with the 6-in. (150- mm)-diameter specimens, the purpose of flexural testing for the 12-in. (300-mm)-diameter joints was to simulate joint rotation induced by heavy truck traffic on the road above the pipe, and to apply this rotation to the joint repetitively to simulate the effects of traffic loads over a 50-year service life. Each pipe was orientated as it had been in the ground. The pipe was fitted with Smith-Blair EBR end caps. The overall length of the sections was approximately 8 ft (2.4 m). Photographs of the flexure test setup are shown in Figure 5.5. The inset in the upper right corner of the right-most figure shows the constant moment imposed across the central portion of the pipe section.

Table 5.2. Testing Conditions for 12-in. (300-mm)-Diameter Cast Iron Pipe Specimens

| | Years | Pressure[a] |
|---|---|---|
| Vehicle loadings/bending cycles (1 M cycles) | Up to 50 | 15 psig |
| Undermining excavation event (1) | 1 | 15 psig |
| Additional vehicle loadings/bending cycles (100 K cycles) | + 5 | 15 psig |
| Thermal expansion/contraction cycles (50 cycles)[b] | 1 - 50 | 15 psig |
| Vehicle loadings/bending cycles (another 1 M cycles) | 50 - 100 | 15 psig |
| Excavation event (1) | 1 | 15 psig |
| Additional vehicle loadings/bending cycles (another 100 K cycles) | + 5 | 15 psig |
| Thermal expansion/contraction cycles (another 50 cycles) | 50 - 100 | 15 psig |
| Post-Testing Verification Pressure | 1 | 90 psig |

1 psig = 6.89 kPa.
a – Nitrogen gas used for mechanical aging tests and post-testing verification tests.
b – See Table 5.3 for special conditions for Specimen 12-2

The pipe specimens were pressurized for the flexural testing to 15 psig (414 kPa) using nitrogen. As with the prior flexural testing, rotations of the joint were calculated using measurements from either DCDTs or string pot displacements.

Consistent with previous testing, one million cycles of pipe deflections simulated truck loading on the joint over a 50-year service life. As described previously, 20,000 cycles of vehicular loading is equivalent to one year of service. During the test the load cycles were applied at a rate of approximately one cycle per second. At this rate the test duration for each 50-year service period was approximately 12 days.

The testing regimen for the 12 in. (300 mm) specimens is given in Table 5.2. The testing consisted of vehicular loading followed by thermal cycles, representing 50 years of service, and then both sets of aging tests were repeated representing an additional 50 year of service, followed by pressure test verification. Additional testing was performed on Specimen 12-2 between the first 50 years of vehicular traffic, and the thermal loadings. Table 5.3 lists these additional considerations. The purpose of these additional observations was to further substantiate the internal condition of the pipe specimen.

Table 5.3. Special Conditions for Specimen 12-2 after Initial Vehicle Loadings

| Specimen 12-2 | |
|---|---|
| After first 50 years of vehicle loadings but prior to first fifty years of thermal expansion/contraction cycles | After one thermal cycle, depressurize and take photos, pressure check to 60 psig (414 kPa), re-pressurize to 15 psig (103 kPa) and complete remaining 49 cycles |

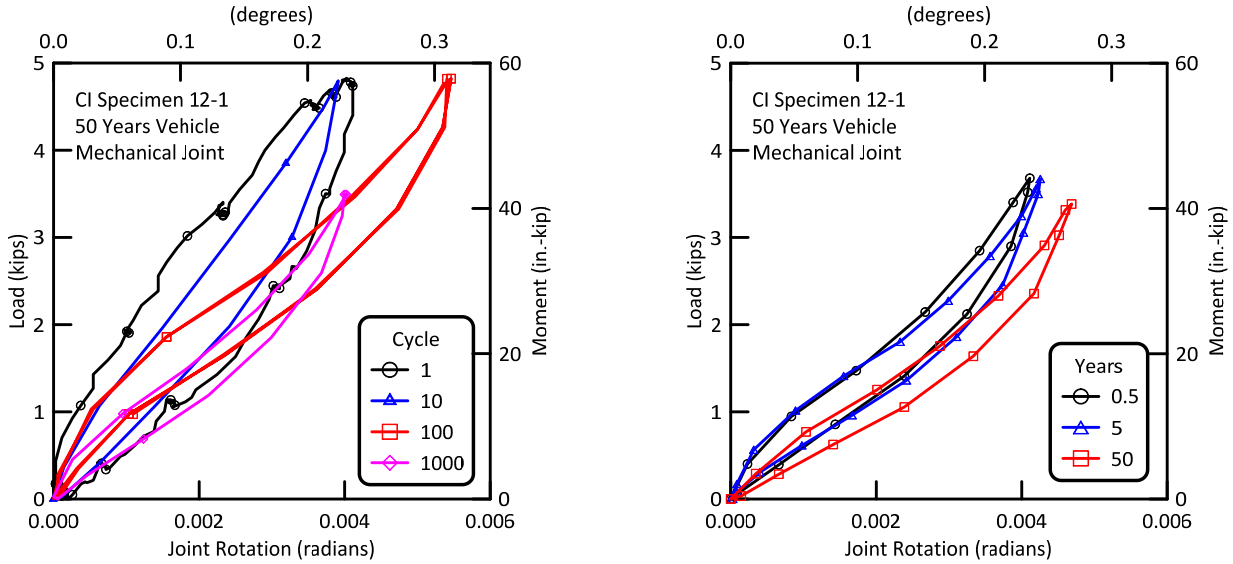


a) Specimen 12-1, Cycles 1 – 1,000

b) Specimen 12-1, Years 0.5 – 50

Figure 5.6. First 50 Years Vehicle Loading Results for Specimen 12-1

### 5.3.1 Specimen 12-1: First 50 Years of Vehicular Loadings

The test results for cycles 1, 10, 100, and 1,000 for Specimen 12-1 are shown in Figure 5.6(a). These cycles are not converted to years (divide cycles by 20,000) because the numerical values are so low. The data for the first 1,000 cycles are nearly identical. The data in Figure 5.6 show that the rotational stiffness of the joint is on the order of $k_\theta$ = 11,760 in.-kip/rad (1,330 m-kN/rad). This was the "as-received" condition of the pipe section. Figure 5.6(b) shows the testing measurements for years 0.5 – 50 (cycles 10,000 – 1,000,000). There is not a significant change in the joint response during the 50-year-equivalent testing.

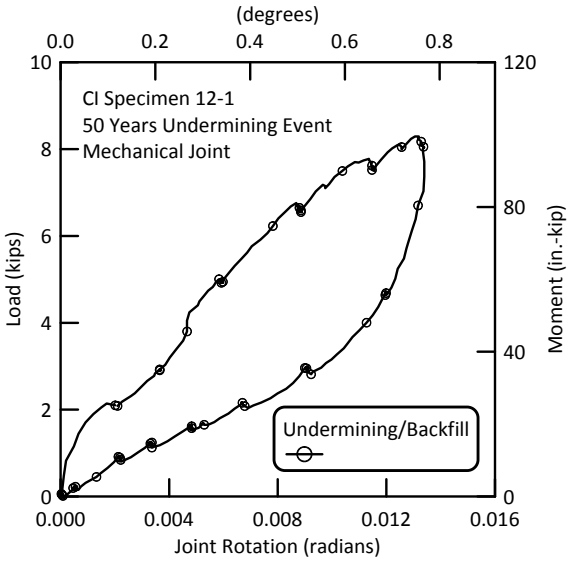


Figure 5.7. First Vehicle Loading for Undermining/Backfill Event for Specimen 12-1

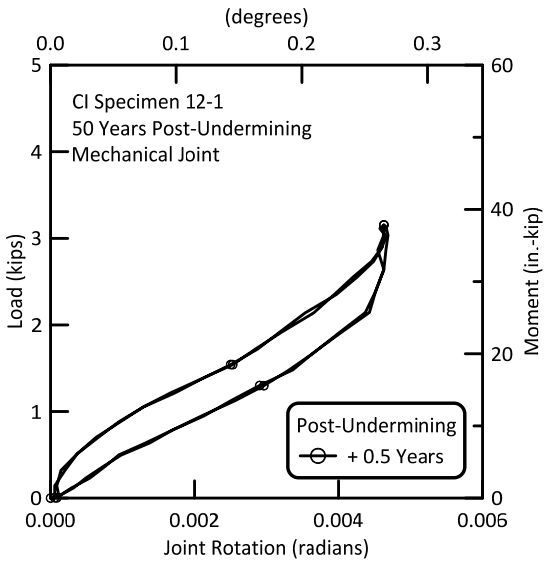


Figure 5.8. First Post-Undermining + 0.5 Years Vehicle Loading for Undermining/Backfill Event for Specimen 12-1

### 5.3.2 Specimen 12-1: First Undermining/Backfill Event

The undermining/backfill episode represents a relatively severe loading condition, as described in Section 3. The backfill was modeled a having low to moderate stiffness, thereby providing less pipe support than the soil associated with one million cycles of traffic load. The test results for Specimen 12-1 in response to repetitive vehicular loading for the undermining/backfilling event are given in Figure 5.7. Note that there is a scale change in Figure 5.7 as compared to the data shown in Figure 5.6. The response to the undermining/backfilling event is roughly three times as large as the prior cyclic loading. Figure 5.8 gives the results for vehicular loading for an additional 100,000 cycles, equivalent to 5 years, beyond the undermining/backfilling event. Again, note that the rotational stiffness of Specimen 12-1 is nearly constant during the first 50 years of vehicular load testing.

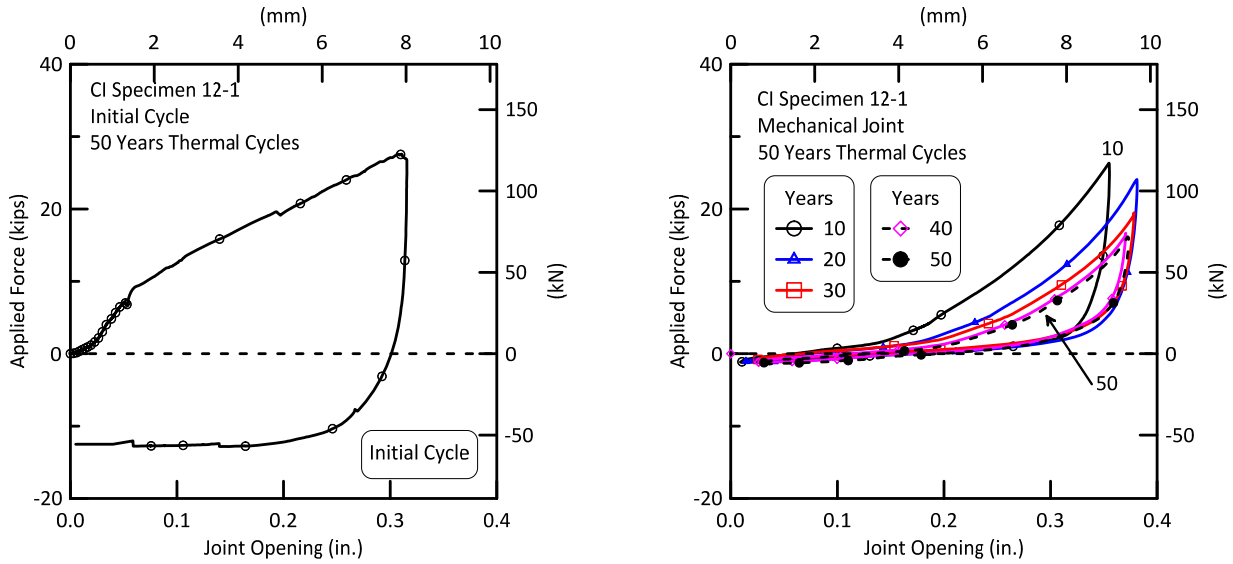


a) Initial Thermal Cycle b) Years 10 through 50

Figure 5.9 Thermal Cycle Joint Openings the First 50 Years, Specimen 12-1

### 5.3.3 Specimen 12-1: First 50 Years of Thermal Loadings

The initial thermal cycle for Specimen 12-1 is shown in Figure 5.9(a). The force-displacement data for years 10 through 50 are given in Figure 5.9(b). The data show similar trends as the thermal data from Specimens 6-1 and 6-2, beyond their first few cycles. There are marked differences for the data from the first cycle, reflecting the effects of thermally-induced debonding of the liner.

### 5.3.4 Specimen 12-1: Second Fifty Years of Vehicular Loadings

After the first 50 years of thermal loading, the specimen was returned to the flexural testing load frame, and subjected to an additional 50 years of vehicular traffic effects. Figure 5.10(a) shows the first few cycles in the second sequence of vehicular loadings, and Figure 5.10(b) shows the force-pipe deflection measurement for years 50.5 through 100 years. The rotational stiffness of Specimen 12-1 for years 50-100 reduced to approximately $k_\theta$ = 3,370 kip-in./rad (420 m-kN/rad). This is about one order of magnitude lower than that measured on Specimen 12-1 without prior thermal cycles. This reduction again indicates that the effect of thermal cycling on the rotational stiffness of the lined pipe is significant.

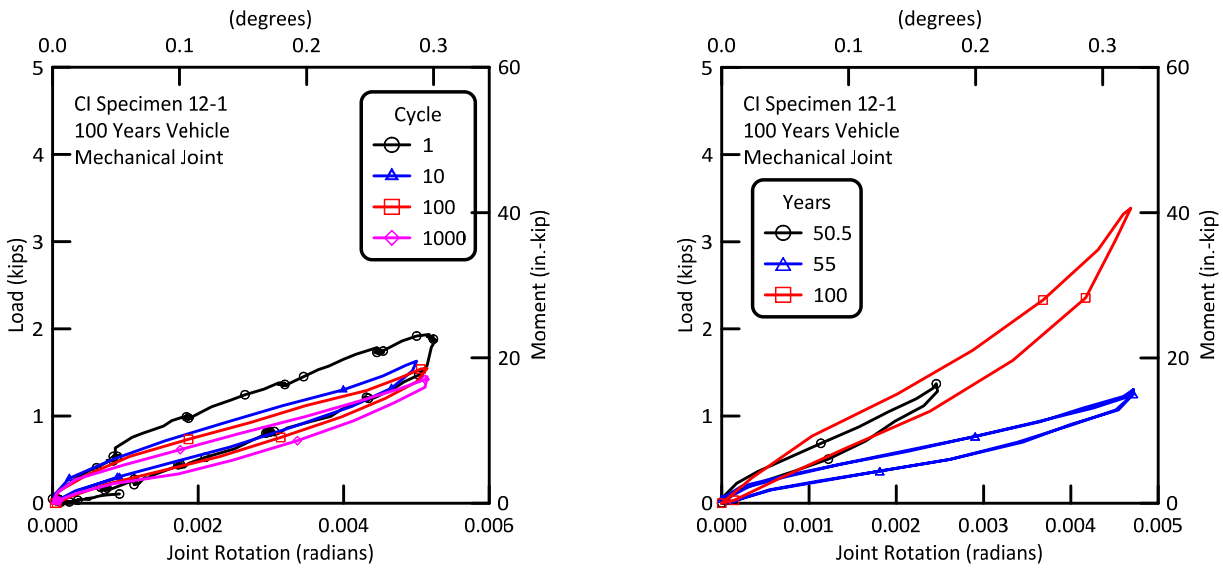


a) Specimen 12-1, Cycles 1 – 1,000

b) Specimen 12-1,Years 0.5 – 50,

Figure 5.10. Second 50 Years (100 Years Total) Vehicle Loading Results for Specimen 12-1

### 5.3.5 Specimen 12-1: Second Undermining/Backfill Event

The response of Specimen 12-1 to vehicular loading for the second undermining/backfilling event, which occurs during the 100 year testing, is given in Figure 5.11. Again note that there is a scale change in Figure 5.11 as compared to the data shown in Figure 5.10. The response to the undermining/backfilling event is again roughly twice as large as the prior cyclic loading. Figure 5.12 gives the results for vehicular loading for an additional 0.5 years beyond the undermining/backfilling event. The rotational stiffness of Specimen 12-1 is nearly constant for all of the 50-100 years of vehicular load testing.

### 5.3.6 Specimen 12-1: Second 50 Years of Thermal Loadings

The data for the second 50 years of thermal aging for Specimen 12-1 are shown in Figures 5.13(a) and 5.13(b). The cyclic contraction/expansion curves for the second 50 years of thermal aging are consistent in shape with those for the first 50 cycles. This indicates no major changes in cyclic degradation beyond that which occurred in the initial cycles of thermal aging.

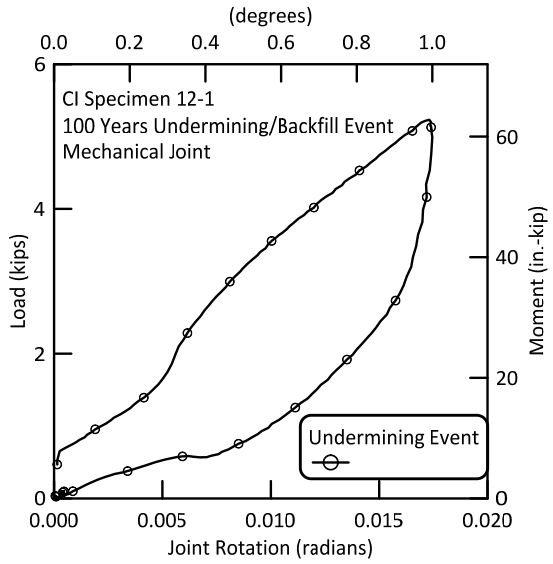


Figure 5.11. Second Vehicle Loading for Undermining/Backfill Event for Specimen 12-1

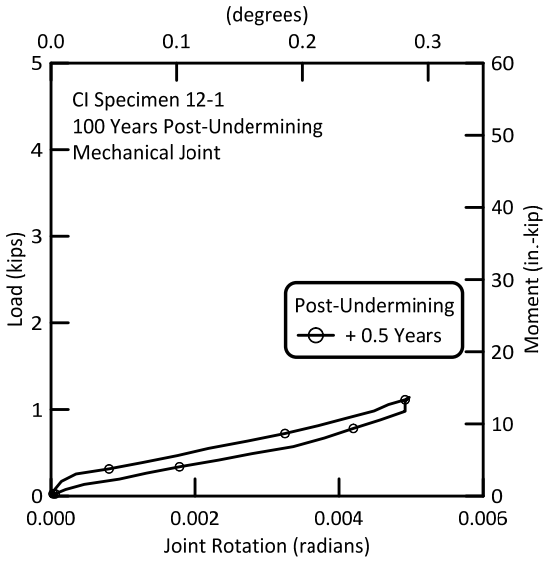


Figure 5.12. Second Post-Undermining + 0.5 Years Vehicle Loading for Undermining/Backfill Event for Specimen 12-1

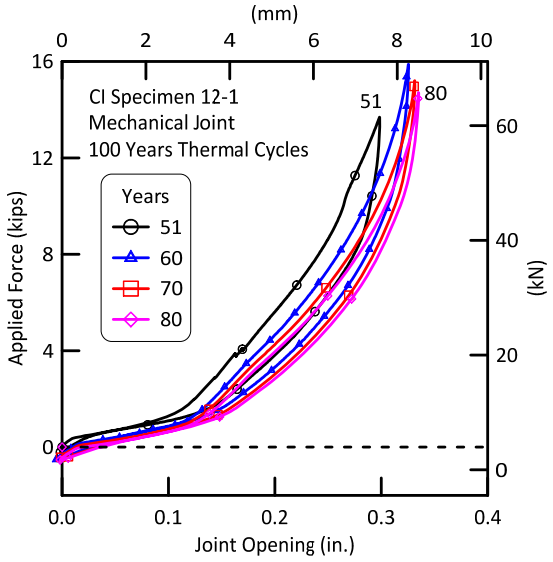


a) Years 51, 60, 70 and 80

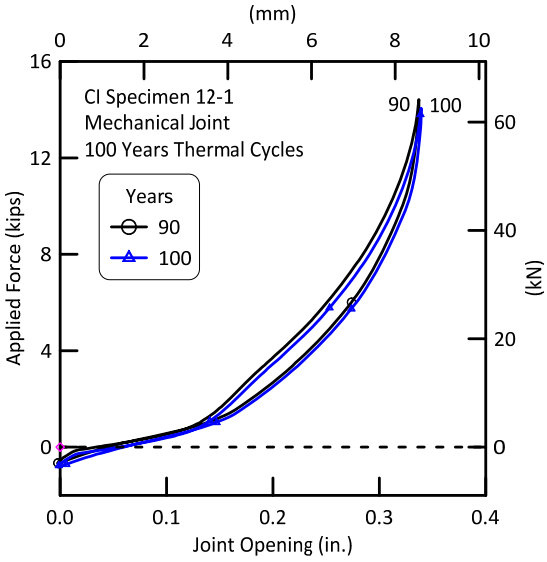


b) Years 90 and 100

Figure 5.13. Thermal Cycle Joint Openings the Second 50 Years (100 Years Total) for Specimen 12-1

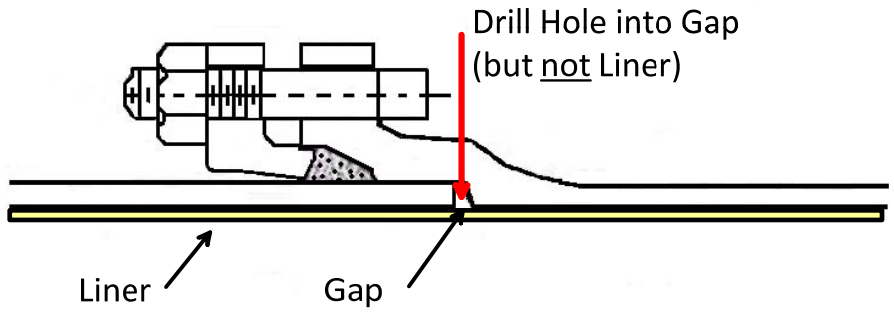


Figure 5.14. Drilling into 12- in. (300)-mm-Diameter CI Bell

### 5.3.7 Specimen 12-1: Post-Test Pressurization

Following the entire set of mechanical aging tests on Specimen 12-1, a pressure verification test was conducted to assure that the liner had not ruptured during the test. Before the pressure testing, a test hole was drilled into the cast iron bell. This is shown schematically in Figure 5.14. The purpose of the drilled hole was to ensure that, if the liner was ruptured, gas would leak through the rupture and out the drilled hole during pressure testing. If the hole had not been present a non-leaking rubber sealing gasket could have prevented any observable liner leak. The pipe was pressure tested to the operating pressure of 60 psig (414 kPa) in roughly 10 psig (7 kPa) increments. There was no leakage. Then the pressure was increased to 90 psig (620 kPa). Again there was no leakage.

### 5.3.8 Specimen 12-1: Additional Comparisons of Mechanical Aging

#### 5.3.8.1 Specimen 12-1: 0 to 100 Years of Vehicular Traffic

Figures 5.15(a) and (b) compare the response of Specimen 12-1 to vehicular loadings for the first 50 years of mechanical aging and the second fifty years of mechanical aging. The data in Figure 5.15(a) is for years 0.5 – 50 (cycles 10,000 – 1,000,000) in the first 50-year sequence of testing. The data in Figure 5.15(b) are for years 50.5 – 100 (cycles 10,000 – 1,000,000) in the second 50-year sequence of testing. They are very similar. The differences in the data for the second 50 years of repetitive traffic aging (Figure 5.15(b)) are not significant.

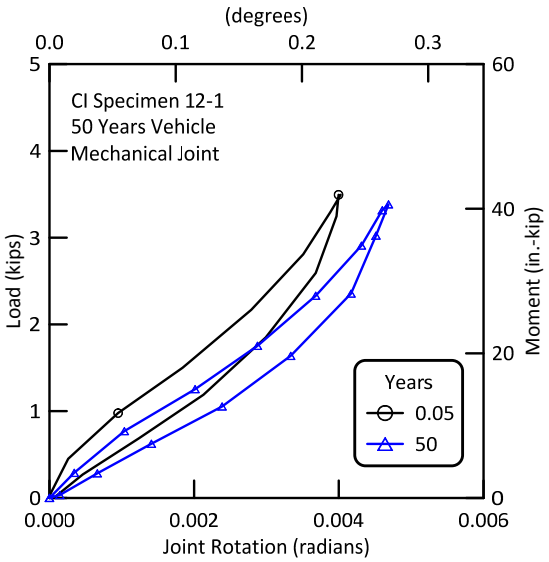


b) Specimen 12-1, Years 0.5 and 50

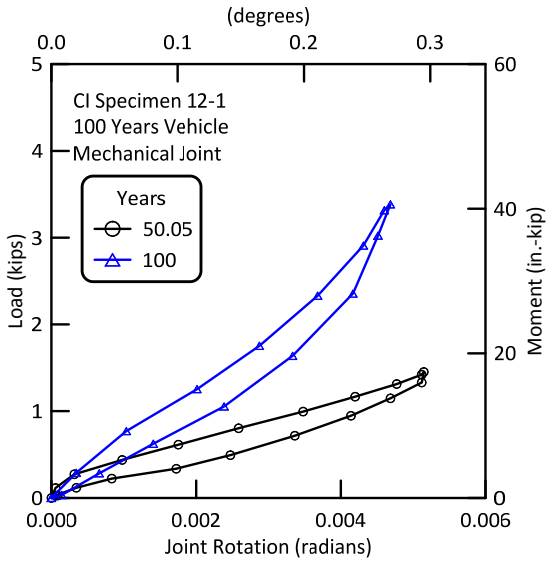


b) Specimen 12-1, Years 50.5 and 100

Figure 5.15. First 50 Years and Second 50 Years Vehicle Loadings for Specimen 12-1

#### 5.3.8.2 Specimen 12-1: Years One through 100 of Thermal Cycling

The weakening of the joint by thermal cycling is further illustrated in Figure 5.16. Here, the initial thermal cycle contraction force is shown for Specimen 12-1 in comparison with the softened contraction/expansion results for years 2 to 100.

### 5.4 Mechanical Aging Test Results for Specimen 12-2

Specimen 12-2 was taken from the same National Grid location in Long Island, NY. Thus, the sampling methodology is the same as described previously. The specimen underwent the same test loading sequence as Specimen 12-1, with the exception of additional inspection, as described previously.

#### 5.4.1 Specimen 12-2: First 50 Years of Vehicular Loadings

The test results for cycles 1, 10, 100, and 1,000 for Specimen 12-2 are shown in Figure 5.17(a). The data for the first 1,000 cycles are very similar. Figure 5.17(b) shows the data through 50 years. The rotational stiffness of the joint was about $k_\theta$ = 11,525 in.-kip/rad (1,300 m-kN/rad). This stiffness is (effectively) the same as measured for Specimen 12-1 with $k_\theta$ = 11,760 in.-kip/rad (1,330 m-kN/rad).

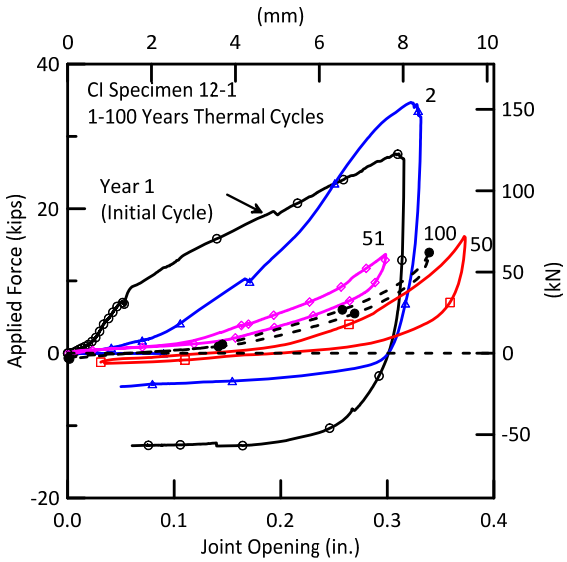


Figure 5.16. Years One through 100 of Thermal Cycling for Specimen 12-1

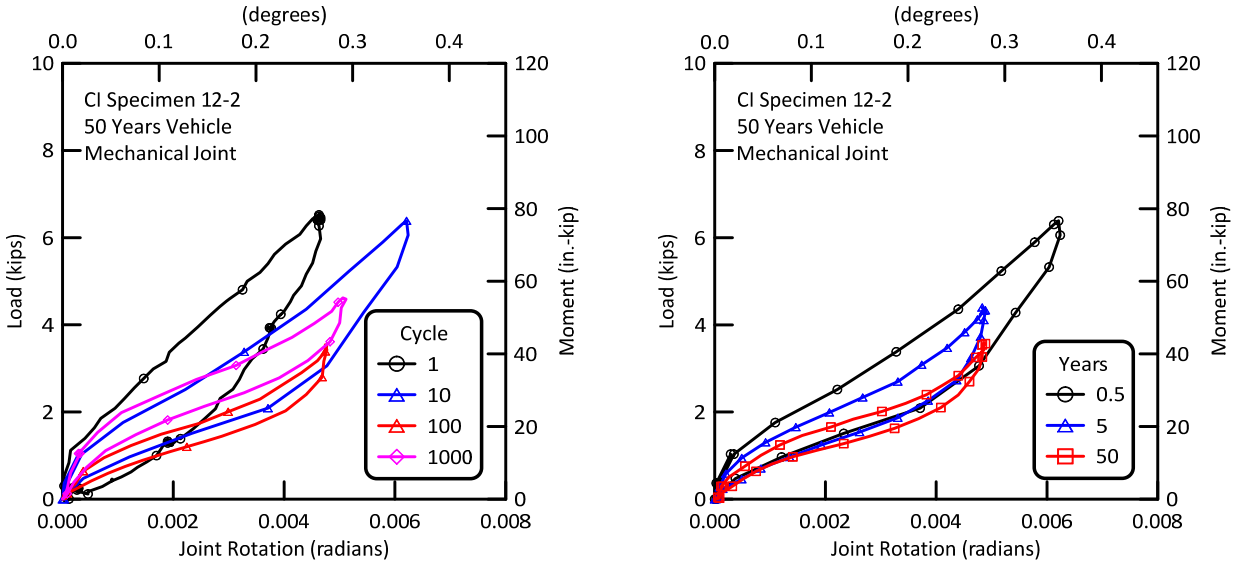


a) Specimen 12-2, Cycles 1 – 1,000

b) Specimen 12-2, Years 0.5 – 50

Figure 5.17. First 50 Years Vehicle Loading Results for Specimen 12-2

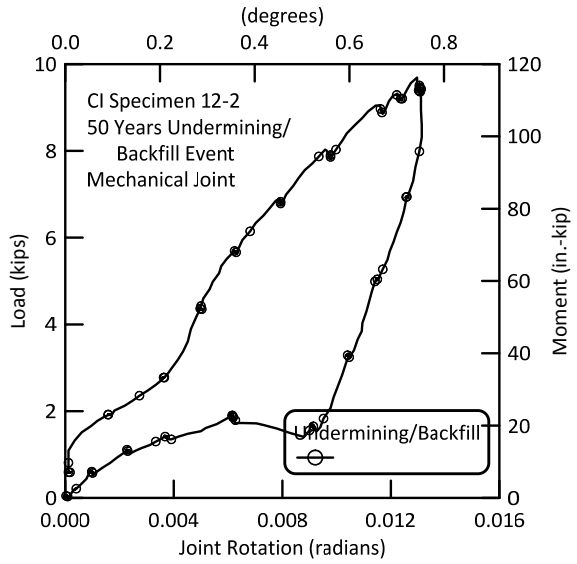


Figure 5.18. First Vehicle Loading for Undermining/Backfill Event for Specimen 12-2

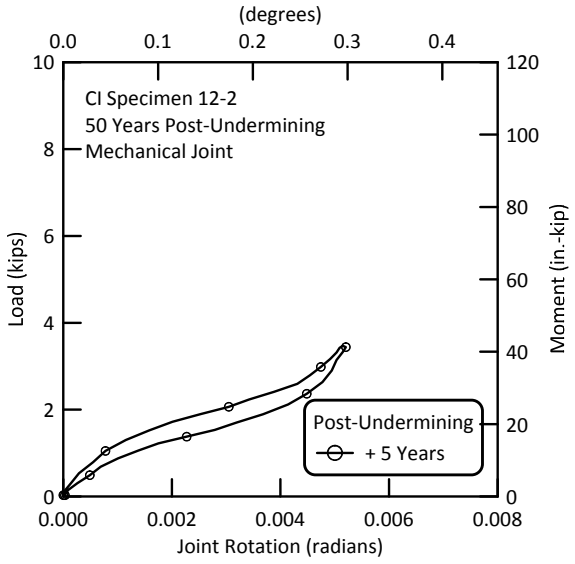


Figure 5.19. First Post-Undermining + 5 Years Vehicle Loading for Undermining/Backfill Event for Specimen 12-2

### 5.4.2 Specimen 12-2: First Undermining/Backfill Event

The test results for Specimen 12-2 in response to the vehicle loading for the undermining/backfilling event are given in Figure 5.18. Note that there again is a scale change for the joint rotation of Figure 5.18 as compared to the data shown in Figure 5.17. The response to the undermining/backfilling event is roughly twice as large as that for the prior cyclic loading (similar to Specimen 12-1). Figure 5.19 gives the results for vehicular loading for an additional 0.5 years beyond the undermining/backfilling event. The response is slightly softer for the post-undermining data, but not dramatically so. The rotational stiffness of Specimen 12-2 is nearly constant during the first 50 years of vehicular loading testing.

### 5.4.3 Specimen 12-2: First 50 Years of Thermal Loadings

The initial thermal cycle for Specimen 12-2 is shown in Figure 5.20(a). Figure 5.20(a) is indicative of the difficulty in gripping the 12-in. (300-mm)-diameter CI. During the first thermal load cycle, the grips on the clamp would often slip and require tightening. With CI pipe, tightening the grips requires great care and experience. If the grips are tightened too aggressively, the CI pipe can crack. If tightening is not sufficient, the grips will slip again,

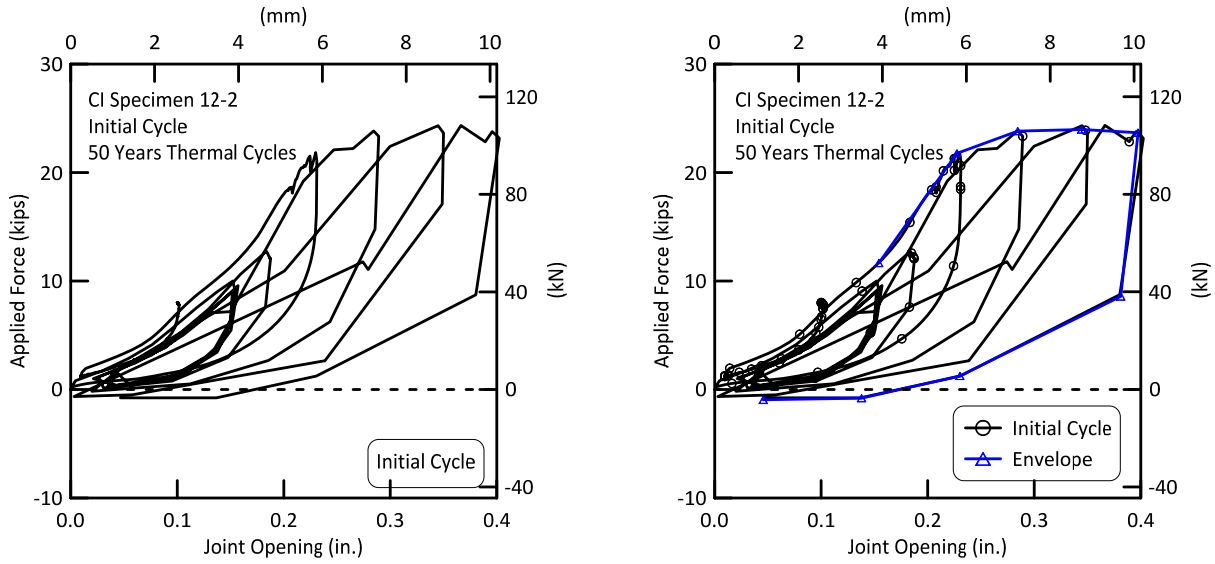


a) Cycle 1 (Year 1)

b) Envelope for Cycle 1 Data

Figure 5.20. Initial Thermal Cycle for Specimen 12-2

requiring another round of adjustment. Figure 5.20(b) shows an envelope of the peaks for the successively increasing forces as tightening was repeated. Figures 5.21(a) and 5.21(b) show the joint opening vs. force for years 3 through 50 years. As was observed in previous specimens, beyond the initial cycles the joint strength is considerably weakened. The effects of debonding are again observed in the CIPL load vs. displacement stiffness reduction during the initial thermal loading cycles.

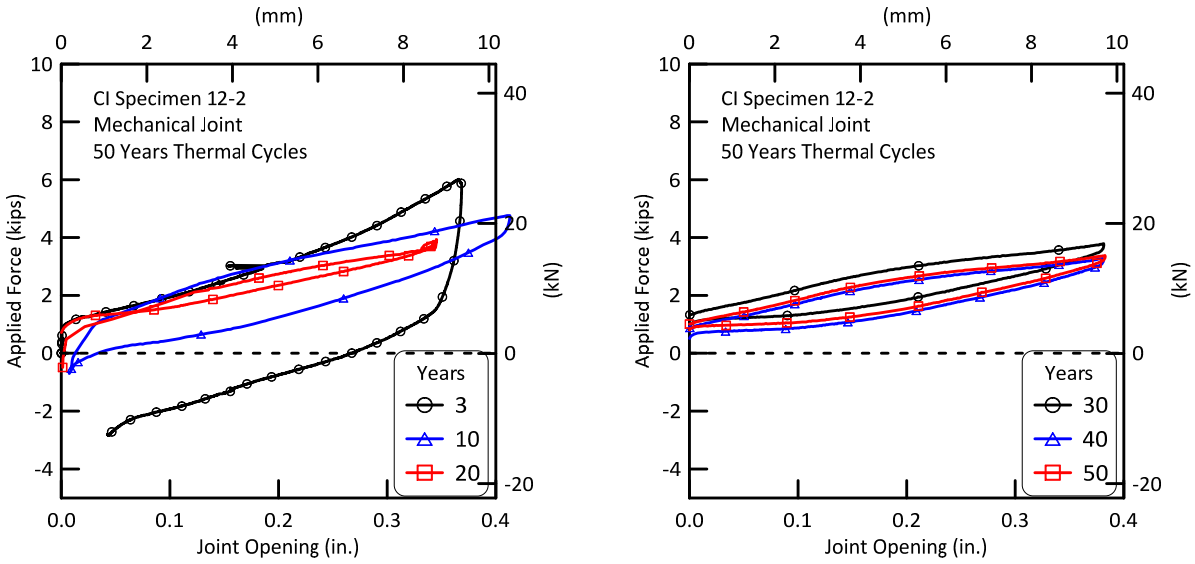


a) Years 3, 10, and 20 b) Years 30, 40 and 50

Figure 5.21. Thermal Joint Openings the Years 3 - 50, Specimen 12-2

### 5.4.4 Specimen 12-2: Second 50 Years of Vehicular Loadings

After the first 50 years of thermal loading, the specimen was returned to the flexural testing load frame, and subjected to an additional 50 years of vehicular traffic effects. Figure 5.22(a) shows the first few cycles in the second round of Specimen 12-2 vehicular loadings and Figure 5.22(b) shows the force-pipe deflection measurement for 50.05 through 100 years. The rotational stiffness for years 50-100 on Specimen 12-2 is now approximately $k_\theta$ = 2,570 kip-in./rad (290 m-kN/rad), which is very close to that of Specimen 12-2 after imposing similar loading conditions.

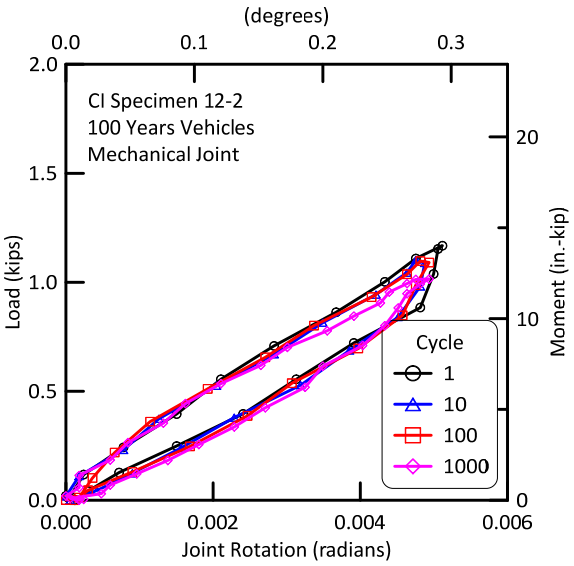


a) Specimen 12-2, Cycles 1 – 1,000

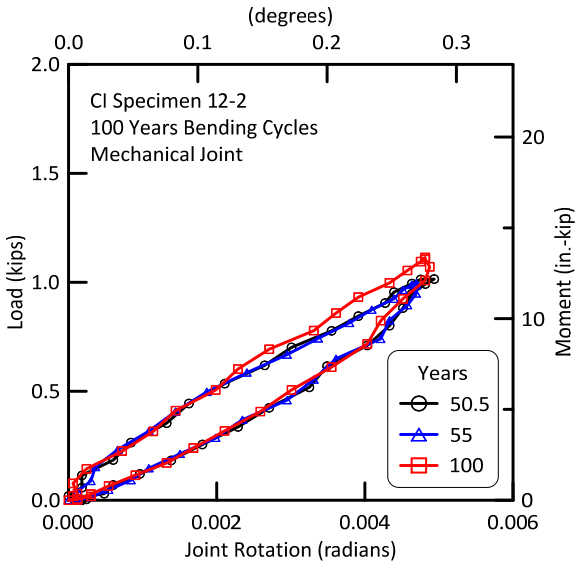


b) Specimen 12-2, Years 0.05 – 50

Figure 5.22. Second 50 Years (100 Years Total) Vehicle Loading Results for Specimen 12-2

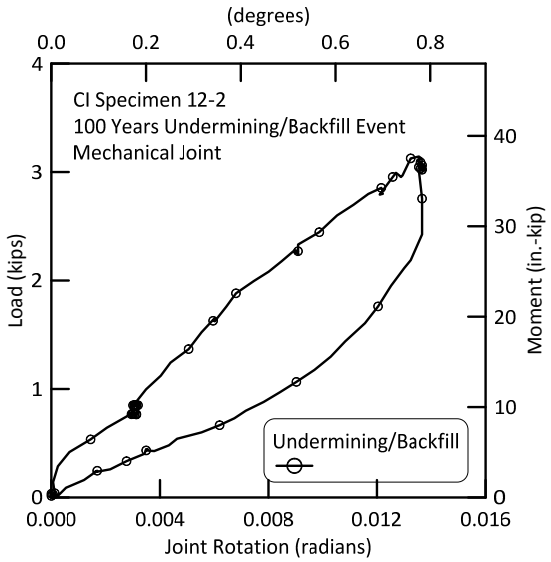


Figure 5.23. Second Vehicle Loading for Undermining/Backfill Event for Specimen 12-2

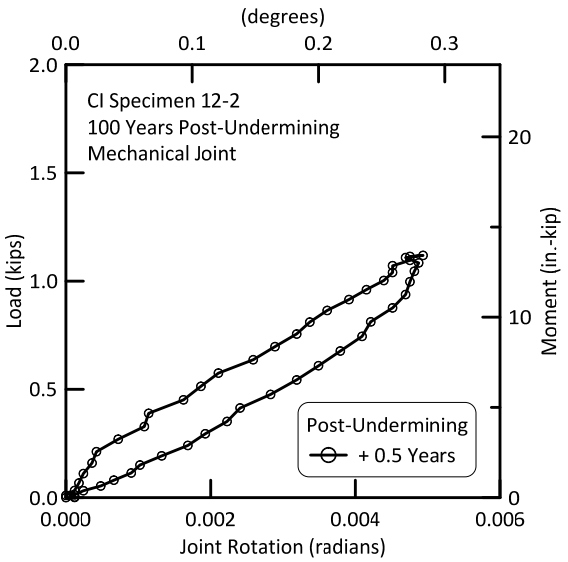


Figure 5.24. Second Post-Undermining + 0.5 Years Vehicle Loading for Undermining/Backfill Event for Specimen 12-2

### 5.4.5 Specimen 12-2: Second Undermining/Backfill Event

The test results for the second undermining/backfill episode for Specimen 12-2, which occurs in the 100 year testing regimen, are given in Figure 5.23. Again note that there is a scale change in Figure 5.23 as compared to the data shown in Figure 5.22. The response to the undermining/backfilling event is again roughly twice as large as the prior cyclic loading. Figure 5.23 gives the results for vehicular loading for an additional 0.5 years beyond the undermining/backfilling event. Also note that the rotational stiffness of Specimen 12-2 is nearly constant during the second 50 years of vehicular load testing.

### 5.4.6 Specimen 12-2: Second 50 Years of Thermal Loadings

The data for the second 50 years of thermal aging for Specimen 12-2 are shown in Figures 5.25(a) and 5.25(b). The cyclic load-unload curves for the second 50 years of thermal aging consistent in shape with those for the first 50 cycles. This indicates no major changes in cyclic degradation beyond that which occurred in the first few cycles of thermal aging.

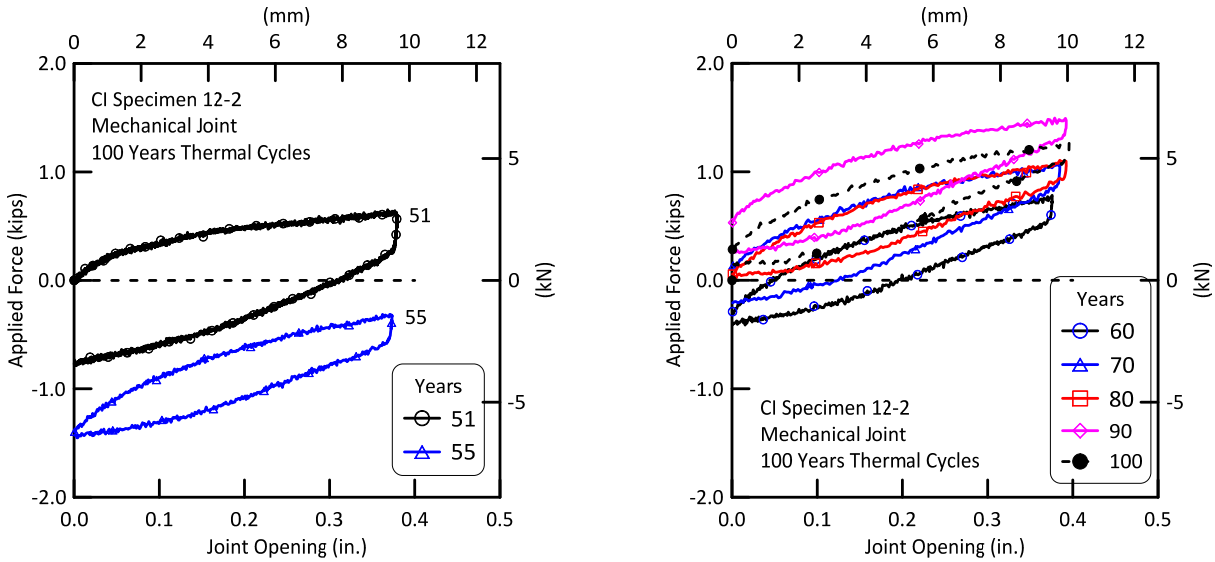


a) Years 51 and 55 b) Years 60 - 100

Figure 5.25. Thermal Cycle Joint Openings the Second 50 Years (100 Years Total) for Specimen 12-2

### 5.4.7 Specimen 12-2: Post-Test Pressurization

Following the entire mechanical aging sequence on Specimen 12-2, a pressure verification test was conducted to assess the pressure integrity of the liner. Again, a small hole was drilled in the bell to assure that any liner rupture was detected during pressurization. The pipe was pressure tested to 60 psig (414 kP) in roughly 10 psig (7 kPa) increments. There was no leakage. Then the pressure was increased to 90 psig (620 kPa). Pipe Specimen 12-2 did not leak after all mechanical aging tests and did not leak after a pressure verification test to 90 psig (620 kPa.).

Visual observations of the liner in the pipe were made after all tests were finished. Figure 5.26 shows photographs of the interior of Specimen 12-2 after all mechanical aging tests and pressure verification. Figure 5.26 shows a ring of discoloration where the CI spigot and bell meet. This discoloration occurred because the annular space between the spigot and bell was filled with soapy water to help detect leakage during pressurization. The oxidation, or rusting, of drill cuttings and iron particles in contact with the liner is the likely cause of the discoloration. At the crown of the pipe there is visible debonding of the CIPL. Figure 5.26(b) shows the interior of the pipe crown. The white circle shows a zone of the liner that has experienced some distress. It is believed that this distress was caused by the first thermal loading, which caused substantial debonding and apparent damage. Figure 5.26(c) is an enlargement of this area. There is some fiber damage visible. However, the liner did not leak. The polyurethane membrane remained intact even though there was some visible liner fabric damage. This is a very important experimental observation. Fiber damage does not mean that the CIPL will leak because additional capacity is provided by the polyurethane membrane. Recall that the internal pressure used in these verification tests was 90 psig (620 kPa). This is 1.5 times the maximum allowable operating pressure (MAOP) of the CI pipeline.

Figure 5.27 shows Specimen 12-2 with a laser shining from outside the pipe through the hole drilled through the bell. The red spot is the laser beam. The photo shows that the portion of the liner in contact with the CI pipe interior surface at this location was in full communication with the atmosphere, and that any liner leakage would have escaped the annular space at the joint created by the still-functioning rubber gasket in the mechanical clamp.

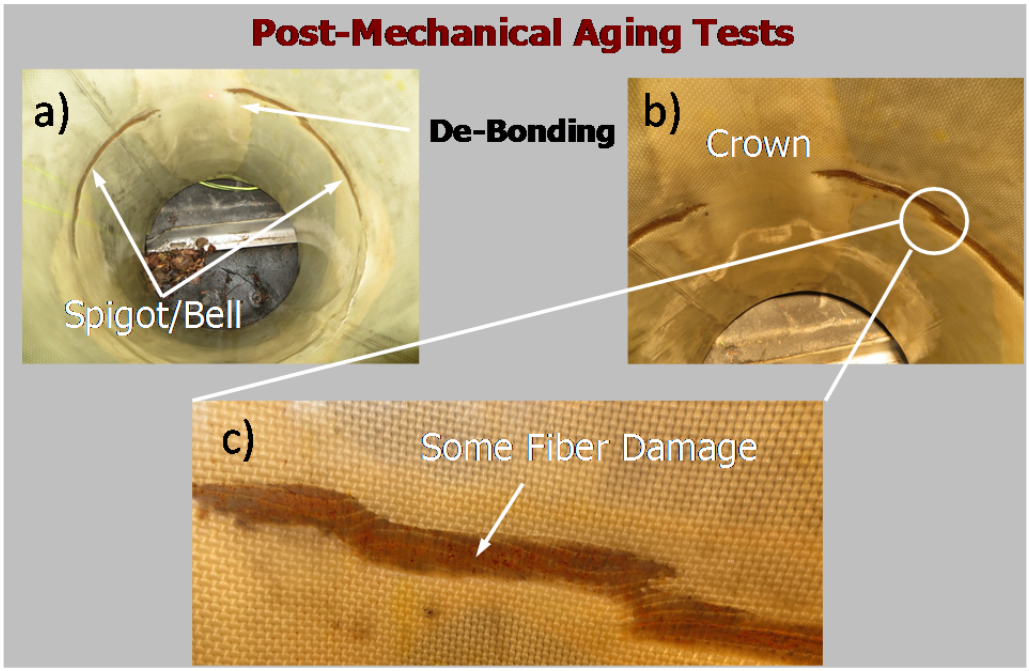


Figure 5.26. Inspection of Specimen 12-2 after All Mechanical Aging Tests

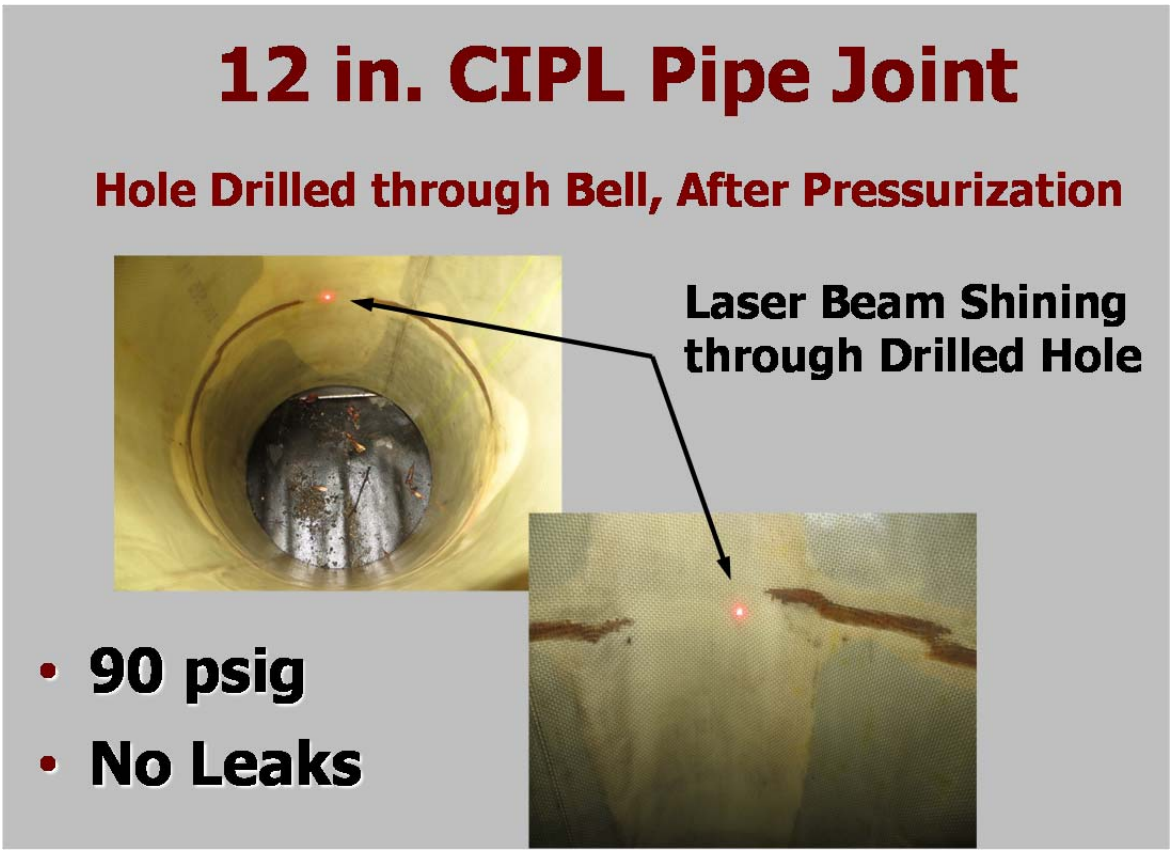


Figure 5.27. Interior of Specimen 12-2 after Pressure Verification Test

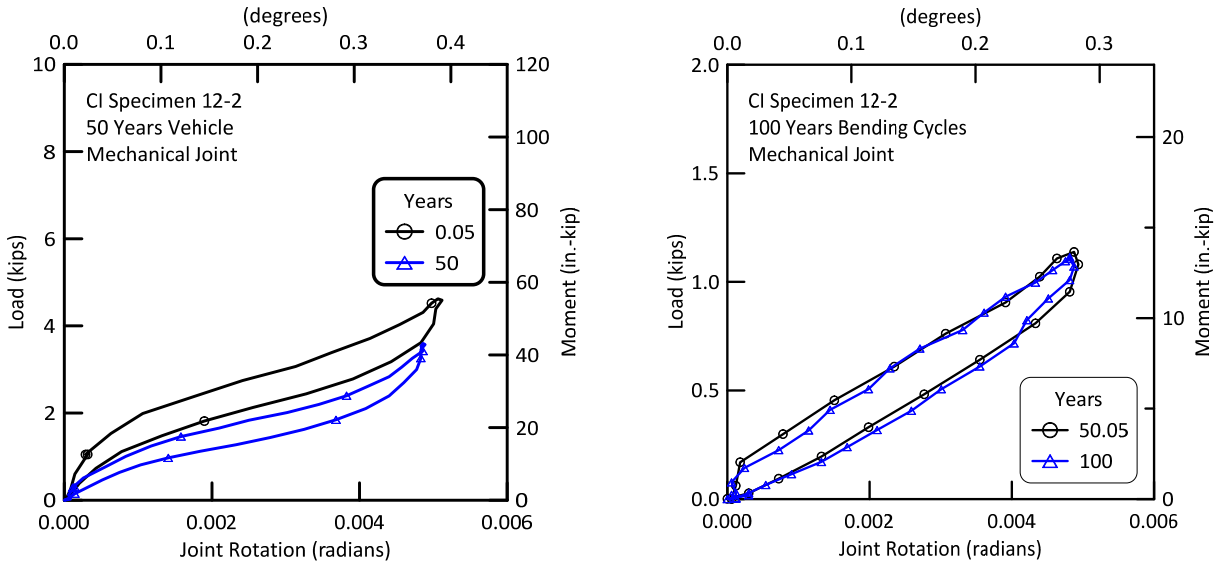


a) Specimen 12-2, Years 0.5 and 50 b) Specimen 12-2, Years 50.5 and 100

Figure 5.28. First 50 Years and Second 50 Years Vehicle Loadings for Specimen 12-2

### 5.4.8 Specimen 12-2: Additional Comparisons of Mechanical Aging

#### 5.4.8.1 Specimen 12-2: 0 to 100 Years of Vehicular Traffic

Figures 5.28(a) and (b) compare the response of Specimen 12-2 to vehicular loadings for the first 50 years of mechanical aging and the second 50 years of mechanical aging. Note that there are different vertical scales in the figures. The rotational stiffnesses are quite different, as will be explained in a following paragraph.

#### 5.4.8.2 Specimen 12-2: 0 to 100 Years of Thermal Cycling

The joint weakening by thermal cycles is further illustrated in Figure 5.29. Here, the initial envelope (shown in Figure 5.20) of the contraction force is shown for Specimen 12-2, along with the softened joint contraction/expansion cycles for years 50, 51, and 100. Clearly the first year (first cycle) is noticeably different and much stiffer than those for the subsequent 100 years of thermal aging.

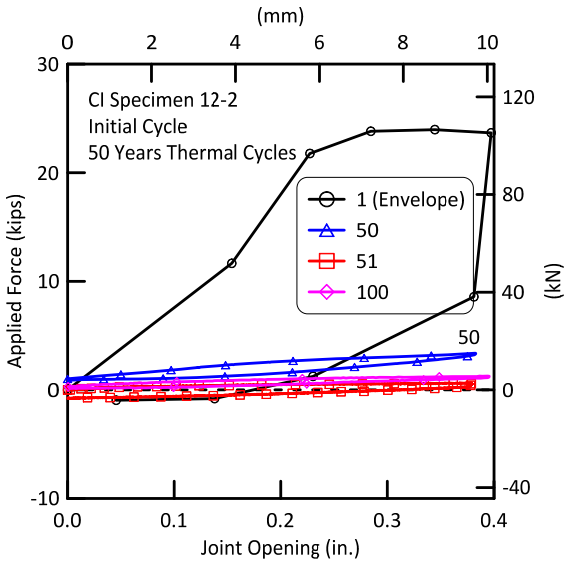


Figure 5.29. Years One through 100 of Thermal Cycling for Specimen 12-2

### 5.4.8.3 Specimen 12-2: Rotational Stiffnesses of Changes and Comparisons to 12-2

During the vehicular loading sequences, the moment-rotation relationships for the 12-in. (300-mm)-diameter cast iron joints can be determined, based on the force-displacement test results given above. Figure 5.30 shows these rotational stiffnesses for two phases of the testing vs. number of loading cycles. In Figure 5.30(a) the upper solid line labeled "12-1 Pre-Thermal Cycles" shows $k_\theta$ = 11,760 in.-kip/rad (1,330 m-kN/rad) for Specimen 12-1 prior to thermal cycling. The dashed line labeled "12-1 Post-Thermal Cycles" shows that the rotational stiffness of Specimen 12-1 has decreased to about 3,730 in.-kip/rad (420 m-kN/rad) due to thermal cycling. Figure 5.30(b) shows similar data for Specimen 12-2. The "12-2 Pre-Thermal Cycles" data shows $k_\theta$ = 11,525 in-kip/rad (1,300 m-kN/rad). The "Post-Thermal" data for Specimen 12-2 indicate that the rotational stiffness has decreased to $k_\theta$ = 2,570 in.-kip/rad (290 m-kN/rad) due the thermal cycling. The rotational stiffnesses for Specimens 12-1 and 12-2 are very nearly the same before thermal cycling. After thermal cycling they also are nearly the same, and substantially lower due to the thermal effects. The rotational stiffnesses of the 12-in. (300-mm)-diameter CI joints are given in Table 5.4. No other data are available for the rotational stiffness of 12-in. (300-mm) CI joints with these types of mechanical clamps.

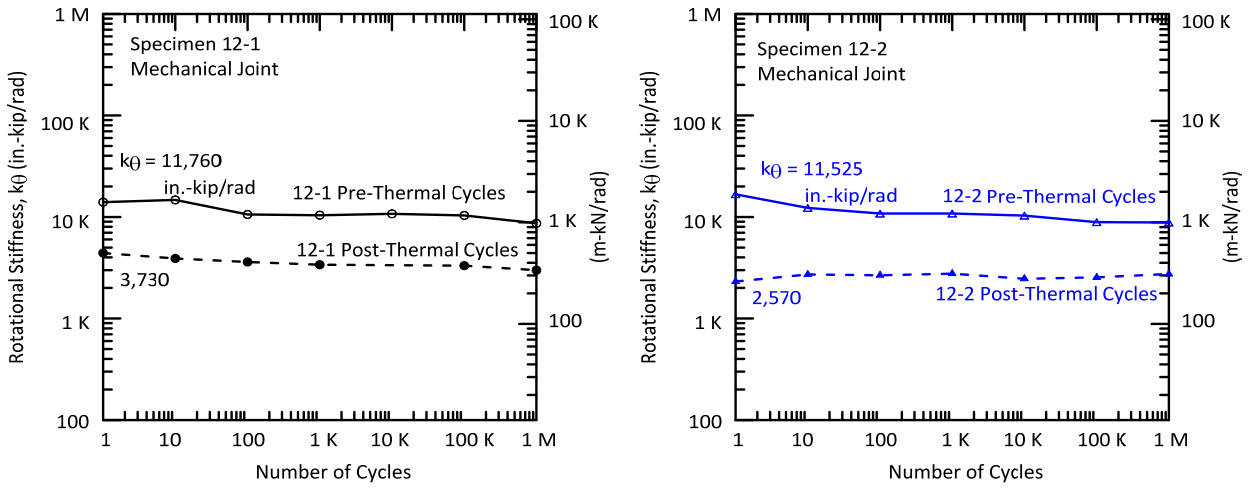


a) Specimen 12-1 b) Specimen 12-2

Figure 5.30. Rotational Stiffnesses of Specimens 12-1 and 12-2

Table 5.4. Twelve-in. (300-mm)-Diameter Cast Iron Joint Rotational Stiffnesses

| 12 in. (300 mm) CI Joint Description | Rotational Stiffness | |
|---|---|---|
| | (in.-kip/rad) | (m-kN/rad) |
| This Study | | |
| Mechanical Clamp, with CIPL[a], No Prior Thermal Cycling (Specimen 12-1) | 11,760 | 1,330 |
| Mechanical Clamp, with CIPL[a], No Prior Thermal Cycling (Specimen 12-2) | 11,525 | 1,300 |
| Mechanical Clamp, with CIPL[a], after Thermal Cycling (Specimen 12-1) | 3,730 | 420 |
| Mechanical Clamp with CIPL[a], after Thermal Cycling (Specimen 12-2) | 2,570 | 290 |

a – Starline®2000

## 5.5 Summary of Mechanical Aging Test Results for Specimen 12-1 and 12-2

Two 12-in. (300-mm)-diameter specimens were retrieved from a National Grid location in South Garden City, Long Island, NY. The CI pipeline initially was installed in 1951 and lined with Starline®2000 in 2004. This pipeline was operating at 60 psig (414 kPa). The pipe specimens were retrieved in August, 2014. A testing program also was developed to simulate 100 years of vehicular loading, several undermining/backfill (excavation for services) operations followed by additional traffic loadings, and 100 years of thermal expansion/contraction cycling using the same temperature range of $\Delta T = 40ºF$ (22ºC). The CI joints had mechanical clamps (Inner-Tite or equivalent), which resulted in initial rotational stiffnesses of approximately $k_\theta$ = 11,000-12,000 in.-kip/rad (1,240 to 1,360 m-kN/rad.). No additional treatment of the joints, other than de-scaling and cleaning, was performed on either specimen before the mechanical aging tests.

The testing program consisted of four-point bending (flexure) tests, simulating two 50-year-rounds of testing. The deflections and rotations of the joints were measured carefully, and any changes in pipe characteristics over the 100-year period were noted.

As with the testing program for the 6-in. (150-mm) pipe sections, the testing program consisted of four-point bending (flexure) tests, simulating two 50-year-sequences of traffic loading. The flexure tests were performed using displacements and joint rotations consistent with those derived using previous Cornell research. Special undermining/backfill events also were replicated in the laboratory testing. The deformations imposed in the pipe from these loading were about two to three times those associated with the normal vehicular loadings. Additional loadings following these events did not indicate any changes in the performance of the CIPL system.

Both 12-in. (300-mm) CI specimens showed substantial changes in their axial contraction/expansion stiffnesses after the first thermal cycle. The first thermal cycle, performed over about 6 hours for the first tension portion, and 4 hours for the completion of the compression cycle, caused substantial debonding of the liner from the pipe, and possible tearing of the liner fibers. As stated previously, this simulated rate of temperature drop is much faster than the $\Delta T = 40ºF$ (22ºC) decrease over about 120 days, the typical rate of cooling at gas pipeline depths in the northeast. In a field environment, the visco-elastic properties of the polyester fibers along with the polyurethane membrane liner would shed stress during slow

cooling. Slow cooling, consistent with the actual seasonal rates of temperature change, would promote local debonding to relieve strain (stress) concentration in the lining. Under these conditions, it is likely that the polyester fabric would have been less damaged.

The debonding also was reflected as a decrease in rotational stiffness after the first round of thermal cycling. As the joints transitioned from the first 50 years to the second 50 years of vehicular traffic loading, the rotational stiffness of both 12 in. (300 mm) pipes was reduced significantly from approximately $k_\theta$ = 11,000-12,000 in.-kip/rad (1,240 to 1,360 m-kN/rad.) to $k_\theta$ = 2,500 to 4,000 in.-kip/rad (289 to 450 m-kN/rad) due to thermal cycling.

During all phases of the mechanical aging tests the specimens did not leak. After the mechanical aging tests the pipes were pressurized with nitrogen. Holes were drilled through the CI bell into the gap between the interior surface of the bell and the CIPL. The primary propose of these drilled holes was to make sure any leaking gas could escape and not be restricted by the rubber gasket in the mechanical clamp. This hole was filled with soapy water to assist in the detection of leakage during pressurization. Each specimen was pressure tested to 60 psig (414 kPa), with no joint leakage. Even when the pressure was increased to 90 psig (620 kPa) the liner maintained its pressure integrity.

After pressure testing, the pipes were inspected, and a laser was directed from the outside of the pipe to illuminate the drilled location on the inside of the CIPL. Even though there was some fabric damage, the liner did not leak at pressure 50 % higher than the pipe MAOP.

# Section 6
# Material Property Tests

## 6. 1 Introduction

This chapter describes the characterization of the residual tensile properties of bonded and debonded liners from both 6-in. and 12-in. (150- and 300-mm)-diameter CI pipe sections retrieved from PSG&E and National Grid service areas, respectively. In addition, lap shear and peel tests were performed to evaluate the strength characteristics along the liner/CI pipe interface.

The material properties were characterized for the CIPL specimens "as received" from the field, and are referred to as being field aged (FA). The FA specimens were taken from a part of the CI pipe where the liner remained bonded to the CI pipe surface. Material properties were also assessed after the mechanical aging procedures were carried out, and are referred to as being field and mechanically aged (FMA). As described in Chapter 3, the mechanical aging procedures consisted of thermal aging (contraction/expansion) and traffic loading cycles equivalent to 100 years of service life in addition to the simulation of undermining effects followed by repetitive vehicular loading of the lined pipe in backfilled soil. The FMA specimens were taken from both bonded and debonded (close to the separation or lip between the spigot and bell) sections of the lining.

The 6-in. (150-mm)-diameter CIPL specimens are distinguished as 1) FA specimens that had undergone "field aging" for 16 years and 2) FMA specimens that had undergone "field aging" for 16 years plus mechanical aging equivalent to 100 years of service life. The 12-in. (300-mm)-diameter CIPL specimens are distinguished as 1) FA specimens that had undergone "field aging" for 10 years and 2) FMA specimens that had undergone "field aging" for 10 years plus mechanical aging equivalent to 100 years of service life.

## 6. 2 Scope

The scope of the material properties testing part of the work was divided into two parts:

1) Characterize the residual tensile properties of the composite liner system as a way to assess the effects of field and mechanical aging on the liner system and its durability, and
2) Characterize the residual liner/CI pipe bond (adhesion) strength and assess the durability

of the bond strength of field and mechanically aged specimens using lap shear and peel tests.

Consistent with the project scope, material property tests were conducted on both FA and FMA specimens and are described below.

## 6. 3 Material Property Tests

Material property tests consisted of both longitudinal and hoop tensile strength tests on samples of the liner as well as lap shear and peel tests of the liner/CI pipe interface. Test descriptions are provided under the headings below.

### 6.3.1 Tension Test

Tension tests on bonded and debonded liner samples for both 6-in. (150-mm) and 12-in. (300-mm)-diameter CI pipes were performed using an Instron universal testing machine (Model 5566) using a modified ASTM D 3039/3039M-00 (ASTM, 2000) procedure. Specimen dimensions were modified to match the earlier testing protocol used by Netravali et al. (2003) for characterizing Starline®2000 PSE-35 liner. A load cell with 2.25 kip (10 kN) full-scale load capacity was used for these tests. Pneumatic grips with serrated steel faces were deployed to hold the specimens without slippage. The liner specimens were tested in both longitudinal and transverse directions. The specimens were cut into dimensions of 0.59 in. (15 mm) width and 7.87 in. (200 mm) length. The test parameters, including gage length (initial distance) between the grips and specimen dimensions, are presented in Table 6.1. Thicknesses of all specimens were measured, and the average thickness is reported in Table 6.1.

### 6.3.2 Lap Shear Test

The lap shear tests were performed on the same Instron universal testing machine (Model 5566) as used for the tension tests to characterize the shear strength between the liners and the CI pipe substrate following a modified ASTM D 3164-97a (ASTM, 1997) procedure. Specimen dimensions were modified to match the earlier testing protocol used by Netravali et al. (2003) for characterizing Starline®2000 PSE-35 liner. A load cell with 2.25 kip (10 kN) full-scale load capacity and pneumatic grips with serrated steel faces were used for these tests. The specimens were 1 in. (25.4 mm) wide and 6 in. (152.4 mm) long, with one end for gripping the liner. The

Table 6.1. Test Parameters and Specimen Dimensions for Tension Tests

| | Values | |
|---|---|---|
| Gauge Length | 2.36 in. | 60 mm |
| Crosshead Speed | 0.78 in./min | 20 mm/min |
| Width | 0.59 in. | 15 mm |
| Thickness<br>6 in. (150 mm) Pipe<br>12 in. (300 mm) Pipe | <br>0.049 in.<br>0.072 in. | <br>1.25 mm<br>1.82 mm |
| Length | 7.87 in. | 200 mm |

Table 6.2. Test Parameter and Specimen Dimensions for the Lap Shear Tests

| Parameter | Value | |
|---|---|---|
| Gauge Length | 3.15 in. | 80 mm |
| Crosshead Speed | 0.39 in./min | 10 mm/min |
| Width | 1.0 in. | 25.4 mm |
| Thickness<br>6 in. (150 mm) Pipe<br>12 in. (300 mm) Pipe | <br>0.049 in.<br>0.072 in. | <br>1.25 mm<br>1.82 mm |
| Length | 6.0 in. | 152.5 mm |
| Overlap | 0.315 in. | 8 mm |

liner overlap with the pipe was fixed at 0.31 in. (8 mm). The specimens were tested in the longitudinal (along the length of the CI pipe) direction. The test parameters and specimen dimensions for the lap shear test are presented in Table 6.2.

### 6.3.3 Peel Test

A modified ASTM D 1876-95 (ASTM, 1995) procedure using a 180° peel test method was employed to obtain the peel strength between the lining system and the CI pipe in tensile mode. Specimen dimensions were modified to match the earlier testing protocol used by Netravali et al. (2003) for characterizing Starline®2000 PSE-35 liner. All tests were performed on the same testing machine and measuring systems used for the tensile and lap shear tests.

Table 6.3. Test Parameters and Specimen Dimensions for Peel Tests

| Parameter | Value | |
|---|---|---|
| Gauge Length | 3.15 in. | 80 mm |
| Crosshead Speed | 5.90 in./min | 150 mm/min |
| Width | 1.0 in. | 25.4 mm |
| Thickness<br>6 in. (150 mm) Pipe<br>12 in. (300 mm) Pipe | <br>0.049 in.<br>0.072 in. | <br>1.25 mm<br>1.82 mm |
| Length | 11.8 in. | 300 mm |

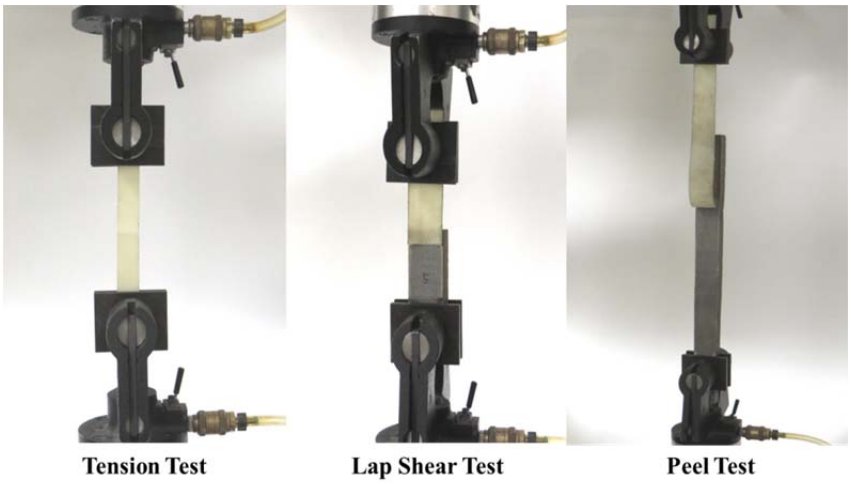


Figure 6.1. Setup for the Tension, Lap Shear and Peel Tests on Instron Universal Tester

Typical specimen dimensions were 1 in. (25.4 mm) wide by 11.8 in. (300 mm) long. The specimens were tested in the longitudinal direction (along the length of the CI pipe). The test parameters and specimen dimensions for the peel tests are presented in Table 6.3. The setups for the tension, lap shear and peel tests on the Instron universal tester are illustrated in Figure 6.1.

### 6.3.4 Field Aging and Mechanical Aging

The test specimens were subjected to both field and mechanical aging, as described under the subheadings that follow.

#### 6.3.4.1 Field Aging

As stated previously, CI gas pipes with the composite lining system were field aged for about 16 years, in the case of 6-in. (150-mm)-diameter pipe, and over 10 years, in the case of 12-in. (300-mm)-diameter pipe, before excavation and transportation to Cornell University. Detailed information about the field aged CI pipe specimen excavations is provided in Sections 4 and 5.

#### 6.3.4.2 Mechanical Aging

Lined CI gas pipes containing a joint were mechanically aged at Cornell, equivalent to 100 years of traffic and thermal expansion/contraction cycling plus undermining and repetitive vehicular loads on lined pipe in the backfilled soil. During the thermal contraction/expansion cycling, the liner debonded locally from the pipe at the joint. The debonding was confined to a small distance either side of the spigot/bell separation, less than one pipe diameter in total width. Both bonded and debonded parts of the liners were characterized for their residual tensile strength.

### 6.5 Test Results

Material properties were measured by performing longitudinal and transverse tensile tests on the FA (bonded) and FMA (bonded and debonded) linings as well as lap shear and peel tests on bonded specimens. Comparisons are made between the tensile strength data for FA and FMA linings. Comparisons are also made between the lap shear and peel test data for the specimens obtained in the present study with similar test data for Starline®2000 PSE-35 liners reported by Netravali et al. (2003). In all cases standard t-tests (Walpole and Myers, 1972) were performed when comparing the data as to assess the statistical significance of the strength comparisons. With only two exceptions, the t-tests confirm that at a 5% level of significance the mechanical aging did not affect the strength properties. One of the exceptions involves peel test results, which are inherently highly variable and affected by small changes in CI pipe/liner interfacial characteristics. The other exception involves 6 in. (150 mm) FMA bonded liner specimen #2 (Specimen 6-2) data for longitudinal tensile strength. Both these exceptions are discussed in conjunction with the appropriate test results under the headings that follow.

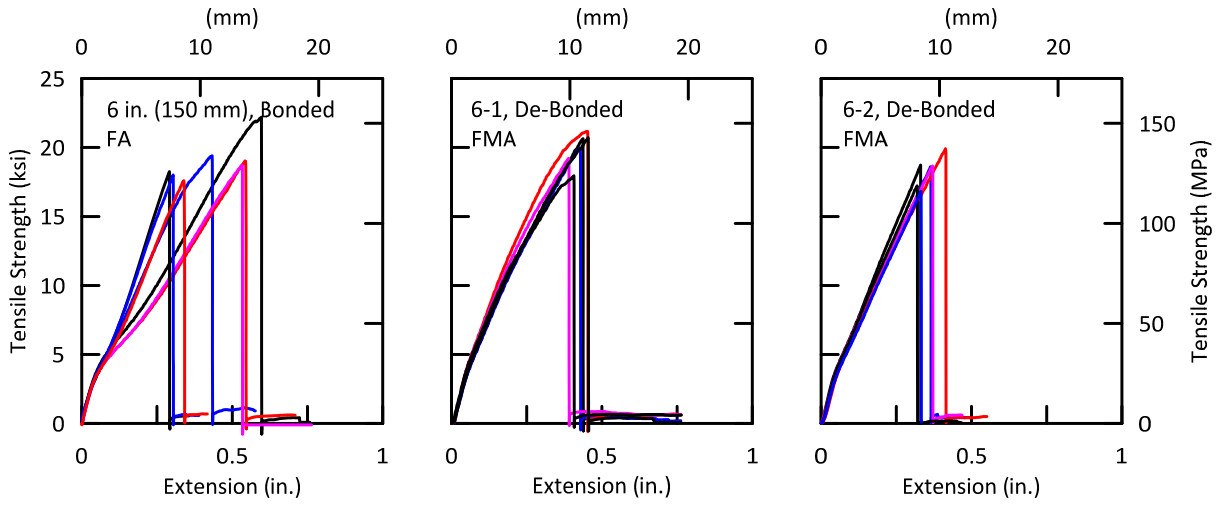


FA = Field Aged for 16 years
FMA = Field Aged + Mechanically Aged at Cornell (equivalent to 100 years of traffic and thermal cycling)

a) Field Aged, Bonded

b) 6-1, Field + Mechanically Aged, De-Bonded

c) 6-2, Field + Mechanically Aged, De-Bonded

Figure 6.2. Tensile Strength vs. Extension for FA (Bonded) and FMA (De-Bonded) Liners in the Longitudinal Direction for 6 in. (150 mm) Pipe

### 6.5.1 Longitudinal Tensile Strength of 6 in. (150 mm) Pipe Liner

Figure 6.2 presents the longitudinal tensile stress vs. extension plots for the FA bonded and FMA debonded liners for 6-in. (150-mm)-diameter CI pipe. In Figure 6.2, the labels 6-1 and 6-2 refer to the specimens taken from the two 6 in. (150 mm) CI pipe sections recovered from the field sites. As mentioned earlier, the debonding of the liners occurred only at the joints where the maximum liner strains and stresses had developed. It is clear from Figure 6.2 that the FMA liners have strength similar to that of the FA liners. Also, the plots for both FA and FMA liners show similar characteristics indicating that there is little to no effect of the mechanical aging on the liner tensile behavior in the longitudinal direction. The mean and percent coefficient of variation (CV%) of the longitudinal tensile strength values for FA bonded and FMA debonded specimens are presented in Table 6.4. The difference between the FA and FMA strengths is not statistically significant.

Table 6.4. Average Tensile Strengths of FA (Bonded) and FMA (De-Bonded) Liners in the Longitudinal Direction for 6 in. (150 mm) Pipe

| | Averages for 6 in. (150 mm) Pipe | | |
|---|---|---|---|
| | Field Aged (FA) | Field + Mechanically Aged (FMA) | |
| Test Value | Bonded | De-Bonded 6-1 | De-Bonded 6-2 |
| ksi (MPa) | 19.03 (131.2) | 19.94 (137.5) | 18.33 (126.3) |
| CV (%) | 7.44 | 5.46 | 5.59 |

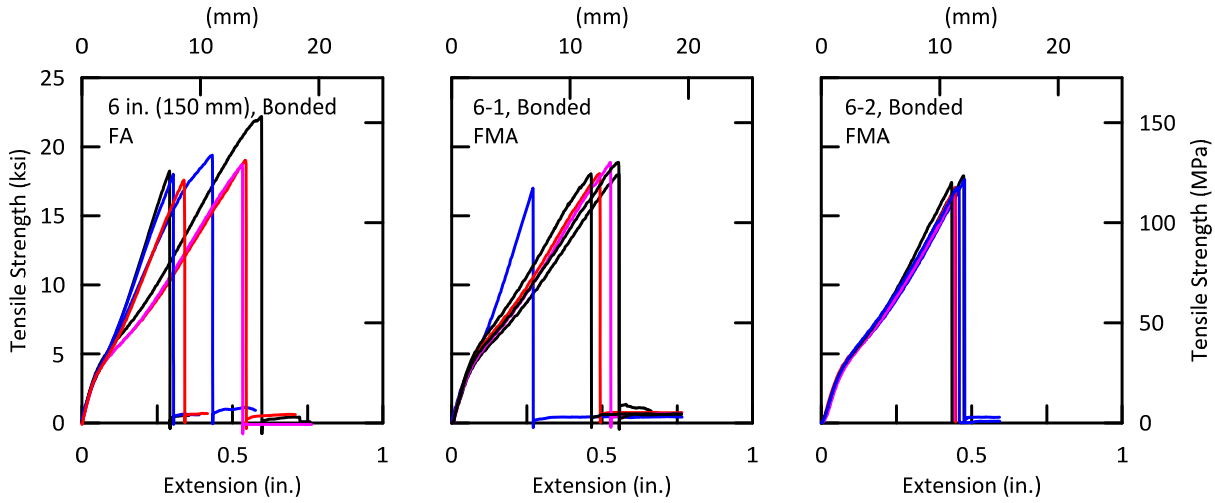


FA = Field Aged for 16 years
FMA = Field Aged + Mechanically Aged at Cornell (equivalent to 100 years of traffic and thermal cycling)

a) Field Aged, Bonded

b) 6-1, Field + Mechanically Aged, Bonded

c) 6-2, Field + Mechanically Aged, Bonded

Figure 6.3. Tensile Strength vs. Extension for FA (Bonded) and FMA (Bonded) Liners in the Longitudinal Direction for 6 in. (150 mm) Pipe

Figure 6.3 shows the longitudinal tensile strength vs. extension plots for bonded FA and bonded FMA liners for the 6 in. (150 mm) CI pipe. These plots show characteristics similar to those in Figure 6.2, indicating that mechanical aging effects did not caused a change in the liner tensile behavior in the longitudinal direction. The mean and percent coefficient of variation (CV%) of the longitudinal tensile strength values for FA and FMA bonded specimens are presented in Table 6.5.

Table 6.5. Average Tensile Strengths of FA and FMA (Bonded) Liners in the Longitudinal Direction for 6 in. (150 mm) Pipe

| | Averages for 6 in. (150 mm) Pipe | | |
|---|---|---|---|
| | Field Aged (FA) | Field + Mechanically Aged (FMA) | |
| Test Value | Bonded | Bonded 6-1 | Bonded 6-2 |
| ksi (kPa) | 19.03 (131.2) | 18.15 (125.1) | 17.23 (118.8) |
| CV (%) | 7.44 | 3.48 | 2.93 |

While there was no difference between the FA bonded and FMA bonded specimen 6-1, at 5% level of significance, specimen 6-2 showed a lower value and was the only one that did not conform to 5% level of significance. It was, however, not significant at 10% level of confidence.

### 6.5.2 Transverse Tensile Strength of 6 in. (150 mm) Pipe Liner

Figure 6.4 presents the transverse tensile stress vs. extension plots of bonded FA and bonded FMA liners for the 6 in. (150 mm) CI pipe. As shown in Figure 6.4, the plots for FA liners have characteristics similar to those for the FMA liners. The mean and coefficient of variation of transverse strength values of FA bonded and FMA bonded specimens are presented in Table 6.6. The average FMA liner strength is very close to that of the FA liner and indicates that there is no significant effect of mechanical aging on the liner strength.

Figure 6.5 shows the transverse tensile strength vs. extension plots for FA (bonded) and FMA (debonded) liners for 6 in. (150 mm) pipe. As shown in Figure 6.5, the FA and FMA liners show very similar tensile behavior. The mean and coefficient of variation of transverse strength values for FA bonded and FMA debonded specimens are presented in Table 6.7. The average FMA liner strength is very close to that of the FA liner and indicates that there is no significant effect of mechanical aging on the liner strength.

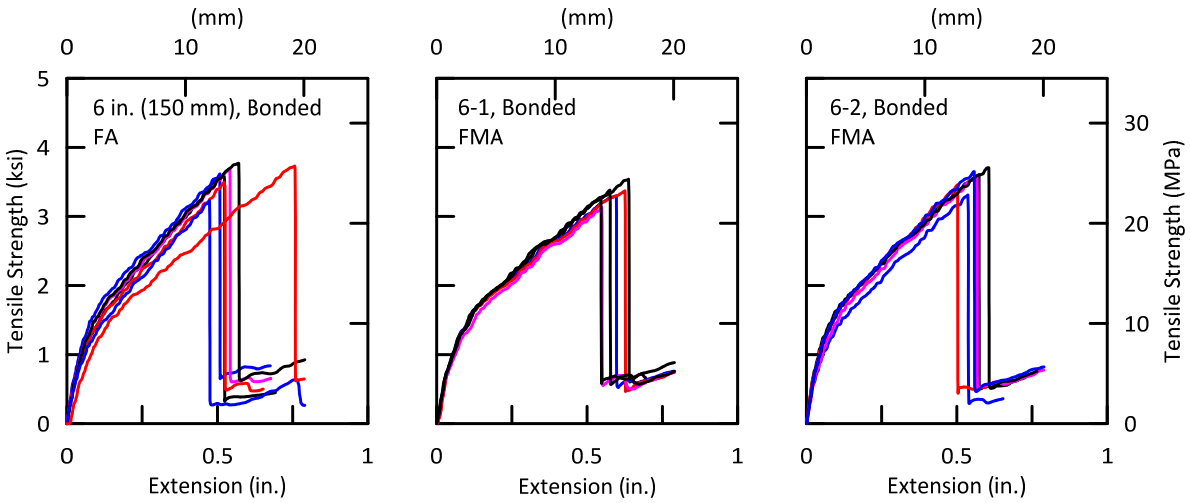


FA = Field Aged for 16 years
FMA = Field Aged + Mechanically Aged at Cornell (equivalent to 100 years of traffic and thermal cycling)

a) Field Aged, Bonded

b) 6-1, Field + Mechanically Aged, Bonded

c) 6-2, Field + Mechanically Aged, Bonded

Figure 6.4. Tensile Strengths vs. Extension for FA (Bonded) and FMA (Bonded) Liners in the Transverse Direction for 6 in. (150 mm) Pipe

Table 6.6. Average Tensile Strengths of FA (Bonded) and FMA (Bonded) Liners in the Transverse Direction for 6 in. (150 mm) Pipe

| | Averages for 6 in. (150 mm) Pipe | | |
|---|---|---|---|
| | Field Aged (FA) | Field + Mechanically Aged (FMA) | |
| Test Value | Bonded | Bonded 6-1 | Bonded 6-2 |
| ksi (MPa) | 3.59 (24.8) | 3.33 (23.0) | 3.55 (24.5) |
| CV (%) | 4.74 | 3.75 | 3.72 |

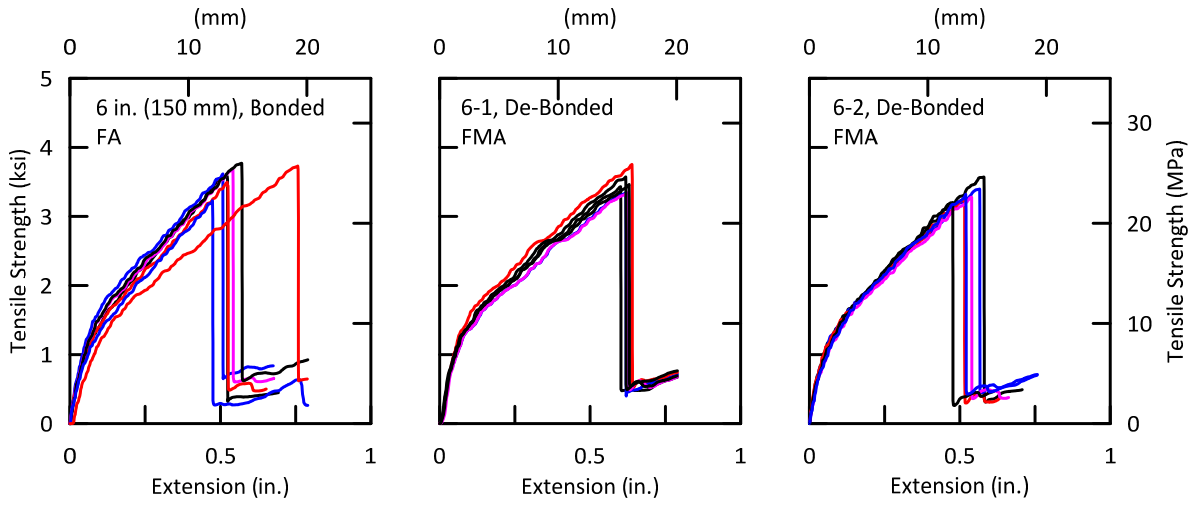


FA = Field Aged for 16 years
FMA = Field Aged + Mechanically Aged at Cornell (equivalent to 100 years of traffic and thermal cycling)

a) Field Aged, Bonded

b) 6-1, Field + Mechanically Aged, De-Bonded

c) 6-2, Field + Mechanically Aged, De-Bonded

Figure 6.5. Tensile Strengths vs. Extension for FA (Bonded) and FMA (De-Bonded) Liners in the Transverse Direction for 6 in. (150 mm) Pipe

Table 6.7. Average Tensile strengths of FA (Bonded) and FMA (De-bonded) Liners in the Transverse Direction for 6 in. (150 mm) Pipe

| | Averages for 6 in. (150 mm) Pipe | | |
|---|---|---|---|
| | Field Aged (FA) | Field + Mechanically Aged (FMA) | |
| Test Value | Bonded | De-Bonded 6-1 | De-Bonded 6-2 |
| ksi (MPa) | 3.59 (24.8) | 3.48 (24.0) | 3.33 (23.0) |
| CV (%) | 4.74 | 4.11 | 3.66 |

### 6.5.3 Longitudinal Tensile Strength of 12 in. (300 mm) Pipe Liner

Figure 6.6 presents the longitudinal tensile stress vs. extension plots for the FA bonded and FMA debonded liners for 12 in. (300 mm) CI pipe. As in the case of 6 in. (150 mm) pipe liners, 12-1 and 12-2 refer to the two 12 in. (300 mm) pipe liner specimens that were tested in this study. As discussed in Section 5, the debonded area of the FMA liner consisted of both visually

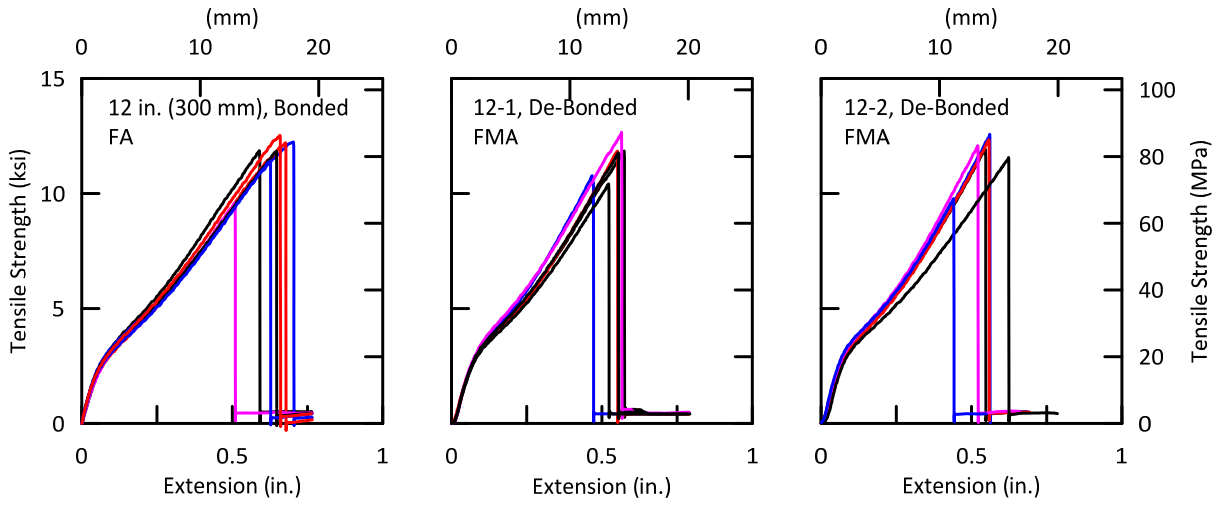


FA = Field Aged for 11 years.
FMA = Field Aged + Mechanically Aged at Cornell (equivalent to 100 years of traffic and thermal cycling).

a) Field Aged, Bonded

b) 12-1, Field + Mechanically Aged, De-Bonded

c) 12-2, Field + Mechanically Aged, De-Bonded

Figure 6.6. Tensile Strengths vs. Extension for FA (Bonded), and FMA (De-Bonded) Liners in the Longitudinal Direction for 12 in. (300 mm) Pipe

Table 6.8. Average Tensile Strengths of FA (Bonded) and FMA (De-bonded) Liners in the Longitudinal Direction for 12 in. (300 mm) Pipe

| | Averages for 12 in. (300 mm) Pipe | | |
|---|---|---|---|
| | Field Aged (FA) | Field + Mechanically Aged (FMA) | |
| Test Value | Bonded | De-Bonded 12-1 | De-Bonded 12-2 |
| ksi (MPa) | 11.67 (80.5) | 11.55 (79.6) | 11.71 (80.7) |
| CV (%) | 7.82 | 6.45 | 7.84 |

undamaged and partially damaged sections in the vicinity of the joint. The results shown in Figure 6.6 and presented in Table 6.8 are those for the undamaged liner sections. Separate results for visually damaged liner sections are presented and discussed in Section 6.4.4.

The plots for both FA and FMA liners show similar characteristics, indicating that there is little to no effect of the mechanical aging on the liner tensile behavior in the longitudinal direction.

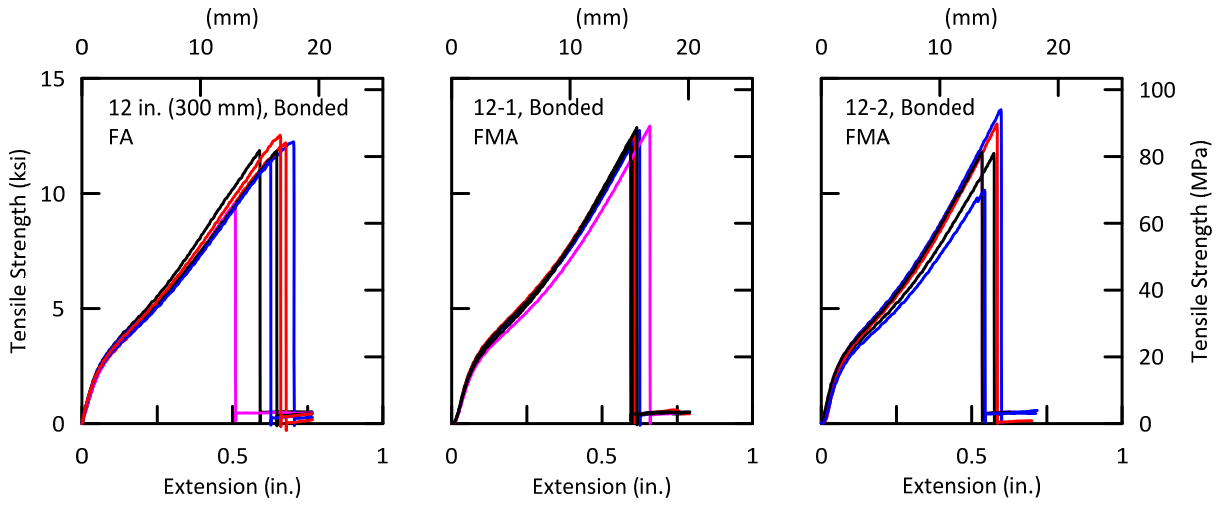


FA = Field Aged for 11 years.
FMA = Field Aged + Mechanically Aged at Cornell (equivalent to 100 years of traffic and thermal cycling).

a) Field Aged, Bonded

b) 12-1, Field + Mechanically Aged, Bonded

c) 12-2, Field + Mechanically Aged, Bonded

Figure 6.7. Tensile Strengths vs. Extension for FA and FMA (Bonded) Liners in the Longitudinal Direction for 12 in. (300 mm) Pipe

The mean and coefficient of variation of the longitudinal tensile strength values for FA bonded and FMA debonded specimens are presented in Table 6.8. From the plots and data it is clear that the difference between the FA and FMA strengths is not statistically significant.

Figure 6.7 shows the longitudinal tensile strength vs. extension plots for bonded FA and bonded FMA liners for the 12 in. (300 mm) CI pipe. These plots show characteristics similar to those in Figure 6.6, indicating that both FA and FMA liners have similar tensile behavior. The mean and CV of the longitudinal tensile strength values for FA and FMA bonded specimens are presented in Table 6.9. The data show that once again there is no significant effect of mechanical aging on the tensile properties of the liner in the longitudinal direction.

Table 6.9. Average Tensile Strengths of FA and FMA (Bonded) Liners in the Longitudinal Direction for 12 in. (300 mm) Pipe

| | Averages for 12 in. (300 mm) Pipe | | |
|---|---|---|---|
| | Field Aged (FA) | Field + Mechanically Aged (FMA) | |
| Test Value | Bonded | De-Bonded 12-1 | De-Bonded 12-2 |
| ksi (MPa) | 11.67 (80.5) | 12.64 (87.2) | 12.02 (82.9) |
| CV (%) | 7.82 | 1.86 | 9.19 |

### 6.5.4 Longitudinal Tensile Strength of Partially Damaged 12 in. (300 mm) Pipe Liner

As mentioned previously, during the mechanical aging (thermal contraction/expansion) process, part of the debonded liner showed visual damage. A typical set of damaged specimens are shown in Figure 6.8. Close inspection of the specimens indicated that the polyester yarns were damaged while the polyurethane membrane remained intact. Most of the polyester yarn damage occurred during the first thermal contraction/expansion cycle, and was likely caused by the high rate of the test that was completed in just 2-4 hours, about 4 orders of magnitude faster than the natural cycle of a few months. All polymers, including polyesters used in the liners, show brittle behavior characterized by reduced fracture strain and high modulus (stiffness) when subjected to high strain rates. The breaking of polyester yarns in the liners under rapid loading is consistent with the typical behavior of polymers.

Damaged liners were tested for their tensile strength in the longitudinal direction. Figure 6.9 shows the tensile strength vs. extension plots of undamaged and damaged FMA (debonded) liners in the longitudinal direction for the 12 in. (300 mm) CI pipe. The plots of the damaged liners essentially reflect the characteristics of the polyurethane membrane, with lower strength and higher fracture strain compared to the undamaged liners.

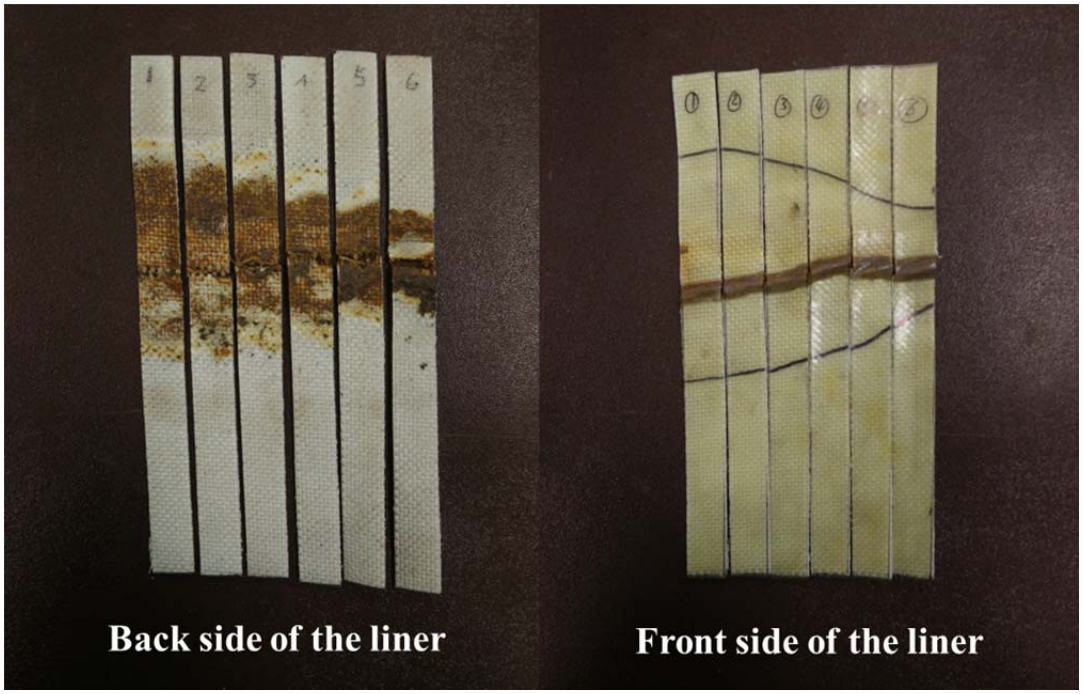


Figure 6.8. Photographs of Partially Damaged Section of the De-Bonded 12 in. (300 mm) Pipe Liner

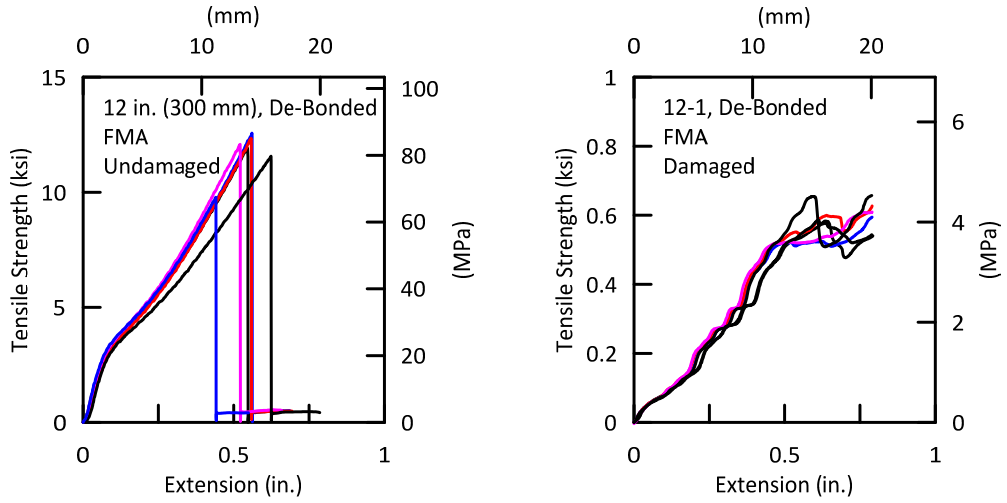


FMA = Field Aged + Mechanically Aged at Cornell (equivalent to 100 years of traffic and thermal cycling).

a) 12 in. (300 mm), Undamaged, De-Bonded

b) 12 in. (300 mm), Damaged, De-Bonded

Figure 6.9. Tensile Strength vs. Extension for a) Undamaged and b) Damaged FMA (De-Bonded) Liners in the Longitudinal Direction for 12 in. (300 mm) Pipe

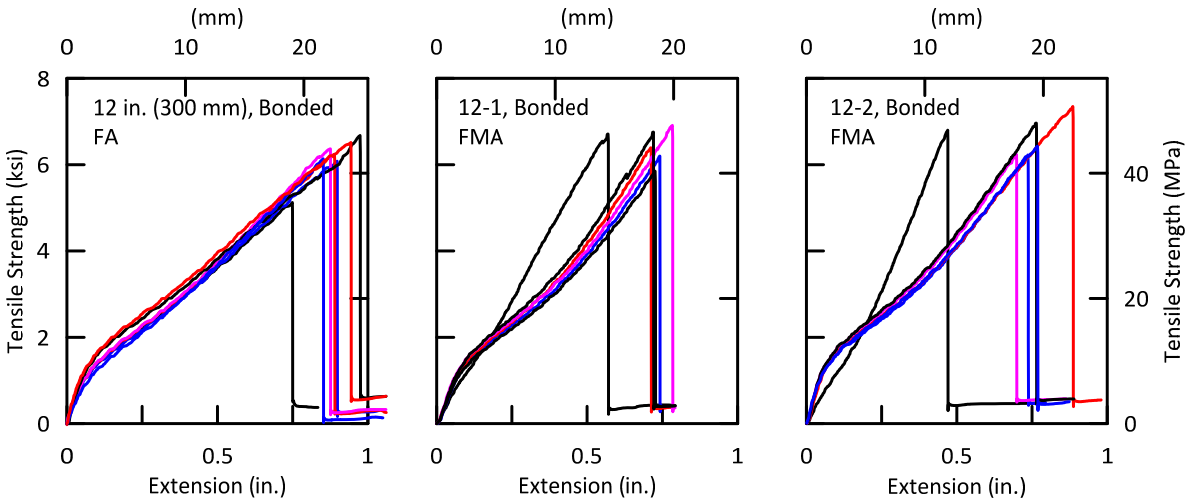


FA = Field Aged for 11 years.
FMA = Field Aged + Mechanically Aged at Cornell (equivalent to 100 years of traffic and thermal cycling).

a) Field Aged, Bonded

b) 12-1, Field + Mechanically Aged, Bonded

c) 12-2, Field + Mechanically Aged, Bonded

Figure 6.10. Tensile Strengths vs. Extension for FA and FMA (Bonded) Liners in the Transverse Direction for 12 in. (300 mm) Pipe

Table 6.10. Average Tensile Strengths of FA and FMA (Bonded) Liners in the Transverse Direction for 12 in. (300 mm) Pipe

| | Averages for 12 in. (300 mm) Pipe | | |
|---|---|---|---|
| | Field Aged (FA) | Field + Mechanically Aged (FMA) | |
| Test Value | Bonded | De-Bonded 12-1 | De-Bonded 12-2 |
| ksi (MPa) | 5.92 (40.8) | 6.47 (44.6) | 6.56 (45.2) |
| CV (%) | 6.00 | 5.63 | 4.30 |

### 6.5.5 Transverse Tensile Strength of 12 in. (300 mm) Pipe Liner

Figure 6.10 presents the transverse tensile stress vs. extension plots of FA (bonded) and FMA (bonded) liners for the 12 in. (150 mm) CI pipe. As shown in Figure 6.10, the plots for FA liners have characteristics similar to those for the FMA liners. The mean and coefficient of variation of transverse strength values for FA bonded and FMA bonded specimens are presented in Table 6.10. The average FMA liner strength is very close to that of the FA liner and indicates that there is no significant effect of mechanical aging on the liner strength.

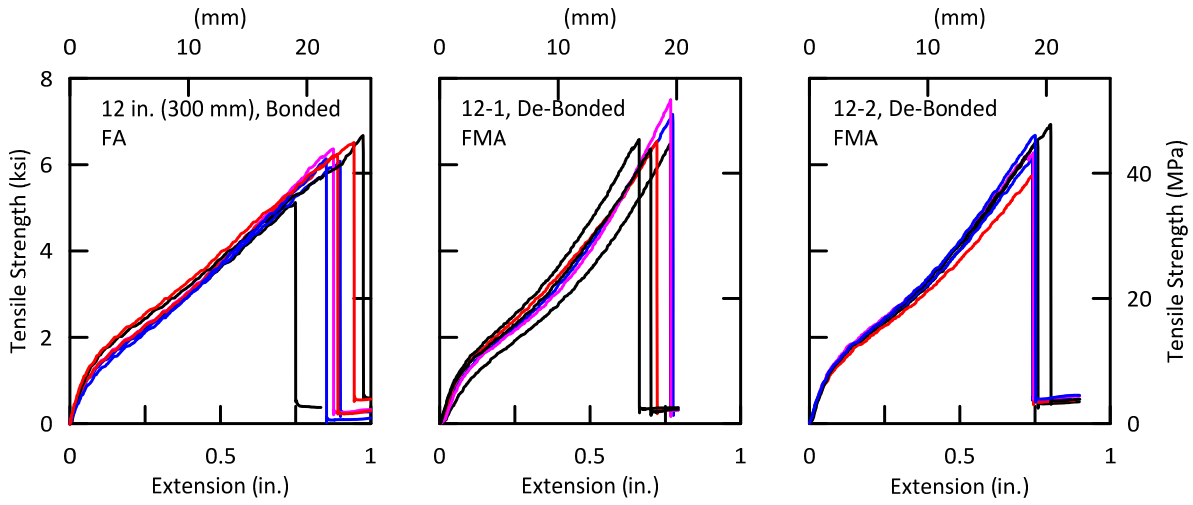


FA = Field Aged for 11 years.
FMA = Field Aged + Mechanically Aged at Cornell (equivalent to 100 years of traffic and thermal cycling).

a) Field Aged, Bonded

b) 12-1, Field + Mechanically Aged, De-Bonded

c) 12-2, Field + Mechanically Aged, De-Bonded

Figure 6.11. Tensile Strengths vs. Extension Plots for FA (Bonded) and FMA (De-Bonded) Liners in the Transverse Direction for 12 in. (300 mm) Pipe

Table 6.11. Average Tensile Strengths of FA (Bonded) and FMA (De-Bonded) Liners in the Transverse Direction for 12 in. (300 mm) Pipe

| | Averages for 12 in. (300 mm) Pipe | | |
|---|---|---|---|
| | Field Aged (FA) | Field + Mechanically Aged (FMA) | |
| Test Value | Bonded | De-Bonded 12-1 | De-Bonded 12-2 |
| ksi (MPa) | 5.92 (40.8) | 6.78 (46.7) | 6.39 (44.1) |
| CV (%) | 6.00 | 6.14 | 6.00 |

Figure 6.11 shows the transverse tensile strength (stress) vs. extension plots of FA (bonded) and FMA (debonded) liners for the 12-in. (300-mm) pipe. As shown in Figure 6.11, the FA and FMA liners show similar tensile behavior. The mean and coefficient of variation of transverse strength values for FA bonded and FMA debonded specimens are presented in Table 6.11. The average FMA liner strength is very close to that of the FA liner and indicates that there is no significant effect of mechanical aging on the liner strength.

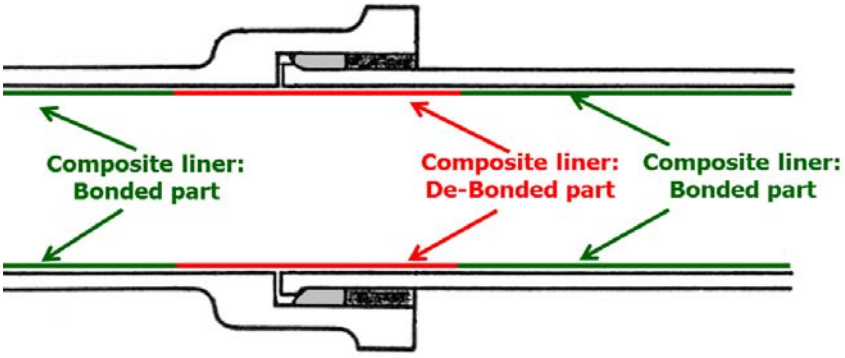


Figure 6.12. Typical Bell and Spigot CI Pipe Joint with Composite Liner Showing both Bonded and De-Bonded Sections of the Pipe after Mechanical Aging Tests

### 6.5.6 Lap Shear Strength

A longitudinal cross-section through typical bell and spigot CI joint with liner is shown in Figure 6.12. When thermal contraction of the CI pipes occurs, the two adjoining pipe sections are pulled apart and maximum tensile stress and strain are exerted on the liner at the gap between the bell and the spigot. The liner, while stretching, generates shear stresses at the CI pipe/liner interface at that location. This results in the CI pipe/liner interfacial failure in the shear mode. As a result, shear is viewed as the primary mode of CI pipe/liner interfacial failure. The debonded region of the liner has been observed to be within one diameter across the joint gap.

During axial joint displacement, the lining tends to reduce in diameter within the debonded region as the spigot is pulled from the bell. The reduction in diameter is resisted by adhesion in the tensile mode between the CI pipe surface and liner, which is measured in the peel test. It should be recognized that this type of adhesion loss is a secondary mode of failure, which is not as important as the shear resistance between the liner and CI pipe surface.

#### 6.5.6.1 Lap Shear Tests for 6 in. (150 mm) Pipe in the Longitudinal Direction

Figure 6.13 shows the plots obtained for the lap shear tests of FA and FMA bonded liners for 6 in. (150 mm) pipe in the longitudinal direction. The characteristic plots of shear vs. extension in both cases are virtually identical. The average lap shear values and CV values for each group are presented in Table 6.12. The results are also compared with control (lab prepared) specimens of Starline®2000 PSE-35 liner and for specimens aged for 48 weeks at 149 °F (65 °C) (equivalent

to about 22 years of aging at room temperature) in the lab (Netravali et al., 2003). From the data it is clear that the lap shear strength values remained essentially unchanged after the mechanical aging, suggesting that there was little or no effect of mechanical aging on CI pipe/liner adhesion.

#### 6.5.6.2 Lap Shear Tests for 12 in. (300 mm) Pipe in the Longitudinal Direction

Figure 6.14 shows the plots obtained for the lap shear tests of FA and FMA bonded liners for 12 in. (300 mm) CI pipe in the longitudinal direction. As in the case of the 6 in. (150 mm) pipes, the characteristic plots of shear vs. extension for FA and FMA specimens follow similar trends. The average lap shear values and CV values for each group are presented in Table 6.13. From the data it is clear that the lap shear strength values did not change after the mechanical aging suggesting that there was little effect of mechanical aging on CI pipe/liner shear strength.

The results from both the 6 in. (150 mm) and 12-in. (300 mm) lap shear specimens in this work were also compared with the results for control (lab prepared) specimens of the Starline® 2000 PSE-35 liner (Netravali et al., 2003) and specimens that were aged for 48 weeks at 149 °F (65 °C) (equivalent to about 22 years of aging at room temperature) in the lab. All results were found to be in very close agreement.

### 6.5.7 Peel Test

#### 6.5.7.1 Peel Tests for 6 in. (150 mm) Pipe in the Longitudinal Direction

Figure 6.15 shows the plots obtained for the 180° peel tests of bonded liners for 6 in. (150 mm) pipe in the longitudinal direction. The average of samples for each group were calculated and shown in Table 6.14. The results were also compared with the results for control (lab prepared) specimens of Starline®2000 PSE-35 liner and specimens that were aged for 48 weeks at 149 °F (65 °C) (equivalent to about 22 years of aging at room temperature) in the lab (Netravali et al., 2003).

In the peel test the CI pipe/liner failure occurs within a very small linear zone. During the peel tests, once that local zone under stress debonds, the stress is released. Further peeling (pulling) builds up the stress on the next zone until it debonds, again reducing stress. This step-by-step process of building and releasing stress continues through the test and, as a result, the plot has typical stick-slip characteristics. Since the failure occurs in a small zone, the peel test is very sensitive to local bond variations. The plots obtained for individual specimens clearly show this

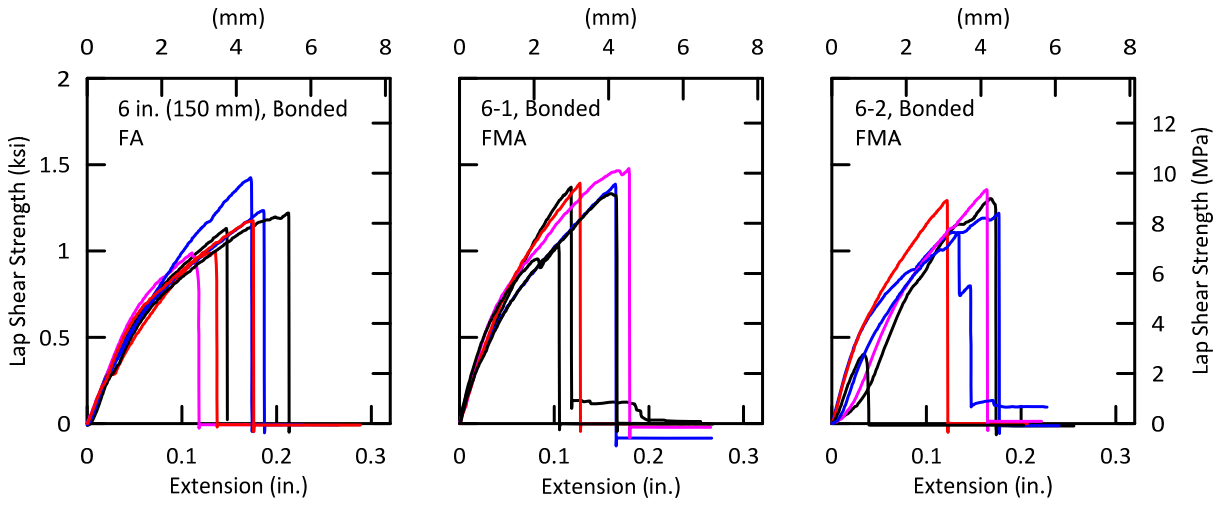


FA = Field Aged for 16 years.
FMA = Field Aged + Mechanically Aged at Cornell (equivalent to 100 years of traffic and thermal cycling).

a) Field Aged, Bonded

b) 6-1, Field + Mechanically Aged, Bonded

c) 6-2, Field + Mechanically Aged, Bonded

Figure 6.13. Lap Shear Strengths for FA and FMA Bonded Liners for 6 in. (150 mm) Pipe in the Longitudinal Direction

Table 6.12. Average Lap Shear Strengths for FA and FMA Bonded Liners for 6 in. (150 mm) (150 mm) Pipe in the Longitudinal Direction

| | | Aged for 48 weeks at 149°F (65°C)[a] | Averages for 6 in. (150 mm) Pipe | | |
|---|---|---|---|---|---|
| | | | Field Aged (FA) | Field + Mechanically Aged (FMA) | |
| Test Value | Control | | Bonded | Bonded 6-1 | Bonded 6-2 |
| ksi (MPa) | 1.1 (7.6) | 1.4 (9.7) | 1.17 (8.1) | 1.33 (9.2) | 1.11 (7.7) |
| CV (%) | 13.20 | 5.70 | 11.91 | 10.56 | 29.41 |

a - Results obtained in 2003 study on Starline®2000 PSE-35 liner.

variation among specimens. However, even within a single specimen, large variations can be seen. Despite the inherent variations, the peel strength values are similar, with the exception of the results for specimen 6-2. The results were also compared with the results for control (lab prepared) specimens of Starline®2000 PSE-35 liner and specimens that were aged for 48 weeks at 149 °F (65 °C) (equivalent to about 22 years of aging at room temperature) in the lab (Netravali et al., 2003).

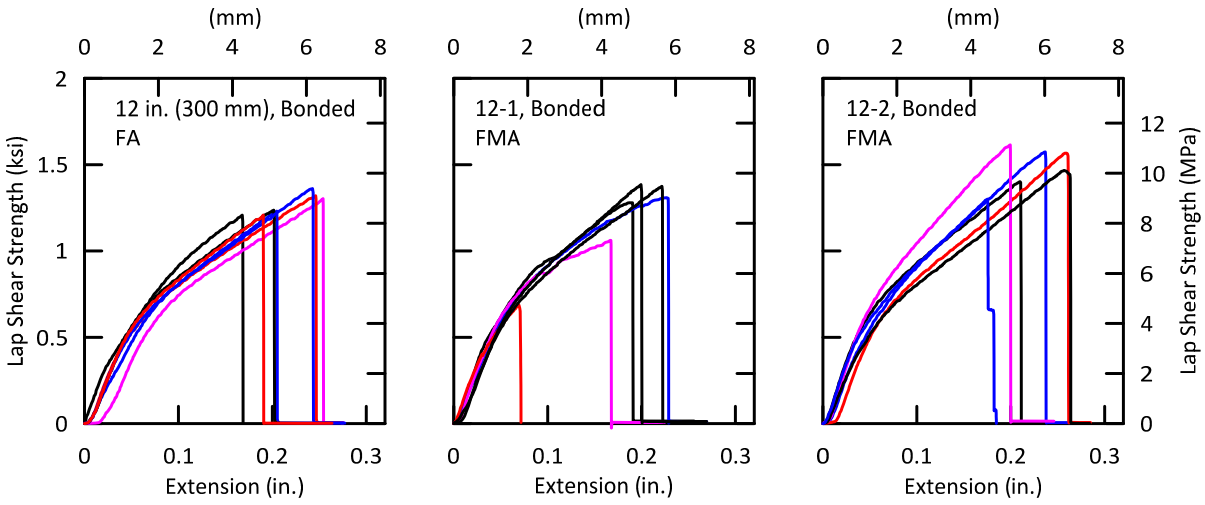


FA = Field Aged for 11 years.
FMA = Field Aged + Mechanically Aged at Cornell (equivalent to 100 years of traffic and thermal cycling).

a) Field Aged, Bonded

b) 12-1, Field + Mechanically Aged, Bonded

c) 12-2, Field + Mechanically Aged, Bonded

Figure 6.14. Lap Shear Strengths for FA and FMA Bonded Liners for 12 in. (300 mm) Pipe in the Longitudinal Direction

Table 6.13. Average Lap Shear Strengths for FA and FMA Bonded Liner for 12 in. (300 mm) (300 mm) Pipe in the Longitudinal Direction

| | | Aged for 16 weeks at 149°F (65°C)[a] | Averages for 12 in. (300 mm) Pipe | | |
|---|---|---|---|---|---|
| | | | Field Aged (FA) | Field + Mechanically Aged (FMA) | |
| Test Value | Control | | Bonded | Bonded 12-1 | Bonded 12-2 |
| ksi (MPa) | 1.1 (7.6) | 1.6 (11.0) | 1.27 (8.8) | 1.18 (8.1) | 1.49 (10.3) |
| CV (%) | 13.20 | 10.10 | 4.46 | 20.82 | 7.40 |

a - Results obtained in 2003 study on Starline®2000 PSE-35 liner

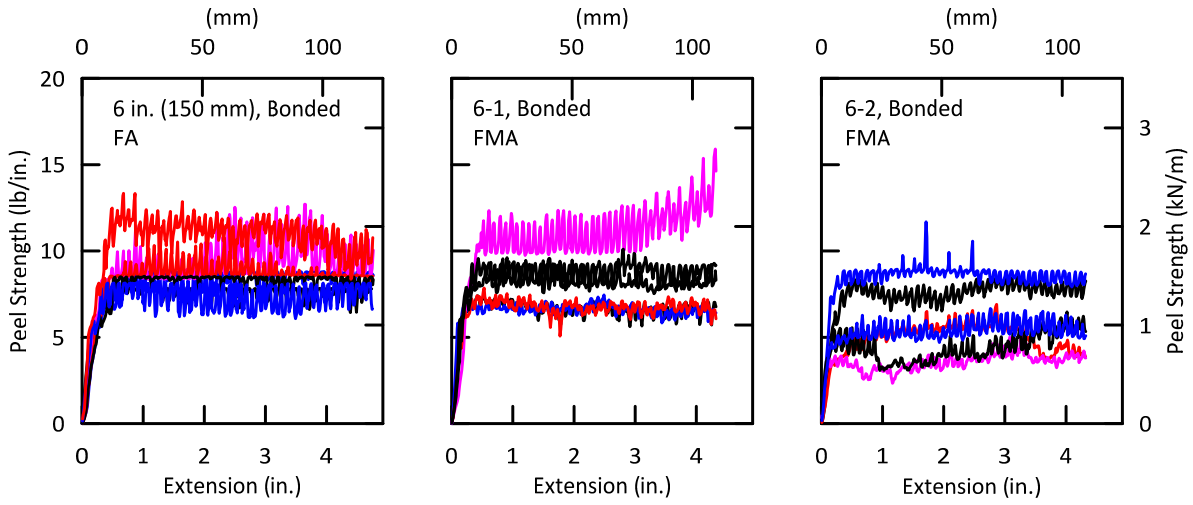


Figure 6.15. Peel Test Strengths for FA and FMA Bonded Liners for 6 in. (150 mm) Pipe in the Longitudinal Direction

Table 6.14. Average Peel Strengths for FA and FMA Bonded Liners for 6 in. (150 mm) Pipe in the Longitudinal Direction

| | | Aged for 48 weeks at 149°F (65°C)[a] | Averages for 6 in. (150 mm) Pipe | | |
|---|---|---|---|---|---|
| | | | Field Aged (FA) | Field + Mechanically Aged (FMA) | |
| Test Value | Control | | Bonded | De-Bonded 6-1 | De-Bonded 6-2 |
| lb/in. (kN/m) | 8.00 (1.40) | 9.70 (1.70) | 8.72 (1.53) | 8.06 (1.41) | 5.83 (1.02) |
| CV (%) | 7.60 | 9.90 | 12.96 | 21.01 | 30.08 |

a - Results obtained in 2003 study on Starline®2000 PSE-35 liner

### 6.5.7.2 Peel Test for 12 in. (300 mm) Pipe in the Longitudinal Direction

Figure 6.16 shows the peel test results of the 12 in. (300 mm) pipe bonded liner in the longitudinal direction. The averages of samples for each group were calculated and shown in Table 6.15. The results were also compared with the results for control (lab prepared) specimens of Starline®2000 PSE-35 liner and specimens aged for 48 weeks at 149°F (65°C) (equivalent to about 22 years of aging at room temperature) in the lab (Netravali et al., 2003). As can be seen from Figure 6.16 large variations were observed between different specimens as well as within single specimens.

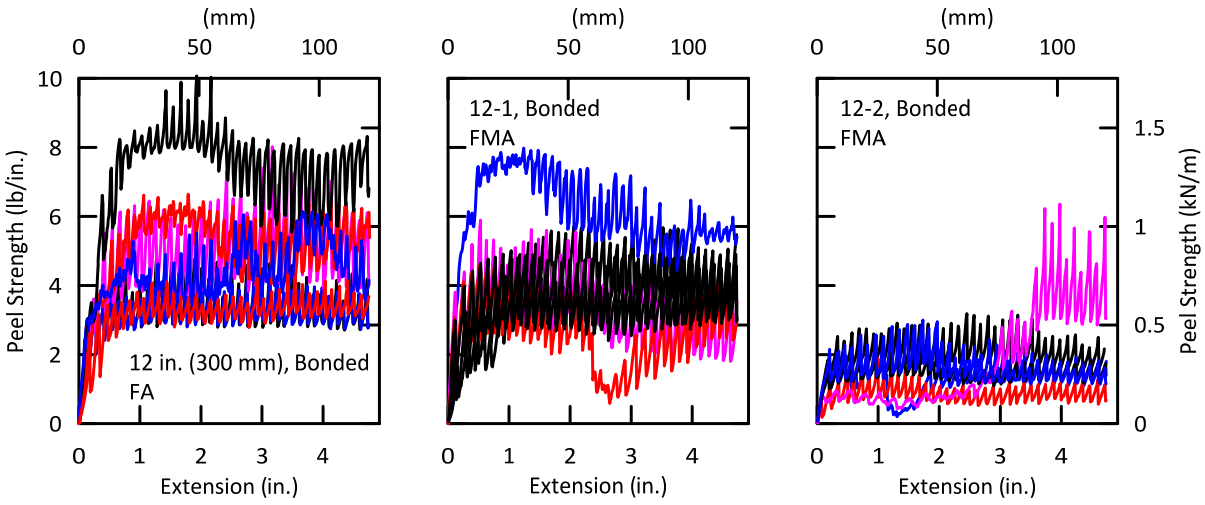


Figure 6.16. Peel Test Strengths for FA and FMA Bonded Liners for 12 in. (300 mm) Pipe in the Longitudinal Direction

Table 6.15. Average Peel Strengths for FA and FMA Bonded Liners for 12 in. (300 mm) Pipe in the Longitudinal Direction

| | | Aged for 16 weeks at 149°F (65°C)[a] | Averages for 12 in. (300 mm) Pipe | | |
|---|---|---|---|---|---|
| | | | Field Aged (FA) | Field + Mechanically Aged (FMA) | |
| Test Value | Control | | Bonded | De-Bonded 12-1 | De-Bonded 12-2 |
| lb/in. (kN/m) | 8.00 (1.40) | 9.70 (1.51) | 4.66 (0.82) | 3.90 (0.68) | 1.56 (0.27) |
| CV (%) | 7.60 | 10 | 31.61 | 29.48 | 25.88 |

a - Results obtained in 2003 study on Starline®2000 PSE-35 liner

The current peel strength values for 12 in. (300 mm) pipe are about half those obtained for the earlier 6 in. (150 mm) pipe study (Netravali et al., 2003). Progressive Pipeline Management personnel were contacted to understand better the field installation procedures for the Starline® 2000 PSE-35 liners. The inversion pressure for 12 in. (300 mm) CI pipe is approximately 8 psig (55 kPa) in contrast to about 25-28 psig (≈ 180 kPa) for 6 in. (150 mm) CI pipe. Since the inversion pressure is directly related to the stress imposed on the liner/CI pipe interface during installation and initial curing, it will influence adhesion that develops in the tensile mode between the liner and the CI pipe interior surface. It is likely, therefore, that the lower pressure is responsible for the reduced peel strength.

## 6.6 Conclusions

The liner tensile testing showed that the liner strengths were comparable for the 6 in. (150 mm) specimens for FA and FMA liner specimens taken from bonded and debonded sections of the liners. Based on these results it can be concluded that 100 years of mechanical aging did not affect the longitudinal tensile strengths of the 6 in. (150 mm) pipe liners. In the hoop direction the liners are also unaffected by mechanical aging.

For the 12 in. (300 mm) pipe liners, tensile strength reduction was measured only in the liner specimens that contained partially damaged yarns, specifically in the debonded sections. Considerable tensile strength was still present in liner specimens with damaged fibers because the stretchable polyurethane membrane was intact. For undamaged specimens removed from the debonded areas, liner strengths were comparable for FA and FMA liner specimens taken from bonded and debonded sections of the liners.

The testing for lap shear and peel strengths of the FA and FMA liner specimens provides an opportunity to determine if the lap shear and peel strengths are affected by mechanical aging. A comparison of the lap shear strengths of FA and FMA specimens from the 6 in. (150 mm) and 12 in. (300 mm) pipe with the lap shear strengths of unaged specimens of cast iron pipe with Starline®2000 PSE-35 liner tested at Cornell in 2003 show no significant difference in the results. Thus, no loss of lap shear strength can be shown over the 10 to 16 years of service life in the field and for the 100 years of mechanical aging imposed on the specimens.

A comparison of the peel strengths of FA and FMA specimens from the 6 in. (150 mm) pipe with the peel strengths of unaged specimens of 6 in. (150 mm) cast iron pipe with Starline®2000 PSE-35 liner tested at Cornell in 2003 show no significant difference in the results. Peel strengths for the 12 in. (300 mm) specimens in this study are not comparable to those of the 6 in. (150 mm) specimens. This is because, as mentioned earlier, installation of the liner in the field involves curing under internal pressure substantially less than that for 6 in. (150 mm) pipe. The lower pressure can be expected to result in a lower peel strength relative to that for the 6 in (150 mm) pipe. The results of this study support this hypothesis. Thus, an important conclusion from this study is that there is no evidence of significant reduction in either lap or peel strength due to field aging over 10 to 16 years in addition to 100 years of mechanical aging when the inversion pressures during CIPL installation are similar.

# Section 7
# Summary

## 7.1 Project Summary

This report presents the results of a project supported by the gas industry and government regulators to evaluate the performance of field-aged cured-in-place pipe liners (CIPL) that had been in service for 10 to 16 years. The liners were a product called Starline®2000, and are a system comprised of a polyester fabric with a tough polyurethane coating. This liner is adhered to the inside of the cleaned and prepared host pipe and allowed to cure in place for a relatively brief period of time. This system is impervious and durable, and is used as a composite renewal system for both gas and water pipelines.

Pipe sections with this lining were retrieved from two field sites and subjected to 100 years of mechanical aging due to vehicular traffic, undermining/backfill events, and thermal cycling simulations. Vehicular traffic simulations were equivalent to 100 years (2,000,000 cycles) of a 40 kip (180 kN) tandem axle with an impact factor of 1.5. Thermal aging was performed by simulating the expected contraction/expansion of a round crack in CI due to a 40 ºF (22 ºC) seasonal temperature variation in the ground at typical pipe burial depths.

## 7.2 Specimen Retrieval

Specimens were retrieved from two field sites for special aging tests done in the laboratory to simulate 100+ years of field service. The 6-in. (150-mm)-diameter specimens were retrieved from a Public Service Electric and Gas location in Elmwood Park, NJ. The CI pipeline was installed in 1949, and a Starline®2000 liner was installed inside the pipeline by Progressive Pipeline Management in 1998. The pipe specimens were extracted in May, 2014 and sent to Cornell University for mechanical aging tests. The 12-in. (300-mm)-diameter specimens were retrieved from a National Grid location in South Garden City, Long Island, NY. The CI pipe was initially constructed in 1951, and a Starline®2000 liner was installed in the pipeline in 2004. The pipe specimens were retrieved in August, 2014, and sent to Cornell University for mechanical aging tests. The joints in the 6 in. (150 mm) pipes were cement/mortar and jute caulking. The pipe joints for the 12 in. (300 mm) sections were mechanical clamps with a rubber sealing gasket.

## 7.3 Mechanical Aging Tests

The mechanical aging tests used pipe joints in place of a pipe section with a round crack. Retrieving a pipe section having had a round crack, then lined with CIPL was not feasible. The joint is intended to simulate a round crack with very small rotational stiffness. The 6-in. (150-mm)-diameter pipe section had stiff, cement mortar joints. When the first 6 in. (150 mm) pipe section was first tested in the thermal loading test frame, the forces necessary to attempt joint opening were very large. If this condition was allowed to remain, it was entirely possible that the epoxy resin in the joint opening could suddenly fail, or the interface bond between the liner and the pipe slip rapidly, causing the CIPL to abruptly rupture. This condition would not have been representative of the magnitude of loading or rate of displacement imposed across a round crack with CIPL liner under expected seasonal temperature variations. Thus, the cement/mortar joint material was removed to weaken the joint. This process was performed on both 6-in. (150-mm)-diameter specimens. After this procedure the joints are referred in this report as "weakened joints." This had the additional testing benefit of providing a potential leakage path for internal pressure drop (indicating leakage) if the CIPL ruptured. The intact cement/mortar in the test joint may have prevented this, and leakage may not have been detected if the CIPL had ruptured.

Mechanical aging tests included flexure testing to simulate vehicular traffic, additional bending after an undermining/backfill event, and thermal cycling to simulate seasonal variations in temperature. The purpose of the flexural tests is to characterize the performance of the lined joints under repetitive deformations imposed on the pipeline due to traffic loads during the pipeline service life. Vehicular surface loads are transmitted through the pavement and soil to the underground pipelines imposing flexure and joint rotation. Among other factors, the magnitude of pipeline deformation and joint rotation greatly depend on the applied load, the relative stiffness of the pipeline with respect to the surrounding soil that supports it, depth of burial, and the stiffness of the joint between individual lengths of pipe. The two important factors for the performance of joints are (1) the magnitude of joint rotation due to the applied load, and (2) ability of the joint to handle the imposed rotation.

The testing program consisted of four-point bending (flexure) tests, simulating two 50-year-sequences of testing. The deflections and rotations of the joints were measured, and any changes in pipe characteristics of the 100-year period were noted. The flexure tests were performed using

displacements and joint rotations consistent with those derived using previous Cornell analytical research, which were validated by full-scale field tests assuming soil and flexible pavement conditions typically found in gas distribution systems. Special undermining/backfill (trenching) events also were replicated in the laboratory testing. The deformations imposed in the pipe from these loadings were about two to three times that used for the normal vehicular loadings. Additional loadings following these events did not indicate any changes in the performance of the CIPL system.

Thermal loads in buried piping are a direct result of temperature changes. Data were summarized for temperature change in New York State and other parts of the Northeast that would be experienced by pipelines at soil depths between 30 and 49 in. (0.8 and 1.2 m), which is in the range of burial depths for typical gas distribution pipe. A comparison of data sets revealed that ground temperatures are relatively consistent throughout the northeast for various conditions. Ground temperatures can fluctuate between 70 and 25 °F (21 and -4 °C) over a period of 6 to 7 months. More typically, the data show that ground temperatures fluctuate between 70 and 30 °F (21 and -1 °C). Thus, the maximum design temperature change due to seasonal variations in ground temperature in the northeastern US for typical distribution pipe depths is taken as $\Delta T = 40°F$ (22°C).

Both 6- and 12-in. (150- and 300-mm)-diameter CI specimens showed a dramatic change in axial pull/push stiffness after the very first thermal cycle. The first thermal cycle, performed over about 6 hours for the first tension portion, and 4 hours for the completion of the compression cycle, caused substantial debonding of the liner from the pipe. This rate of temperature drop is much faster that the $\Delta T = 40$ ºF (22 ºC) decrease over about 120 days, the typical rate of cooling at gas pipeline depths in the northeast. In a field environment, the visco-elastic properties of the polyester fibers along with the polyurethane membrane liner would shed stress during slow cooling. This effect is likely to be extremely significant. Debonding was also reflected as a decrease in rotational stiffness from the first 50 years of vehicular traffic, which had not been subject to thermal cycling, to the second 50 years which had experienced the first round of 50 years of thermal cycles.

During all phases of the mechanical aging tests none of the specimens leaked. Following these mechanical aging tests, Specimen 6-2 was pressure tested to 90 psig (620 kPa) using water, and

the pipe did not leak. The pressure was increased to 150 psig (1,034 kPa) and the pipe continued to maintain pressure integrity.

For the 12 in. (300 mm) specimens holes were drilled through the CI bell and into the gap between the spigot end and the CIPL. The propose of these drilled holes was to make sure any leaking gas could escape and not be restricted by an intact rubber gasket in the mechanical clamp. This hole was filled with soapy water so that any leakage of the liner during pressure verification could be detected. Each specimen was pressure tested to 60 psig (414 kPa) using nitrogen, and the pipes did not leak. The pressure was increased to 90 psig (620 kPa) and the pipe continued to maintain pressure integrity.

After mechanical testing the pipe joints were cut longitudinally for visual inspection. The 6 in. (150 mm) joints with the CIPL showed debonding at the separation between bell and spigot that was confined to a small distance either side of the separation, less than one pipe diameter in total width. This debonding allowed the liner to stretch without experiencing excessive strain, and demonstrates that the CIPL response involves local bonding adjustments that relieve high strain concentrations in the liner. This type of strain reduction is a highly desirable aspect of CIPL performance.

The 12 in. (300 mm) specimens did experience some minor liner damage. It is believed that this distress occurred during the first thermal loading cycle, which caused substantial debonding and some visually observed fiber damage. However, the liner did not leak because the polyurethane membrane remained intact and maintained its capacity to resist high internal gas pressure. The pipe sections did not leak when pressure tested to 90 psig (620 kPa), which is 1.5 time the pipe MAOP. This is a very important experimental observation. Fiber damage does not mean that the CIPL will leak because additional capacity is provided by the polyurethane membrane.

### 7.4 Material Property Characterization

The purpose of the additional material property characterization tests was to:

l) Characterize the residual tensile properties of the Starline®2000 composite liner system as a way to assess the effects of field and mechanical aging on the liner system and their durability, and

2) Characterize the residual liner/CI pipe bond (adhesion) strength and assess the durability

of the bond strength of field and mechanically aged specimens using lap shear and peel tests.

This allowed for an evaluation of whether the longitudinal and hoop tensile strengths of bonded, field-aged (FA) liner specimens are comparable to those for both bonded and debonded field and mechanically aged (FMA) liner specimens. The testing showed that the liner strengths were comparable for the 6 in. (150 mm) specimens for FA and FMA liner specimens taken from bonded and unbonded sections of the liners. Thus, 100 years of mechanical aging did not have a significant effect on either the longitudinal or hoop tensile strengths of the 6 in. (150 mm) pipe liners.

For the 12 in. (300 mm) pipe liners, tensile strength reduction was measured in the immediate vicinity of damaged fibers in the debonded sections of the lining. Considerable tensile strength was still present in lining specimens with damaged fibers because the polyurethane membrane was intact, thus providing resistance to tensile test forces. In locations removed from the vicinity of damaged fibers, liner strengths were comparable for FA and FMA liner specimens taken from bonded and unbonded sections of the liners.

The testing for lap and peel strengths allows for an evaluation of whether the lap and peel strengths of the FA and FMA liner specimens are comparable to those of unaged specimens. A comparison of the lap shear strengths of FA and FMA specimens from the 6 in. (150 mm) and 12 in. (300 mm) pipe with the lap shear strengths of unaged specimens of cast iron pipe with Starline®2000 liner tested at Cornell in 2002 show no significant difference in the results. Thus, no loss of lap shear strength can be shown over the 10 to 16 years of service life in the field and for the 100 years of mechanical aging imposed on the specimens. These findings are important because the strength of the CIPL system depends strongly on the lap shear strength, especially for resistance to thermally induced contraction/expansion of the pipe at round cracks and the bell/spigot separation in a weak, deteriorated joint.

A comparison of the peel strengths of FA and FMA specimens from the 6 in. (150 mm) pipe with the peel strengths of unaged specimens of 6 in. (150 mm) cast iron pipe with Starline®2000 liner tested at Cornell in 2002 show no significant difference in the results. Peel strengths for the 12 in. (300 mm) specimens in this study are not comparable to those of the 6 in. (150 mm) specimens because installation of the liner in the field involves curing under internal pressure

substantially less than that for 6 in. (150 mm) pipe. The reduced pressure will result in a lower peel strength relative to that for the 6 in (150 mm) pipe, which is confirmed by the test results in this study. Thus, a critically important conclusion from the testing is that there is no evidence of significant reduction in either lap or peel strength due to field aging over 10 to 16 years in addition to 100 years of mechanical aging.

## 7.5 Conclusions

The laboratory tests for mechanical and thermal aging and those for material characterization of both field-aged and field plus mechanically aged liners showed that the lined pipe sections were unaffected by both heavy vehicular traffic and special undermining/backfill events for the 100 year equivalent test sequences.

The thermal loading tests revealed that the liner response was greatly affected by the first thermal cycle. This thermal cycle caused debonding between the liner adhesive and the cast iron. The thermal displacements were applied over a 6 to 10 hour expansion/contraction time. This is substantially faster that the slow rate of temperature and displacement rates under field conditions. Research at Cornell on thermal properties of other thermoplastic material under temperature changes has helped quantify the visco-elastic properties of polymers. Additional thermo-mechanical testing under slower rates would help clarify the behavior of the CIPL systems under perhaps more representative field conditions.

During all of the mechanical aging tests, both flexural and thermal, the liners did not leak. Pressure verifications tests were performed at high pressures, well in excess of the pipeline operating pressures. The CIPL systems maintained pressure integrity for all phases of testing.

Additional material characterization tests showed that the liner material had maintained strength characteristics similar to those of unaged laboratory specimens. Lap and peel shear tests showed no evidence of significant reduction in either lap or peel strength due to field aging over 10 to 16 years in addition to 100 years of mechanical aging.

## References


ASTM D1876 (1995), "Standard Test Method for Peel Resistance of Adhesives (T-Peel Test)," ASTM International, West Conshohocken, PA.

ASTM D3164, (1997). "Standard Test Method for Strength Properties of Adhesively Bonded Plastic Lap-Shear Sandwich Joints in Shear by Tension Loading," ASTM International, West Conshohocken, PA.

ASTM D3039/D3039M, (2000)." Standard Test Method for Tensile Properties of Polymer Matrix Composite Materials," ASTM International, West Conshohocken, PA.

Carder, DR, P. Nath, and ME Taylor. (1981). "A Method of Modeling the Effect of Traffic on Undermined Buried Pipelines," *Laboratory Report 1028*, Transport and Road Research Laboratory, Crowthorne, UK, 1981.

Carroll, C, H Schenck Jr. and W Williams. (1966). "Digital Simulation of Heat Flow in Soils," Journal of the Soil Mechanics and Foundations Division, ASCE, Vol. 92, No. SM 4, pgs. 31-49.

Committee on Gas and Liquid Fuel Lifelines. (1984). *Guidelines for the seismic design of oil and gas pipeline systems*, ASCE, New York.

Erlingsson, T. (1971). "A Model for Heat Transfer in Soils," Master of Science Thesis, Cornell Univ., Ithaca, NY, June.

Jeon. S-S, TD O'Rourke and AN Netravali. (2004). "Repetitive Loading Effects on Cast Iron Pipelines with Cast-in-Place Pipe Lining Systems," Journal of Transportation Engineering, ASCE, Nov., pp. 692-705.

Monie, WD and CM Clark. (1974). "Loads on Underground Pipe Due to Frost Penetration," Journal of the American Water Works Association, Vol. 66, No. 6, p. 353-358.

Netravali, AN, TD O'Rourke, SK Shaw, and TK Bond. (2003), "Evaluation of Starline® 2000-PSE Cured-in-Place Lining System for Cast Iron Gas Distribution Pipelines", NYGAS, Contract No. 39802, April.

Northeast Regional Climate Center. (1997). Temperature Sensors Continuously Monitoring Ground Temperature, Cornell University Meteorological Station, Game Farm Road, Ithaca, NY, Dec. 1992-Apr.

Netravali, AN, TD O'Rourke, KI Gerritsen, YP Singh, S-S and DZ Zhao. (2000). "Advanced Pipeline Support and Stabilized Backfill for Gas Mains," Contract No. 31120 Report, NYGAS.

Netravali, AN and Shaw, SK. (2002). "Evaluation of Starline® 2000 PSE-35 Liner System for Cast Iron (CI) Gas Distribution Pipeline," Report submitted to Karl Weiss GmbH & Co., Berlin, Germany, August.

O'Rourke, TD, AR Ingraffea, HE Stewart, CW Crossley, GL Panozzo, JR Blewitt, MS Tawfik, and A Barry. (1988). "State-of-the-Art Review: Practices for Pipeline Crossings at Highways," Topical Report GRI-88/0287, Gas Research Institute, Chicago, IL, Sept., 208 p.

O'Rourke, TD, AN Netravali, SM Pendharkar, A Tonkinson, D Chaudhuri, and S Toprak. (1996). "Evaluating Service Life of Anaerobic Joint Sealant Products and Techniques, Gas Research Institute, Report No. GRI-96/0318, September.

Pocock, RG, GJL Lawrence, and ME Taylor. (1980). "Behavior of a Shallow Buried Pipeline under Static and Rolling Wheel Load." TRRL Laboratory Rep. 954, Transportation and Road Research Laboratory, Crowthorne, Berkshire, U.K.

Stewart, HE, BJ O'Rourke, TD O'Rourke, and BM New. (1989). "Evaluation of Cast Iron Pipeline Response at Excavation Crossings," Geotechnical Engineering Rep. 89-1, School of Civil and Environmental Engineering, Cornell Univ., Ithaca, N.Y.

Stewart, HE, Ö Bilgin, TD O'Rourke, and TM-J and Keeney. (1999). "Improved Design and Construction Practices for Thermal Loads in Plastic Gas Pipelines," Geotechnical Engineering Rep. 99-1, School of Civil and Environmental Engineering, Cornell Univ., Ithaca, N.Y.

Taki, H, and TD O'Rourke. (1984). "Factors Affecting the Performance of Cast Iron Pipe," Geotechnical Engineering Rep. 84-1, School of Civil and Environmental Engineering, Cornell Univ., Ithaca, N.Y.

Walpole, RE and RH Myers. (1972). Probability and Statistics for Engineers and Scientists, Macmillan Publishing Co., Inc.

# Appendix A

## Equivalent Years vs. Report Terminology for Vehicle Loadings

### A. 1 Introduction

One objective of this report was to subject specimens of CIPL to cycles of vehicular loading simulating 100 years of traffic, which would convert to 2,000,000 cycles of laboratory flexural loadings. So, 1 year is equal to 20,000 vehicle cycles. In the figures of this report the first 1,000 cycles were not shown as equivalent years because the number of years would be too small to have any meaningful significance. The laboratory simulations were done in two test sequences, separated by a 50-year-equivalent set of thermal aging cycles. Each sequence of vehicle testing also included one cycle of an undermining/backfill event followed by an additional 100,000 cycles of vehicular loading. These additional 100,000 cycles were intended to see whether the undermining/backfill event had a significant effect of the subsequent specimen behavior. Thus, the vehicle traffic simulates slightly more than 100 years. The vehicle traffic loading response in the pipe sections became nearly constant after a few thousand cycles, at most. The effect of vehicle traffic is insignificant relative to the effect of thermal loading. Thus, there is no practical difference in pipe response to the flexural loadings at 1,000,000 cycles and 1,100,000 cycles.

For simplicity of the report the first 50 years are referred to as the first 1,000,000 cycles, while the 100,000 cycles after the undermining are referred to as "+ 0.5 years". To be entirely consistent, the first sequence of testing could have been represented as 50.5 years of vehicle loading, and carry this "extra" half year throughout the cycle conversion of the next loading sequence. To provide clarity the report does not include this additional half year of vehicular loading. Table A.1 gives the full representation of the testing, and the actual "Equivalent Years" of testing vs. the years used in this report in describing figures, tables, etc. The conversion divided lab cycles by 20,000 to obtain years.

Table A.1. Equivalent Years vs. Report Terminology for Vehicle Loadings

| First 50 Years Test Sequence | | |
|---|---|---|
| | Equivalent Years | Report Terminology |
| Cycle 1 | - | Cycle 1 |
| Cycle 100 | - | Cycle 100 |
| Cycle 1,000 | - | Cycle 1,000 |
| Cycle 10,000 | 0.5 | 0.5 |
| Cycle 100,000 | 5 | 5 |
| Cycle 1,000,000 | 50 | 50 |
| 100,000 Cycles Post-Undermining | 50 + 0.5 = **50.5** | 50 |
| Second 50 Years Test Sequence | | |
| Cycle 1 | - | Cycle 1 |
| Cycle 100 | - | Cycle 100 |
| Cycle 1,000 | - | Cycle 1,000 |
| Cycle 10,000 | 50.5 + 0.5 = 51 | 50.5 |
| Cycle 100,000 | 50.5 + 20 = 70.5 | 70 |
| Cycle 1,000,000 | 50.5 + 50 = 100.5 | 100 |
| 100,000 Cycles Post-Undermining | 100.5 + 0.5 = **101** | 100 |